SEX-SPECIFIC EFFECTS OF DEVELOPMENTAL DIELDRIN EXPOSURE ON SYNUCLEINOPATHY

By

Aysegul Ozgur Gezer

A DISSERTATION

Submitted to
Michigan State University
in partial fulfillment of the requirements
for the degree of

Cell and Molecular Biology—Doctor of Philosophy

2020

ABSTRACT

SEX-SPECIFIC EFFECTS OF DEVELOPMENTAL DIELDRIN EXPOSURE ON SYNUCLEINOPATHY

By

Aysegul Ozgur Gezer

Human and animal studies have shown that exposure to the organochlorine pesticide dieldrin is associated with increased risk of Parkinson's disease (PD). Previous work showed that developmental dieldrin exposure increased neuronal susceptibility to MPTP toxicity in male C57BL/6 mice, possibly via changes in dopamine (DA) packaging and turnover. However, the relevance of the MPTP model to PD pathophysiology has been questioned. We therefore studied dieldrin-induced neurotoxicity in the α-synuclein (α-syn)-preformed fibril (PFF) model, which better reflects the α-syn pathology and toxicity observed in PD pathogenesis. Specifically, we used a "two-hit" model to determine whether developmental dieldrin exposure in mice increases susceptibility to α-syn PFF-induced synucleinopathy. Dams were fed either dieldrin (0.3 mg/kg, every 3-4 days) or vehicle corn oil starting 1 month prior to breeding and continuing through weaning of pups at postnatal day 22. At 12 weeks of age, male and female offspring received intrastriatal PFF or control saline injections. Consistent with the male-specific increased susceptibility to MPTP, our results demonstrate that developmental dieldrin exposure exacerbates PFF-induced toxicity in male mice only. Specifically, in male offspring, dieldrin exacerbated PFF-induced motor deficits on the challenging beam and increased DA turnover in the striatum 6 months after PFF injection. However, male offspring showed neither exacerbation of phosphorylated α-syn (p-syn) aggregation in the substantia nigra (SN) at 1 or 2 months post-PFF injection, nor exacerbation of PFF-induced TH and NeuN loss in the SN 6

months post-PFF injection. Collectively, these data indicate that developmental dieldrin exposure produces a male-specific exacerbation of synucleinopathy-induced behavioral and biochemical deficits. This sex-specific result is consistent with both previous work in the MPTP model, our previously reported sex-specific effects of this exposure paradigm on the male and female epigenome, and the higher prevalence and more severe course of PD in males. The novel two-hit environmental toxicant/PFF exposure paradigm established in this project can be used to explore the mechanisms by which other PD-related exposures alter neuronal vulnerability to synucleinopathy in sporadic PD. We also assessed the expression of total α-syn, DAT and VMAT2 by western blotting, inflammation by TaqMan Mouse Immune Array, and levels of dopamine (DA) and DA metabolites by HPLC in striatal tissue following developmental dieldrin exposure. We found that while developmental dieldrin exposure had no effect on total α-syn, DAT or VMAT2 levels or on striatal DA levels in both male and female F1 pups, exposure produced distinct effects on the male and female inflammatory gene profile. Finally, we also characterized the α-syn PFF model in female animals for the first time. Our results showed that female mice have reduced loss of nigral DA neurons and a behavioral resilience to the same level of DA loss compared to their male counterparts. This is the first study to show sex differences in sensorimotor function in the PFF model and suggests that the PFF model may be a valuable tool to model sex-differences in PD pathology and etiology that does not require any additional surgery or other treatments to manipulate hormonal state.

In memory of
DENIZ

ACKNOWLEDGEMENTS

I have been beyond lucky to have Dr. Alison Bernstein as my mentor during my training, a great role model who I always look up to. I learned an immense amount in a short period of time from her and felt very supported from my first day in the lab. I just could not have asked for a better mentor.

I would like to thank Dr. Jack Lipton and Dr. Caryl Sortwell for trusting me and supporting me throughout the most challenging part of the graduate school.

I would like to thank my committee members, Dr. Tim Collier, Dr. Caryl Sortwell, Dr. Cheryl Rockwell, and Dr. Gina Leinninger for guiding me throughout my training, and for their support.

Many thanks to Dr. McCormick for believing in me from the beginning, Bethany Heinlen for her generosity and support, Dr. Schutte and Michelle Volker for their support and commitment to making the DO/PhD program better, CMB program and Dr. Sue Conrad for the support and guidance.

There are many people who helped me and supported me during this journey. My lab, Dr. Joe Kochmanski for being generous with his time to help me anytime I needed, for his support and friendship. Allyson Cole-Strauss for all the help I received from her and for her support and patience. Dr. Joe Patterson for being very generous with his time to teach me and helping me with every single one of my endless questions. Sarah VanOeveren for all the help, endless support, and friendship. Chris Kemp for his help with experiments.

One of my strongest support during my PhD was from Katie. I cannot imagine this journey without her support and friendship. I owe a big thank you to my friends and family who have been very patient with me during this journey, loved me and supported me. Particularly Funda for supporting me during the most difficult times, I cannot thank her enough. Irem for being always on my side even when we were far away. My boyfriend Sam for being loving, encouraging, supportive and for just making every day better.

Lastly, I am eternally thankful for my family for being very patient with me as always, during my PhD. I felt their love and support every day despite the distance. Thank you for believing in me and supporting my decisions even when they included crossing an ocean for a decade long program. I love you.

PREFACE

At the time of writing this dissertation, Chapter 2, 3, and 4 have been reviewed by Neurobiology of Disease as one manuscript and revisions have been submitted. All data for published figures will be deposited in Mendeley Data upon publication of the manuscript. GraphPad Prism files can be viewed in the free Viewer mode or data can be extracted by viewing files in a text editor. R and RStudio are freely available.

TABLE OF CONTENTS

LIST OF TABLES

LIST OF FIGURES

KEY TO ABBREVIATIONS

α-syn	α-Synuclein
6-OHDA	6-hydroxydopamine
CNS	Central nervous system
COMT	Catechol-O-methyltransferase
DA	Dopamine
DAT	Dopamine transporter
DOPAC	3,4-Dihydroxyphenylacetic acid
GABA	Gamma aminobutyric acid
GPe	Globus Pallidus externus
GPi	Globus Pallidus internus
GWAS	Genome wide association study
GxE	Gene environment interactions
HVA	Homovanillic acid
L-DOPA	Levodopa
MAO	Monoamine oxidase
MPP+	1-methyl-4-phenylpyridinium
MPTP	1-methyl-4-phenyl-1,2,3,6-tetrahydropyridine
OCs	Organochlorine pesticides
p-syn	Phosphorylated α-Synuclein
PD	Parkinson's Disease
PFF	Pre-formed fibrils

POP	Persistent organic pollutant
ROS	Reactive oxygen species
SN	Substantia nigra
SNc	Substantia nigra pars compacta
SNP	Single nucleotide polymorphism
SNr	Substantia nigra pars reticulata
STN	Subthalamic nucleus
STR	Striatum
TH	Tyrosine hydroxylase
VMAT2	Type II vesicular monoamine transporter

Chapter 1 Introduction

Parkinson's disease: Overview

Parkinson's disease (PD) was first described in 1817 by British physician James Parkinson in a monograph entitled "An Essay on the Shaking Palsy" as:

> "Involuntary tremulous motion, with lessened muscular power, in parts not in action and even when supported; with a propensity to bend the trunk forwards, and to pass from a walking to a running pace: the senses and intellects being uninjured (1)."

Although initially described as a motor disorder, PD has since been recognized as a multisystem disorder with a significant non-motor component (2,3). PD is a debilitating disorder with no definitive treatment, adversely affecting patients' quality of life (4,5).

PD Demographics

PD is the second most common neurodegenerative disorder after Alzheimer's disease and the most common neurodegenerative movement disorder (6). Age is the biggest risk factor for PD, with incidence increasing in each decade of life. In the US, prevalence rates have been estimated at 0.01% for the population under 45 and about 1% for the population over 65 (7,8). Given current demographic trends, PD is expected to impose an increasing social and economic burden as the population ages, particularly in the developing world (6,8). For example, the number of individuals with PD is expected to more than double from 2005 to 2030 (9).

PD is more common in males than in females across all ages, with twice as many men suffering from PD than women in any given age range (10). In males, the incidence rate rises from 3.59 per 100,000 persons at 40-49 years to 132.72 per 100,000 at 70-79 years (4). The corresponding incidence rate is lower in females: 2.94 per 100,000 at 40-49 years and 104.99 per 100,000 at 70-79 years (4). For both sexes, incidence declines after age 80, with peak

incidence rates between 70-79 years (4). In addition, average age of onset is approximately 2 years earlier in men than women (11,12). Not only is PD more common in males than females, but the disease course also tends to be more severe in males (10–19). Specifically, women present more often with tremor-dominant PD, which is associated with milder motor deterioration and striatal degeneration (11). While the mechanisms underlying these sex differences are unclear, it has been hypothesized that higher estrogen in females leads to higher dopamine levels in the striatum, which protects against PD (11).

Clinical Symptoms

Motor Symptoms

Clinically, parkinsonism is primarily defined by six cardinal motor features: tremor at rest, bradykinesia, rigidity, loss of postural reflexes, flexed posture, and freezing (reviewed in Fahn, 2006). At least two features are required for diagnosis and at least one must be tremor at rest or bradykinesia.

- **Tremor at rest:** an involuntary tremor that occurs when muscles are relaxed, often seen as "pillrolling," which is a tremor of the hands and figures where the movements resemble rolling of pills in the hand
- **Bradykinesia:** slowness of movement, manifests as slow and smaller handwriting, decreased amplitude of arm swing and leg stride when walking, loss of facial expressions, and a softer voice

PD is one potential cause of parkinsonism. Clinically, three symptoms differentiate PD from other forms of parkinsonism:

- **Asymmetrical onset of symptoms:** In PD, symptoms begin on one side of the body and gradually progress to the other side; other forms of parkinsonism often present with onset of bilateral symptoms such as rigidity and bradykinesia.
- **Tremor at rest:** Although resting tremor may be absent in patients with PD, resting tremor is almost always absent in other forms of parkinsonism.
- **Substantial clinical response to adequate levodopa (L-DOPA) therapy:** Other forms of Parkinsonism that usually do not respond to L-DOPA therapy. In PD, resting tremor tends to be responsive to L-DOPA, while symptoms such as flexed posture, freezing, and the loss of postural reflexes are not L-DOPA responsive (20–22).

The presence of the clinical motor symptoms described above are sufficient for a clinical diagnosis; however, symptomology of PD is heterogeneous among patients, making clinical diagnosis challenging. As a result, conclusive diagnosis is only possible by postmortem confirmation of its pathological hallmarks.

Non-motor Symptoms

While the motor symptoms of PD are the most recognizable and are required for clinical diagnosis, many patients also experience non-motor symptoms, often starting decades before motor symptom onset and diagnosis (reviewed in (23–25)) (Figure 1.1). In addition, patients report that these non-motor symptoms have a greater negative impact on quality of life (24,26). In addition, these symptoms can be debilitating and lead to institutionalization that imposes a considerable economic burden on patients, their families and society (24,26). Many patients do not report these symptoms, either because they are embarrassed or unaware that they are related to PD (25,27). As such, these symptoms often go unrecognized and untreated.

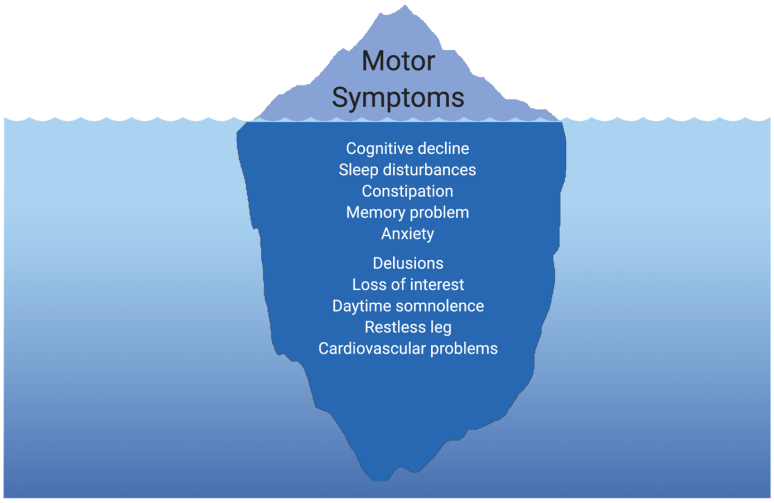

Figure 1.1: Non-motor symptoms of Parkinson's disease. PD patients experiences a diverse range of non-motor symptoms that often unreported and unrecognized by patients and clinicians. Non-motor symptoms include, but are not limited to, those listed on the hidden part of the iceberg.

PD-related non-motor symptoms include autonomic symptoms, sleep disturbances, psychological and cognitive symptoms, with gastrointestinal, urinary and sleep symptoms most commonly reported (Table 1.1). Gastrointestinal symptoms include difficulty swallowing (dysphagia), nausea, constipation, and bowel incontinence. Urinary tract dysfunction is also very common, with patients complaining of urinary urgency, and frequent urination at night. Many PD patients experience sleep disturbances including REM sleep behavior disorder, insomnia, restless leg syndrome, and daytime somnolence. Other less prevalent non-motor symptoms are the loss of sense of smell, neuropsychiatric symptoms and cognitive decline. Like motor symptoms, these non-motor symptoms are progressive and worsen in the later stages of disease (24,25).

Autonomic symptoms	Sleep symptoms	Neuropsychiatric symptoms	Other
GI dysfunction Urinary dysfunction Cardiovascular dysfunction Thermoregulatory dysfunction Sexual dysfunction	REM sleep behavior disorder Excessive daytime sleepiness	Anxiety Depression Cognitive impairment	Olfactory deficits

Table 1.1 Categories of common non-motor symptoms in PD.

Basal ganglia anatomy

The basal ganglia are a group of subcortical nuclei; dysfunction of this circuit is the primary driver of motor symptoms in PD. The structures that make up the basal ganglia include: the striatum (caudate and putamen; STR), the globus pallidus externus (GPe) and internus (GPi), the substantia nigra pars compacta (SNc) and pars reticulata (SNr), and the subthalamic nucleus (STN) (Figure 1.2).

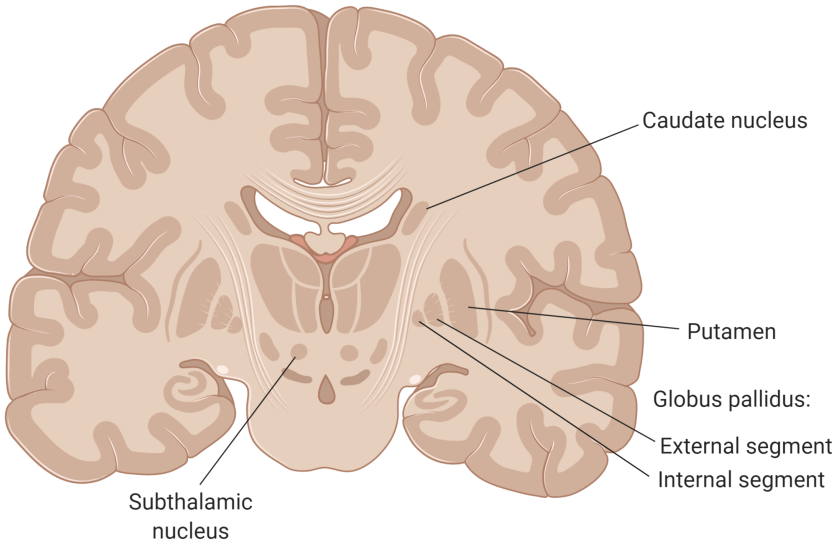

Figure 1.2: Basal ganglia circuitry. Modulation of movement in healthy individuals is controlled in the basal ganglia. This coronal section shows the subcortical nuclei that make up the basal ganglia: the striatum (caudate nucleus and putamen), globus pallidus, and the subthalamic nucleus. The substantia nigra pars compacta is not shown since it is found caudal to the section shown.

The STN and striatum are the primary input nuclei of the basal ganglia (Figure 1.3). The striatum receives input from sensorimotor, cognitive, and limbic cortical areas, excitatory input from thalamic nuclei, and dopaminergic input from the SNc and the ventral tegmental area. GABAergic neurons in the striatum project to the basal ganglia output nuclei, the GPi and SNr (direct pathway) and the GPe (indirect pathway). The STN also receives input from sensorimotor, cognitive, and limbic cortical regions, as well as indirect pathway inputs from the GPe. STN output is primarily glutamatergic to the basal ganglia output nuclei (SNr and GP).

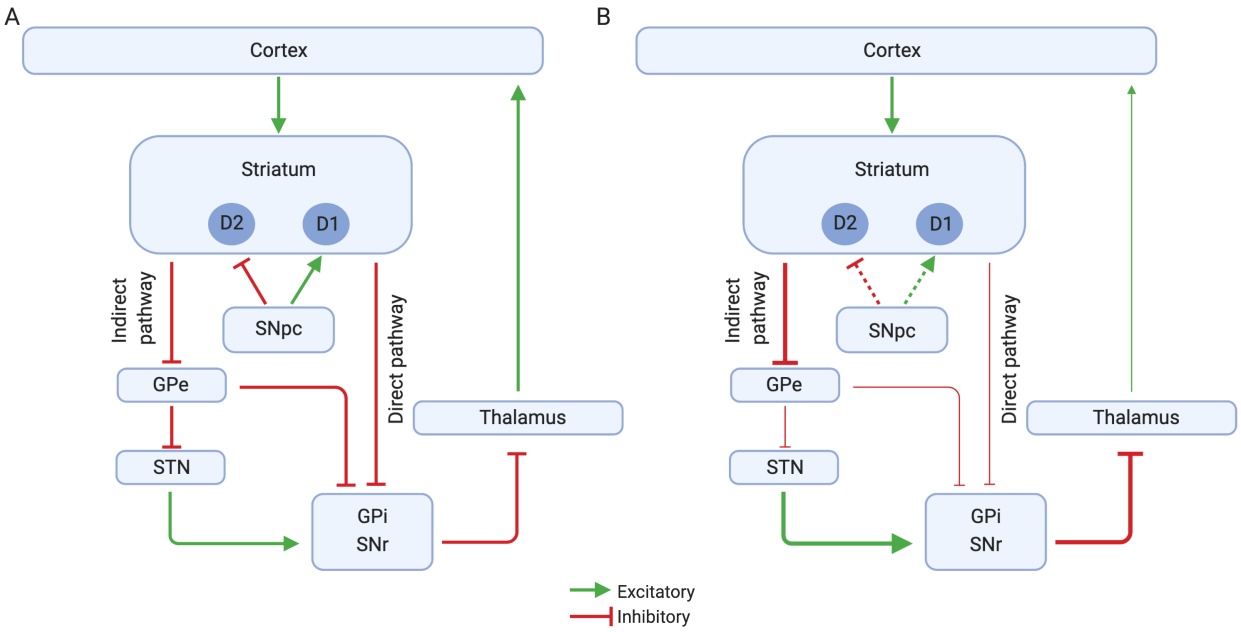

Figure 1.3: Basal ganglia circuits. A) In healthy individuals, voluntary movement is controlled by a balance between the direct and indirect pathways. Excitation of the direct pathway and inhibition of the indirect pathway lead to a net excitation of the motor cortex. B) In individuals with PD, degeneration of the nigrostriatal pathway (indicated as dotted lines) leads to an overall decrease in excitation of the motor cortex. Thickness of lines indicates level of activity compared to a health brain (A). GPe: Globus pallidus externa; GPi: Globus pallidus interna; STN: Subthalamic nucleus; SNpc: Substantia nigra pars compacta SNr: Substantia nigra reticulate; D1: D1 dopamine receptors; D2: D2 dopamine receptors.

Direct and indirect pathways

Striatal neurons in the direct pathway express D1 dopamine receptors, which depolarize the cell in response to dopaminergic signals from the SNc. In turn, output nuclei (GPi and SNr) receive inhibitory input from the GABAergic neurons of the striatum (Figure 1.3A) (28).

Striatal neurons in the indirect pathway express D2 dopamine receptors, which hyperpolarize the cell in response to dopaminergic signals from the SNc. The output nucleic (GPi and SNr) receive indirect excitatory input from the striatum via the GPe (inhibitory) and STN (excitatory) (28).

The GPi and SNr project inhibitory neurons to the thalamus, which then projects excitatory neurons back to the cortex. The net results of this circuit are that 1) the direct pathway has a net *excitatory* effect on the thalamic neurons that project to the cortex, exciting the cortex and 2) the indirect pathway has a net *inhibitory* effect on the thalamic neurons that project to the cortex, reducing excitation to the cortex. It is traditionally thought that this basal ganglia circuit controls movement through a balance between these two pathways (28).

Basal ganglia in PD

In healthy individuals, dopaminergic projections from the SNc to the striatum, known as the nigrostriatal pathway, modulate both the direct and indirect pathways (Figure 1.3A). In PD, this dopaminergic innervation of the striatum degenerates, leading to increased activity in the indirect pathway and decreased activity in the direct pathway. Overall, this leads to decreased excitation of the cortex by the thalamus, producing the motor phenotypes observed in PD (29) (Figure 1.3B).

Neuropathology

There are two pathological hallmarks required for a definitive PD diagnosis: the loss of dopaminergic neurons in the nigrostriatal pathway and the presence of Lewy bodies that contain α-synuclein (α-syn). As mentioned above, a definitive diagnosis of PD can only be confirmed postmortem by the presence of these two hallmarks.

Degeneration of the nigrostriatal pathway

Degeneration of the nigrostriatal pathway and the resulting dysregulation of the basal ganglia circuitry are thought to be responsible for the motor symptoms of PD, while extranigral pathology is thought to underly the majority of non-motor symptoms. This degeneration leads to reduced cortical excitation by the thalamus resulting in reduced movement. Generally, by the time motor symptoms appear and patients receive a diagnosis, there is greater than 60% reduction in striatal dopamine and a 50% loss of nigrostriatal dopamine neuron cell bodies (30,31). The loss of striatal innervation precedes nigral neuronal loss with early striatal dysfunction leading to a retrograde degeneration of nigrostriatal axons and eventual loss of the cell bodies in the SNc (31).

Lewy bodies

Lewy bodies were first described and named after Friedrich H. Lewy in 1912 (32). Lewy bodies are intracellular proteinaceous inclusions that are found in both axons (Lewy neurites) and the cell bodies of the surviving neurons by postmortem analysis. They are found in both the central and peripheral nervous systems of PD patients. In the central nervous system, they are found in many regions, including the substantia nigra, nucleus basalis of Meynert, cortex, and dorsal vagal nucleus and the spinal cord (33). In the peripheral nervous system, Lewy bodies

have been observed in the enteric nervous system, gastrointestinal system, sympathetic ganglia, sciatic nerve and the vagus nerves (34–36).

In 2003, Braak described the temporal and regional distribution of Lewy pathology in PD. It is generally accepted that the earliest lesions develop in non-nigral sites including the vagus nerve, olfactory bulb and, possibly, the enteric nervous system (37). As the disease progresses, pathology develops in an ascending manner to the brain stem and midbrain. In later stages of the disease, pathology develops in the limbic and neocortical regions (38,39). However, how this pattern of pathology arises remains an open question. Braak and colleagues have proposed that, once the aggregates are formed, they are capable of propagating trans-synaptically from nerve cell to nerve cell in a virtually self-promoting pathological process (40). A competing hypothesis known as the threshold theory posits that there is parallel degeneration of both central nervous system and peripheral nervous systems in PD and that the functional threshold varies between systems. According to this hypothesis, regions with lower thresholds underly the emergence of early symptoms, whereas regions with higher thresholds produce the classical motor symptoms of PD that appear later in disease (41).

Alpha synuclein

α-synuclein (α-syn), a small, natively unfolded 140 amino acid protein, is the major protein component of Lewy bodies (42). It is abundantly expressed throughout the brain, with highest expression levels in the neocortex, hippocampus, substantia nigra, thalamus and cerebellum. α-syn represents about 1% of all protein in the neuronal cytosol and is primarily localized to presynaptic terminals (43).

α-syn is a natively unfolded, intrinsically disordered protein that shows dynamic changes in confirmation depending on the environment (44). Such proteins are characterized by lack of a tertiary structure (45). α-syn, like other natively unfolded proteins, requires the presence of molecular interaction partners in order to take on a specific tertiary confirmation (34,45,46). For example, in the presence of acidic lipid membranes, or with membranes with high curvature, the N-terminus of the protein folds into an alpha-helix structure that interacts with membranes (47–52).

α-syn can also interact with itself to form multimers (53). α-syn fibrillization requires formation of protofibrils of highly organized secondary structure (54). These protofibrils form as intermediates in the fibrilization process and the resulting α-syn fibrils form the primary structural component of Lewy bodies (55). Presumably, this process presumably starts with a conformational shift of the monomeric protein, followed by the step-wise formation of larger multimeric protein species from monomers to oligomers to protofibrils to fibrils (56). X-ray diffraction analysis of α-syn fibrils show the characteristic pattern of a β-sheet structure such that the β strands lie perpendicular to the long fiber axis similar to amyloid fibrils (57). The kinetics of α-synuclein aggregation exhibit an initial lag, followed by an exponential growth period, followed by a leveling off as fibril formation comes to a halt (58).

Evidence suggests that soluble oligomeric/protofibrillar aggregates are the most neurotoxic forms of α-syn. Such species may potentiate pathology by acting as seeds for the formation of additional aggregates (56). When α-syn is mutated, very highly expressed (e.g. genomic duplication or triplication), or under conditions of oxidative stress, α-syn self-assembly increases, resulting in a formation of insoluble α-syn aggregates (34,57,59,60).

Other components of Lewy bodies

While α-syn is the primary component of Lewy bodies, many additional components have been identified (33). These include, but are not limited to, structural proteins like neurofilament, α-syn binding proteins, synphilin-1-binding proteins, components of the ubiquitin-proteasome system, cell cycle proteins, proteins associated with phosphorylation, cytochrome-c, tau, tubulin and lipids (33,61,62). A recent study identified vesicular structures and dysmorphic organelles, including mitochondria, within Lewy bodies (63).

Etiology of PD

An estimated 5-10% of PD cases are caused by inherited monogenic mutations, and the etiology of the remaining sporadic cases involves a combination of genetic and environmental factors. Age is the primary risk factor for PD, with incidence and prevalence increasing with age.

Genetics

Familial forms of PD are cause by highly penetrant, rare mutations that follow Mendelian inheritance patterns. In contrast, the majority (>90%) of cases are caused by the combination and interaction of common genetic polymorphisms with weak to moderate effect sizes and environmental exposures. Thus, there is a range of genetic variants underlying PD etiology from common polymorphisms with modest effects to rare highly penetrant variants (64). Known familial PD genes are summarized in Table 1.2; for the purposes of this dissertation, we discuss only the genes that are most commonly mutated in familial PD.

Gene	Inheritance pattern	Frequency	Phenotype
SNCA	Autosomal dominant	Very rare	Early onset
LRRK2	Autosomal dominant	Most common Highly penetrant	Classical PD
VPS35	Autosomal dominant	Very rare	Classical PD
POLG	Autosomal dominant	Rare	Atypical PD
DNAJC13	Autosomal dominant	Unknown	Unknown
UCHL1	Autosomal dominant	Unknown	Unknown
HTRA2	Autosomal dominant	Unknown	Unknown
PRKN	Autosomal recessive	Rare	Often early onset
DJ-1	Autosomal recessive	Very rare	Unknown
PINK1	Autosomal recessive	Rare	Often early onset
DNAJC6	Autosomal recessive	Unclear	Unknown
ATP13A2	Autosomal recessive	Unclear	Atypical PD
FBXO7	Autosomal recessive	Very rare	Often early onset
PLA2G6	Autosomal recessive	Rare	Often early onset
DNAJC6	Autosomal recessive	Very rare	Often early onset
SYNJ1	Autosomal recessive	Very rare	Often atypical PD
GIGYF2	Unclear	Unknown	Unknown
GBA	Autosomal dominant	Incomplete penetrance	Unknown
EIF4G1	Unclear	Unknown	Unknown
TMEM230	Unclear	Unknown	Unknown
VPS13C	Autosomal recessive	Rare	Unknown
LRP10	Autosomal dominant	Unknown	Unknown
GCH1	Unclear	Unknown	Unknown
CHCHD2	Unclear	Unknown	Unknown
Hsp40	Unclear	Unknown	Unknown

Table 1.2: Familial PD genes. Modified from Blauwendraat et al., 2019 (65)

Familial PD

Autosomal dominant PD genes: SNCA, LRRK2, VPS35

SNCA, which encodes α-syn, was the first gene to be associated with inherited PD (66). Missense mutations (A53T, A30P, E46K, and G51D) in *SNCA*, as well as duplications and triplications of *SNCA*, cause autosomal dominant forms of PD (Table 1.2) (5,66–71). These mutations in *SNCA* tend to cause early onset forms of the disease. Many of these missense

mutations are thought to increase the propensity of α-syn to form fibrils and aggregate, and multiplications of the gene lead to higher α-syn protein levels, which are also thought to increase the fibrilization and aggregation (59,72,73). Familial cases of PD caused by these mutations in *SNCA* are quite rare.

Missense mutations in *LRRK2* (leucine-rich repeat kinase 2) are the most commonly mutated gene in familial PD (74,75). *LRRK2* mutations lead to toxic gain of function and have autosomal dominant inheritance leading to classical PD (Reviewed in Blauwendraat, Nalls, & Singleton, 2019).

The VPS35 gene encodes for vacuolar protein sorting associated protein 35 that is a component of a multimeric protein complex involved in retrograde transport of proteins from endosomes to the trans-Golgi network. Missense mutations in *VSP35* cause loss of function of the protein that leads to classical PD in an autosomal dominant pattern (76).

Autosomal recessive PD genes: Parkin, DJ-1, PINK1

Mutations in these genes, and other autosomal recessive genes listed in Table 1.2, are relatively rare in the general population but are responsible for a substantial proportion of early onset PD (77). The most commonly mutated autosomal recessive PD gene is *PRKN*, which encodes Parkin, an E3 ubiquitin ligase (78) (65). Disease-linked mutations in *PRKN* include missense and loss of function mutations (65). *PINK1* encodes a mitochondrial serine/threonine kinase and PD-linked missense mutations lead to loss of function (65). Missense mutations in *DJ-1* also lead to early onset PD through a loss of function of the protein deglycase DJ-1, which has chaperone activity and can inhibit α-syn aggregation under oxidative conditions (65,79).

Mutations in *PRKN, PINK1* and *DJ-1* often result in early onset PD (65). Exon rearrangements in *PINK1* and DJ-1 genes are also responsible for some cases of autosomal recessive PD (80,81).

Sporadic PD

The genes discussed in the above section account for less than 10% of PD cases; the remaining cases are thought to arise from a combination of multiple genetic and environmental risk factors acting together. The vast majority of PD is genetically complex, i.e. it is caused by the combined action of common genetic variants in concert with environmental factors. Candidate gene studies and genome-wide association studies have identified many common single nucleotide polymorphisms (SNP) that are associated with increased risk of PD.

The biggest genetic risk factor for sporadic PD is mutation of *GBA*, a gene that encodes β-glucocerebrosidase, a lysosomal enzyme. Results of a large multicenter study of more than 5000 patients with PD and an equal number of matched controls showed an odds ratio greater than 5 for any *GBA* mutation in Parkinson's disease patients versus controls (5,82).

In the most recent and largest GWAS in the field, 7.8 million SNPs were analyzed in 37,688 cases, 18,618 proxy-cases, and 1.4 million controls. This study identified 90 independent genome-wide significant risk signals across 78 genomic regions, including 38 novel independent risk signals in 37 loci (83). *SNCA* was one of the top hits and some of the other top hits include *HLA-DQB1, MCC1, TMEM175*, and *VPS13C* (64,83,84). Similar to other genetically complex diseases, on their own, these show only moderate associations with PD risk. Increasing this etiologic complexity, many of the involved genetic and environmental risk factors likely interact with each other in a complex manner (85).

Gene-environment interactions

Despite considerable evidence for a large environmental component to PD risk (see Section 0 below), to date, only two studies of gene-environment (GxE) interactions have been published. Both used the same dataset, which was derived from a relatively small clinic-based convenience sample of 1500 cases and 900 controls. The first genome-wide interaction analysis reported for this sample cohort highlighted a potential genome-wide significant interaction of coffee consumption and SNP rs4998386 in GRIN2A (glutamate ionotropic receptor NMDA type subunit 2A) (86). The other GxE analysis reported a suggestive result for an association between 2 SNPs upstream of the *SV2C* (synaptic vesicle protein 2C) gene and smoking history (87). These findings have been difficult to replicate in other populations for two reasons: 1) a lack of exposure data in large cohorts and 2) GxE studies require larger cohorts to achieve adequate statistical power. In order to generate robust and replicable results for GxE interactions, specific population-based datasets of sufficient size with exposure data must be complied to detect or refute GxE effects on a genome-wide scale (reviewed in (64)).

Environmental factors

Epidemiology

Epidemiological studies have shown that environmental factors are associated with PD risk. However, many of these studies suffer from high heterogeneity, signal bias and other issues that make it difficult to infer causation (88). Fortunately, a recent umbrella review by Bellou and colleagues assessed a wide-range of epidemiological meta-analyses to determine the strength of the evidence for these environmental risk factors and PD, summarized below

(88). Relevant to this dissertation, effects of risk factors and protective factors differ between males and females (89).

Protective exposures

- Epidemiological studies have consistently suggested an association between alcohol intake, coffee consumption and smoking and decreased risk of PD (88,90,91).
- Physical activity has also been associated with a decreased risk of PD with convincing statistical evidence for this association compared to other factors (88,92).
- Studies also suggest an association between both dietary consumption of dairy products and vitamin E intake, and decreased PD risk but these studies are also only suggestive (88,93,94).

Environmental risk factors

Many exposures to toxic environmental chemicals have been studied for an association with PD risk. In the umbrella review by Bellou and colleagues, rural living, farming, well-water drinking, welding, and exposure to hydrocarbons, organic solvents, and pesticides all showed suggestive evidence for as association with increased risk of PD (91,95–98).

While epidemiological studies alone cannot inform us about causation, they can shed light on which factors affect PD risk. In the context of environmental risk factors, when epidemiological evidence is combined with postmortem, mechanistic and *in vivo* studies, a role for specific toxic compounds emerges.

Persistent organic pollutants

For the environmental risk factors described above, a common thread is exposure to a group of compounds known as persistent organic pollutants (POPs). POPs have low volatility, are highly lipophilic, and are resistant to degradation, causing them to persist in the environment. Due to these properties, they also tend to accumulate in fatty tissues of the body. POPs include certain types of pesticides and industrial toxicants. Manufacture and use of many POPs been phased out, but their effects linger due to their persistence. In addition, some POPs are still commonly used, like PFAS (per- and polyfluoroalkyl substances). There is an extensive body of literature from epidemiological, postmortem, in vitro and in vivo studies suggesting an association between exposure to POPs and an increased risk of PD (99–115). Of note, these compounds are not thought to explicitly cause PD on their own; instead, they facilitate the pathogenesis of PD through interactions with other genetic or environmental factors (reviewed in (108)).

Industrial toxicants and PD

Industrial toxicants are a broad and diverse class of compounds that are utilized in the manufacture and production of commercial and household products. Exposure occurs mainly in occupational settings, but also via contaminated water or their presence in everyday household products. Specific industrial compounds, such as halogenated POPs (polychlorinated biphenyls and polybrominated biphenyls), trichloroethylene, and heavy metals, have been associated with increased risk of PD (103,116–118).

Pesticides and PD

A large body of epidemiological literature exists concerning pesticides and PD including case reports, descriptive studies, cohort studies, and case control studies (99,101–105,107–115,119,120). As discussed above, there are several other risk factors related to pesticide exposure that are also associated with increased risk of PD, such as rural living, well-water consumption, and farming, raising a question of whether pesticides are causally linked to PD or simply confounded with other environmental factors. In support of a direct link between pesticides and PD, longer durations of exposure to pesticides are associated with a greater increase in risk of PD (119). Unfortunately, due to limitations in study design, most studies are not able to determine on their own if these environmental factors are independent risk factors or simply correlated with pesticide exposure (100). As such, while the overall weight of epidemiological evidence is sufficient to conclude that a generic association between pesticide exposure and PD exists, it is insufficient to conclude that this is a casual relationship or that such a relationship exists for any particular compound (119).

Pesticides that are also POPs are of particular concern due to their tendency to accumulate in fatty tissues, including the brain. Organochlorine pesticides (OCs) are a particular class of POPs that were heavily used during the 1950s-1970s in food and non-food crops such as corn, wheat, and tobacco. Despite being phased out in the US starting in the late 1970s, exposure to organochlorine pesticides is a continuing concern, especially for the aging population who was exposed prior the phase-out (111). OCs are acutely toxic at high doses, but most human exposure is not acute. Rather, exposure is chronic and at much lower doses, with the primary route of exposure through food.

Growing data support a role for OCs in increasing the risk of PD, including a recent family-based case-control study that demonstrated such association (111,121).This association between OCs and increased risk of PD is largely driven by a class of compounds called cyclodienes, likely due to their effects on the dopaminergic system (111,122). Aldrin and its metabolite dieldrin are cyclodienes that have been specifically implicated in PD etiology through a combination of epidemiological, *in vitro* and *in vivo* studies (111,120,123–127). It is thought that these compounds increase PD risk through their action at the dopamine synapse, primarily through disruption of DA neurotransmission and packaging of DA.

Synaptic and vesicular integrity in PD

The dopamine synapse

The central synapse that degenerates in PD is the synapse of nigral DA neurons onto medium spiny neurons on the striatum. Within the cytosol of dopaminergic neurons, dopamine is synthesized from the amino acid tyrosine by tyrosine hydroxylase (TH) to produce L-DOPA; this is the rate limiting step in DA synthesis. L-DOPA is then rapidly converted to DA by DOPA decarboxylase. After the synthesis of DA, it is rapidly transported into synaptic vesicles by the type II vesicular monoamine transporter (VMAT2) for subsequent release into the synaptic cleft (Figure 1.4). This vesicular packaging serves two functions: 1) to package dopamine within the vesicle for subsequent release into the synaptic cleft and 2) to protect the cell from cytosolic DA.

For DA release, in response to an action potential and resulting calcium influx, dopaminergic vesicles fuse to the plasma membrane and the release their contents into the synaptic cleft (Figure 1.4). Upon release from synaptic vesicles, DA binds to the postsynaptic DA

receptor to exert its biological function. DA activity at the synapse is terminated through metabolism by catechol-O-methyltransferase (COMT) and monoamine oxidase (MAO) and by reuptake into the presynaptic neuron by DAT (Figure 1.4). DA that has been taken up in the terminal is then repackaged into synaptic vesicles by VMAT2, completing the cycle. Synaptic vesicles are essential for neurotransmission; when their function is disrupted, neurotransmitter release is decreased.

The second function of vesicular packaging in DA neurons is to prevent oxidation of cytosolic DA (Figure 1.4) (128). Under normal conditions, low levels of DA are present in the cytosol following synthesis from DOPA, plasmalemmal transport by the DAT, and vesicular leak. Cytosolic DA is metabolized by enzymatic deamination or broken down by autoxidation, producing reactive, harmful products. When cytoplasmic DA increases due to faulty vesicular DA packaging, this creates oxidative stress leading to toxicity (128). In fact, altered expression of transporter proteins may produce a state in which the ratio of DAT:VMAT2 is increased. This in turn causes insufficient packaging of DA into vesicles, leading to increased levels of cytosolic DA and oxidative stress within the neuron. Therefore an increased ratio of DAT:VMAT2 is thought to render neurons more susceptible to damage (129).

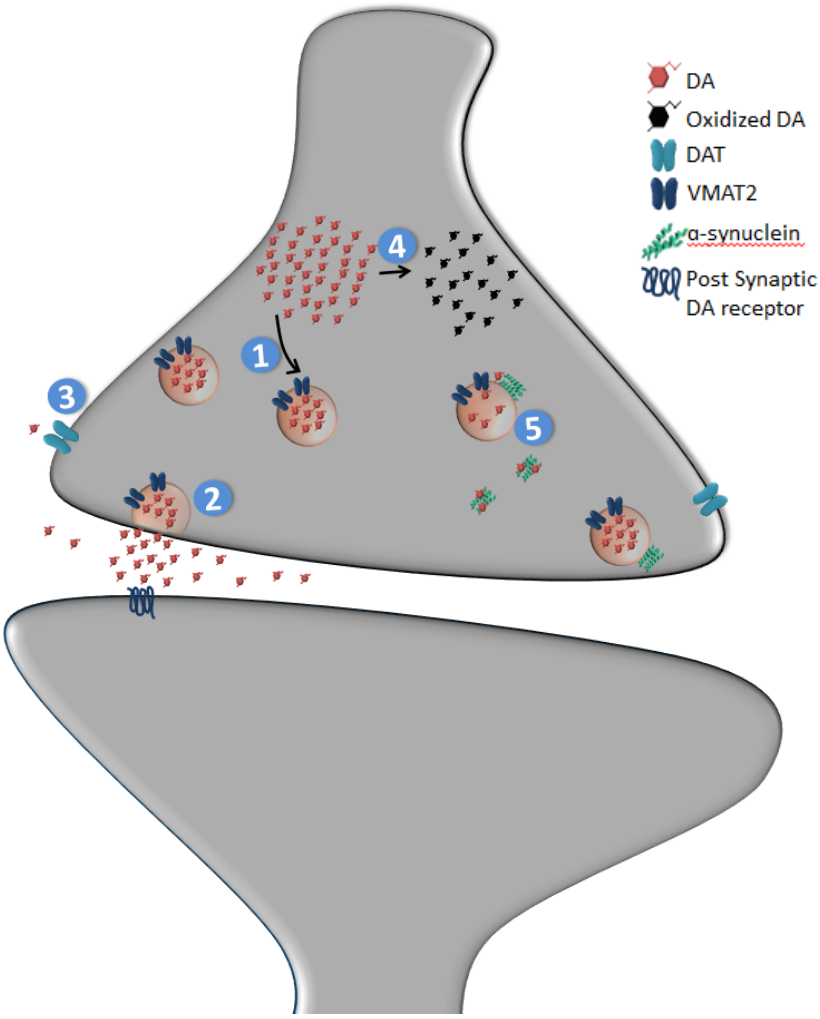

Figure 1.4 Dopaminergic synaptic terminal. 1) DA is transported into vesicles by VMAT2 and stored in vesicles 2) DA vesicles fuse to plasma membrane and release their content 3) DA is taken back into the cell via DA transporter, DAT 4) If not stored in vesicles, cytoplasmic DA is prone to oxidation 5) α-syn interacts with vesicles and DA at the presynaptic terminal

Role of α-syn at the synapse

α-syn is a predominantly neuronal protein that plays an important role in a wide range of cellular functions, such as regulation of synaptic transmission, mitochondrial homeostasis, gene expression, protein phosphorylation, and fatty acid binding (34). Within the presynaptic terminal, α-syn is known to interact with synaptic vesicles. Thus, one of the endogenous functions of α-syn may be to regulate vesicular trafficking, docking and endocytosis

(34,128,130–134) . Furthermore, monomeric α-syn has been shown to reversibly bind and interact with vesicle membranes (47). α-syn also regulates the size of the recycling pool for DA as observed in cultured hippocampal neurons (135). In line with these observations, α-syn null mice show decreased DA stores (136).

α-syn interacts with virtually every major protein involved in DA biosynthesis and handling (34), including the rate limiting enzyme of DA synthesis, TH. α-syn inhibits TH activity by decreasing TH phosphorylation or by altering interactions between TH and its binding proteins (34,137–142). In a rat model of viral α-syn overexpression, TH expression was reduced, suggesting that α-syn also regulates TH expression (143). Furthermore, α-syn increases the amount of VMAT2 on vesicles, interacts with and modulates activity of DAT, and increases DAT insertion into the presynaptic membrane (144–149).

α-syn-DA cycle

Maintenance of the integrity of the synapse and the vesicles within it are critical to the function and health of dopamine neurons; disruption of the synapse is thought to be integral part of PD etiology (128,150). In dopaminergic neurons, decreased sequestration of transmitter into vesicles leads to increased cytoplasmic DA levels, thereby leading to oxidative stress mediated by excessive auto-oxidation and enzymatic deamination of DA (128).

Given the critical functions of α-syn in maintaining proper vesicular and synaptic function, it is easy to envision how dysfunction of α-syn would lead to disturbances to dopaminergic homeostasis. Moreover, as handling of dopamine is affected, there is additional oxidative stress on the neurons and oxidative damage to α-syn. It is increasingly evident that

combined actions of cytosolic DA and α-syn form a toxic and self-reinforcing cycle of neurotoxicity- leading to DA neuronal dysfunction and eventual cell death (Figure 1.5).

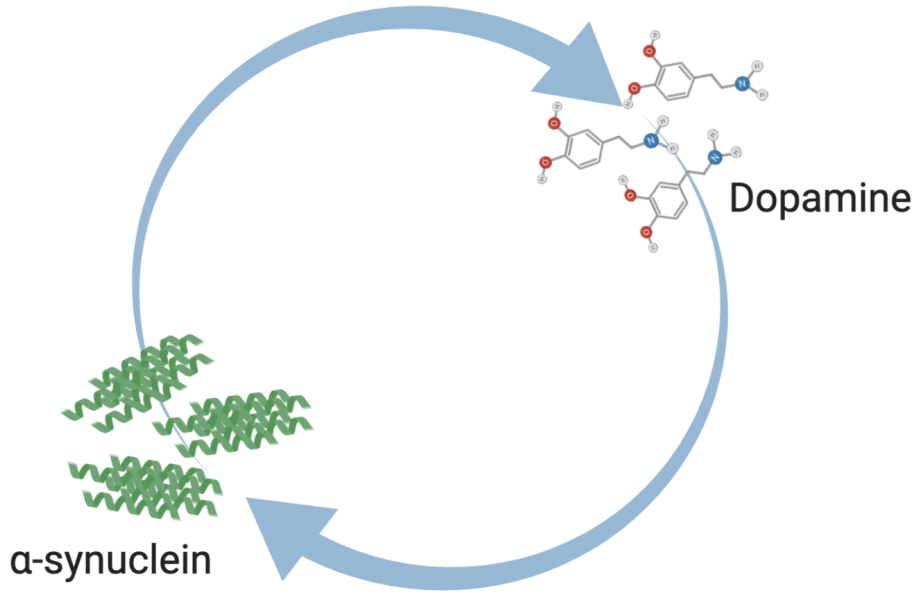

Figure 1.5 Cycle of neurotoxicity

Disruption of proper DA handling and the resulting increase in cytosolic DA and toxic DA byproducts can contribute to α-syn pathology supporting the idea that mishandling of DA can directly affect α-syn aggregation and induce-PD like pathology (128,151–156). In addition, evidence from variety of model systems indicates that one of the endogenous functions of α-syn is to regulate DA homeostasis and release at multiple levels, including biosynthesis and homeostasis, vesicle fusion and release, and trafficking of vesicles between pools, suggesting that disruption of α-syn can disrupt DA turnover, vesicular sequestration, and DA transmission, contributing to this toxic cycle(157–159). Moreover, oxidized DA covalently binds α-syn and stabilizes the protofibril intermediates (160). α-syn protofibrils permeabilize vesicle

membranes, leading to leakage of vesicular DA into the cytoplasm and disruption of the electrochemical gradient through the vesicular membrane (161). Further supporting the role of α-syn in dopamine-related neurotoxicity, rats overexpressing α-syn have reduced dopamine vesicle density and reduced motor activity (162).

Disease models

Many animal models have been developed in an attempt to elucidate the mechanisms of PD pathogenesis. Genetic-based approaches to model Parkinson's disease include transgenic models and viral vector-mediated models targeting genes linked to monogenic Parkinson's disease, including *SNCA, LRRK2, UCH-L1, PRKN, PINK1*, and *DJ-1*, as well as manipulation of dopaminergic transcription factors. Because of the prominent role that α-syn plays in PD pathology, many α-syn-based mouse models have also been developed (reviewed in (34)). Each of these existing models mimic some aspect of the disease but few show α-syn pathology, nigrostriatal degeneration AND motor deficits; even fewer recapitulate non-motor deficits. One transgenic model that successfully recapitulates many of the key aspects of Parkinson's disease is a mouse model that expresses ~5% of normal VMAT2 levels (VMAT2 LO). VMAT2LO mice display age-associated nigrostriatal dopamine degeneration, increased accumulation of α-syn, and progressive non-motor and L-DOPA-responsive motor deficits (151). In this project, we aim to investigate the imprinted effects of dieldrin exposure developmentally on α-syn; therefore, α-syn genetic models are unlikely to be useful for this question.

In addition to genetic models, toxicant models that induce dopaminergic loss and degeneration have been developed to model PD. Classic toxicant models include: 6-hydroxydopamine (6-OHDA), 1-methyl-4-phenyl-1,2,3,6-tetrahydropyridine (MPTP), rotenone,

and paraquat (reviewed in (163)). 6-OHDA is a metabolite of DA that has been used to model aspects of PD. In this model, 6-OHDA is administered via stereotactic injection into the brain, typically into the striatum or medial forebrain bundle. Since it shares structural similarities to DA, 6-OHDA can be taken up by dopaminergic neurons and induce oxidative damage and eventual degeneration of the nigrostriatal pathway (164). When administered by unilateral stereotactic injection into the striatum or median forebrain bundle, 6-OHDA typically produces unilateral degeneration of the nigrostriatal DA neurons, causing dyskinetic limb movements on the affected site and quantifiable circling motor abnormality in animals where DA-releasing compounds such as amphetamine induces asymmetrical rotation (165).

MPTP (1-methyl-4-phenyl-1,2,3,6-tetrahydropyridine) is a prodrug of the neurotoxin MPP^+ (1-methyl-4-phenylpyridinium). MPTP is not toxic itself but is a lipophilic compound that can cross the blood brain barrier. Once inside the brain, MPTP is converted by astrocytes to its toxic metabolite, MPP^+, which is then transported into dopaminergic neurons by the dopamine transporter (DAT). MPP^+ is thought to kill dopaminergic cells by inhibiting ATP production and stimulating superoxide radical formation (166). In animal models, MPTP is given by a number of different routes, including oral gavage and stereotaxic injection into the brain. Dosing paradigms vary by dose, duration and frequency of administration. The most common, reliable and reproducible lesion is caused by its systemic sub-cutaneous or intraperitoneal administration (167).

Rotenone is a commonly used insecticide and piscicide. Rotenone is a mitochondrial complex I inhibitor that easily gains access to brain where it impairs the oxidative phosphorylation in mitochondria. Chronic systemic administration of rotenone causes selective

degeneration of nigral dopaminergic neurons with histopathological hallmarks of PD and PD-like locomotor symptoms in animal models (168).

Paraquat is potent herbicide that has been developed into a PD model based on structural similarity to rotenone. Paraquat toxicity is mediated by redox cycling with cellular diaphorase yielding reactive oxygen species. Inconsistent results have been obtained with paraquat toxicity in mice when it is administered systemically, but direct injection into the brain produces more consistent toxicity (reviewed in (169)). While injection of a strong oxidant directly into nigral neurons will damage those neurons, whether or not this model is toxicologically relevant or not to human PD remains controversial (169).

While these neurotoxicant models do lead to DA depletion and nigrostratial degeneration, they have two major limitations as disease models: 1) they fail to mimic the protracted course of PD and 2) most do not reproduce the α-syn pathology. While there is evidence for α-syn aggregation after chronic administration of MPTP, rotenone, and paraquat, this may be due to supraphysiological levels of oxidative stress produced by administration of these toxicants rather than reflecting the real-life progression of the α-syn pathology. Thus, for questions relating to the consequences of DA loss, these models can be appropriate, but they are unlikely to be useful for questions about how environmental exposures affect the pathogenesis of sporadic PD.

Dieldrin toxicity

Dieldrin is an organochlorine pesticide that has been associated with increased risk of PD in epidemiological and post-mortem studies. (111,120,123,124,126,127,170) (See above:

Pesticides and PD). Mechanistic studies also support a role for this compound in the etiology of sporadic PD.

Dieldrin: in vitro cell culture studies

The direct effects of dieldrin on cells have been studied using a variety of cell lines and suggest that at sufficiently high concentrations, dieldrin can have a direct toxic effect on dopaminergic neurons. In PC12 cells, dieldrin (30–1000 μM) alters the mitochondrial membrane potential and induces cytochrome-c release. This dieldrin-induced cytochrome-c release is attenuated by pretreatment with a reactive oxygen species (ROS) scavenger, MnTBAP, indicating that ROS is an initiator of cytochrome-c release in dieldrin-induced neurotoxicity in PC12 cells (171). Similarly, dieldrin (40 μM) induces ROS production in SN4741, a mouse nigral mesencephalic cell line, and N27 cells, a rat dopaminergic neural cell line (123,172,173). In N27 cells, dieldrin (3 to 70 μM) can also alter the ubiquitin-proteasome system by decreasing proteasomal activity in a dose-dependent manner; this effect is more pronounced in cells overexpressing α-syn (174). In primary mesencephalic cultures from fetal rat brain, dieldrin (0.01 to 100 μM) causes a dose-dependent decrease in the number of TH immunoreactive cells, with non-TH cells susceptible only at higher concentrations of dieldrin (175). While these studies clearly demonstrate that direct dieldrin exposure is toxic to dopaminergic cells, it is unclear if the concentrations used are relevant to concentrations found in human brain tissue.

Dieldrin: in vivo studies

In vivo studies also provide evidence for dieldrin-induced toxicity to the dopaminergic system in many species. In birds and rodents (ring doves, ducks and rats), chronic low doses of

dieldrin by ingestion significantly deplete brain levels of DA and norepinephrine (176–178). In mice, adult exposure to dieldrin (1mg/kg and 3mg/kg) via intraperitoneal injections for 30 days produces increased oxidative stress and α-syn expression in the striatum and decreases striatal DAT levels and function, in the absence of degeneration of nigral DA neurons (179).

Developmental dieldrin exposure model

In this dissertation, we have used a developmental exposure paradigm designed to mimic human exposures at a critical developmental period to similar body burden in an animal model, male pups developmentally exposed to dieldrin show an increased susceptibility later in life to the dopaminergic toxicant, MPTP (129). In this paradigm, female mice were fed dieldrin (0.3, 1 or 3 mg/kg/day) in a corn oil/peanut butter vehicle every 3 days. Feeding continued throughout mating, pregnancy, and, and lactation, until pups are weaned (Figure 1.6).

We used a developmental dieldrin exposure model that is based on the developmental origins of health and disease (DOHaD) hypothesis(129,180). This hypothesis posits that environmental exposures such as chemicals, diet, and pesticides during critical periods of development can alter disease risk late in life (180). In particular, evidence suggests that exposures during the prenatal and perinatal period can increase or decrease the risk of a disease throughout the life course (Figure 1.7) (181). Although PD is a disease of the aged, the neurodegenerative process begins long before clinical diagnosis, and early life exposures during critical periods of development may contribute to sporadic PD. For example, prenatal and perinatal exposures may cause persistent changes in the dopaminergic system that produces a "silent neurotoxicity"; they do not cause overt dysfunction on their own, but instead increase vulnerability to future parkinsonian insults (129,182).

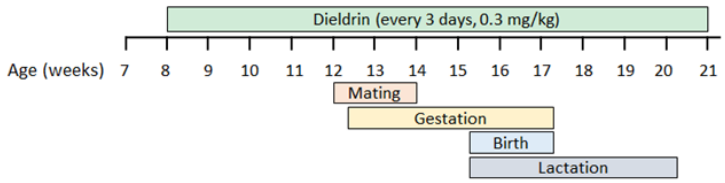

Figure 1.6 Developmental dieldrin exposure paradigm

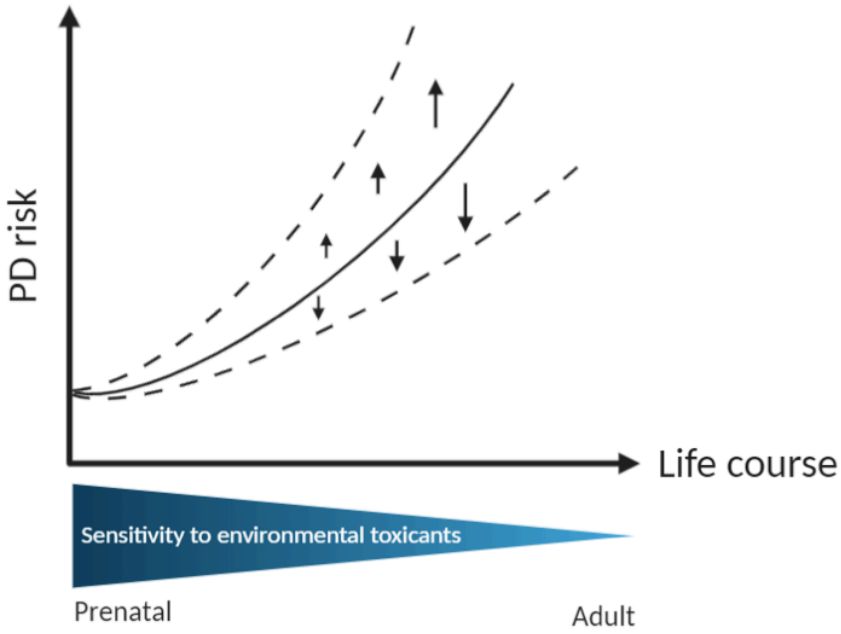

Figure 1.7 Developmental origins of health and disease

In a previous study, pups were assessed at 12 weeks of age for the effects of developmental dieldrin exposure on the dopaminergic system(129). Both male and female pups showed a dose-dependent increase in DAT and VMAT2 expression. In male pups specifically, at all doses tested, these changes in expression produced an increase in the DAT to VMAT2 ratio and a corresponding increase in DA turnover (measured as the ratio of the DA metabolite DOPAC to DA). Such increase in DAT: VMAT2 ratio is important as when the DAT increases to a further degree and exceeds that VMAT2, DA is taken up from the synaptic cleft into the cytosol yet, but cannot get packaged into vesicles as fast by the VMAT 2 (Figure 1.4). This leads to

cytosolic free DA that is susceptible to being oxidized, potentially rendering the neuron more vulnerable to subsequent insults. In this same previous study, at 12 weeks of age, pups were exposed to MPTP to assess susceptibility to dopaminergic toxicants. Reflecting the male-specific effect on DA packaging, at all dieldrin doses tested, male pups developmentally exposed to dieldrin were more susceptible to MPTP toxicity, as measured by striatal DA loss, than vehicle exposed controls(129). Male pups also showed increased MPTP-induced expression in GFAP and α-syn. To elucidate the possible mechanisms for the increase in DAT and VMAT2, this study also assessed the levels of a transcription factor called NURR1 that is known to regulate DAT and VMAT2 expression during development. NURR1 mRNA levels were found to be increased in both male and female offspring, but the increase was more prominent in males (129). However, dieldrin was only detectable by mass spec in the striatum of pups at 12 weeks of age at the highest doses tested; levels were not tested at earlier time points. As a result, from this study, it remains unclear if the effects of developmental exposure are the result of direct or indirect dieldrin exposure on the developing brain.

Since MPTP toxicity depends on the function of DAT and VMAT2 to bring the toxic metabolite MPP^+ to the site of toxic action, the authors assessed striatal MPP^+ levels and found similar levels of MPP^+ in the striatum of male and female pups. However, this does not provide information on whether MPP^+ is the cytosol, where it can carry out its toxic action, or in vesicles, where it is sequestered from its site of toxic action (183). Thus, it is possible that this effect is specific to MPTP due to its dependence on DAT and VMAT2. The experiments conducted in this dissertation project aim to address this issue by testing if this developmental

dieldrin exposure paradigm alters susceptibility of dopaminergic neurons to parkinsonian toxicity in models not dependent on DAT and VMAT2.

The exact mechanism by which dieldrin exposure damages PD-relevant cells and circuits is not clear. The primary mechanism of dieldrin toxicity is through inhibition of chloride ion flux through $GABA_A$ receptors (184). $GABA_A$ receptors are an important part of the basal ganglia circuitry (Figure 1.3) as many basal ganglia synapses are GABAergic (all output from GPe, striatum to GP, and output from GPi and SN to thalamus). Specifically, the γ2 subunit of $GABA_A$ receptor is highly expressed in dopamine neurons in the SNpc (185). In addition, GABA acts a trophic signal in the development of dopaminergic system (and other monoaminergic systems). (186)

It has been proposed that inhibition of chloride flux in the dopamine neurons of SNpc causes increased neuronal activity and burst firing of dopamine neurons (Figure 1.8) (129,184–190). This net increase in neuronal activity could modify the dopamine system through persistent changes in epigenetic mechanisms, leading to dysregulation of genes important for dopamine neuron development and maintenance. These stable changes could then alter the susceptibility of this system to future insults (190,191). Increased neuronal activity also activates Nurr1 transcription, which regulates expression of target genes, including DAT and VMAT2, producing a state in which the ratio of DAT:VMAT2 is increased (129).

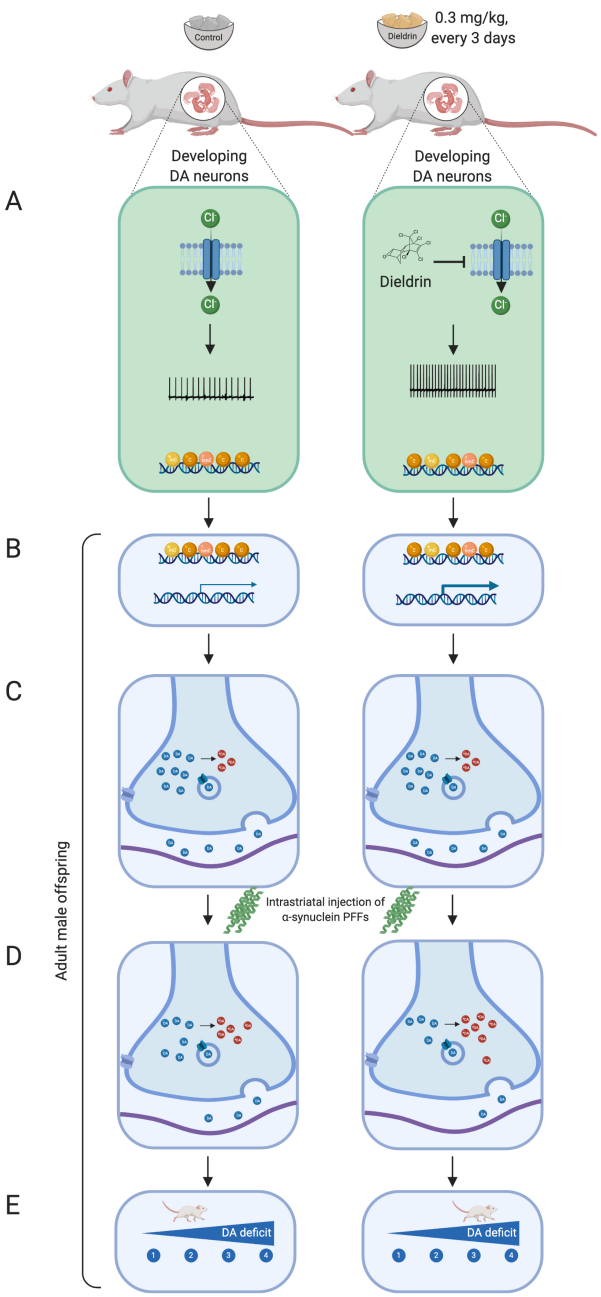

Figure 1.8 Proposed mechanism by which developmental dieldrin exposure leads to exacerbation of PFF-induced toxicity. Dams are fed vehicle or dieldrin containing food starting 1 month prior to mating and continuing through weaning of F1 pups. Dieldrin inhibits chloride influx through $GABA_A$ receptors resulting in increased neuronal activity (A). This change in activity produces epigenetic changes throughout the lifespan even when dieldrin is no longer present (B). These epigenetic changes affect dopamine neuron development and maintenance, producing stable changes in striatal dopamine synapse function (C). These synaptic changes lead to increased susceptibility to PFF-induced synucleinopathy (D, E). Created in BioRender.

Consistent with differential susceptibility by sex, studies in our lab and others' have identified sex-specific dieldrin-induced changes that may be responsible for male specific increased susceptibility to PD models (129,191) (Chapter 2, Chapter 3). Specifically, we have previously identified sex-specific epigenetic changes in DNA methylation and transcriptional profiles in pups developmentally exposed to dieldrin (191). The sex-specific nature of these dieldrin-induced changes and the increased susceptibility to MPTP in male mice exposed to dieldrin are both reminiscent of the increased incidence of PD in men. As discussed in Section 0, epidemiological studies have shown that males are at increased risk for developing PD at all ages and in all nations studied.

α-syn PFF model of PD

While L-DOPA and related dopaminergic therapies help to manage motor symptoms in PD, there are no current therapies to slow or stop nigrostriatal degeneration in PD. This is partly due to the failure of animal models to recapitulate critical aspects of human disease such as Lewy Body formation and PD behavioral deficits (192). MPTP is the gold standard for pre-clinical testing, but, as discussed above (Section 0), this model does not replicate specific key aspects of PD pathogenesis such as α-syn pathology, the progressive disease course, and behavioral deficits (192). Previous α-syn-based models do show some of these missing characteristics such as α-syn pathology, but many rely on overexpression to supraphysiological levels that are never seen in human brain. The α-syn preformed fibril (PFF) model of synucleinopathy has been developed in rats and mice in order to create a model that addresses these limitations (193,194). This model shows protracted course of synuclein pathology and nigrostriatal

degeneration, produces motor deficits without super physiological levels of α-syn protein, and progressive neuropathological and behavioral phenotypes (193–195).

In this model, α-syn fibrils are generated from recombinant α-syn monomers and sonicated into smaller fragments that are about 50 nm in length. When applied to cells in culture or injected directly in the brain of mice or rats, these fragments are taken into the synaptic terminals where they seed the formation of endogenous α-syn into insoluble phosphorylated α-syn (p-syn) inclusions. This eventually leads to neuronal dysfunction and degeneration within the context of normal physiological levels of endogenous α-syn. PFFs applied to primary neurons that lack α-syn or α-syn knockout mice do not induce toxicity, indicating that the toxicity of α-syn PFFs depends on the recruitment of endogenous α-syn (193,195–198).

This model was first reported in mice in 2012 in a seminal paper and was later replicated in rats (193,199–202). In mice, intrastriatal injection of α-syn PFFs leads to deposits of hyperphosphorylated p-syn in regions that innervate the injection site. These p-syn deposits can be detected at the injection site in striatum, in cortical layers 4 & 5, and in the olfactory bulb ipsilateral to the injection site within the first 30 days after PFF injections. p-syn containing inclusions develop progressively, evolving from pale cytoplasmic accumulations at 1 month post PFF to dense perinuclear inclusion at 3 month post PFF in mice (194). The amygdala shows bilateral p-syn deposits consistent with its bilateral connections to the striatum. By 180 days post injection, p-syn immunoreactivity increases in affected regions and extends into contralateral neocortex, ventral striatum, thalamus, occipital cortex, commissural and brainstem fibers. Particularly relevant for studies of PD, p-syn aggregates also form in the SNc,

with a peak at 2-3 months post-injection (194). Furthermore, striatal DA levels are reduced 3 months following PFF injections, and significant loss of TH and motor deficits are seen 6 months after the PFF injections (194) (Figure 1.9).

The α-syn PFF model has also been replicated and optimized in rat (193,200,202,203). The timeline of events is slightly different in rat, but the overall effect is similar. As in mice, actual neurodegeneration lags behind loss of TH phenotype (Figure 1.9) (193). Meanwhile, only rats show PFF-induced contralateral degeneration 6 months post-PFF injection. While this contralateral degeneration has not been observed in mice, it may appear at unmeasured later time points, as mice have a slower time course of degeneration than rats in this model (193,199).

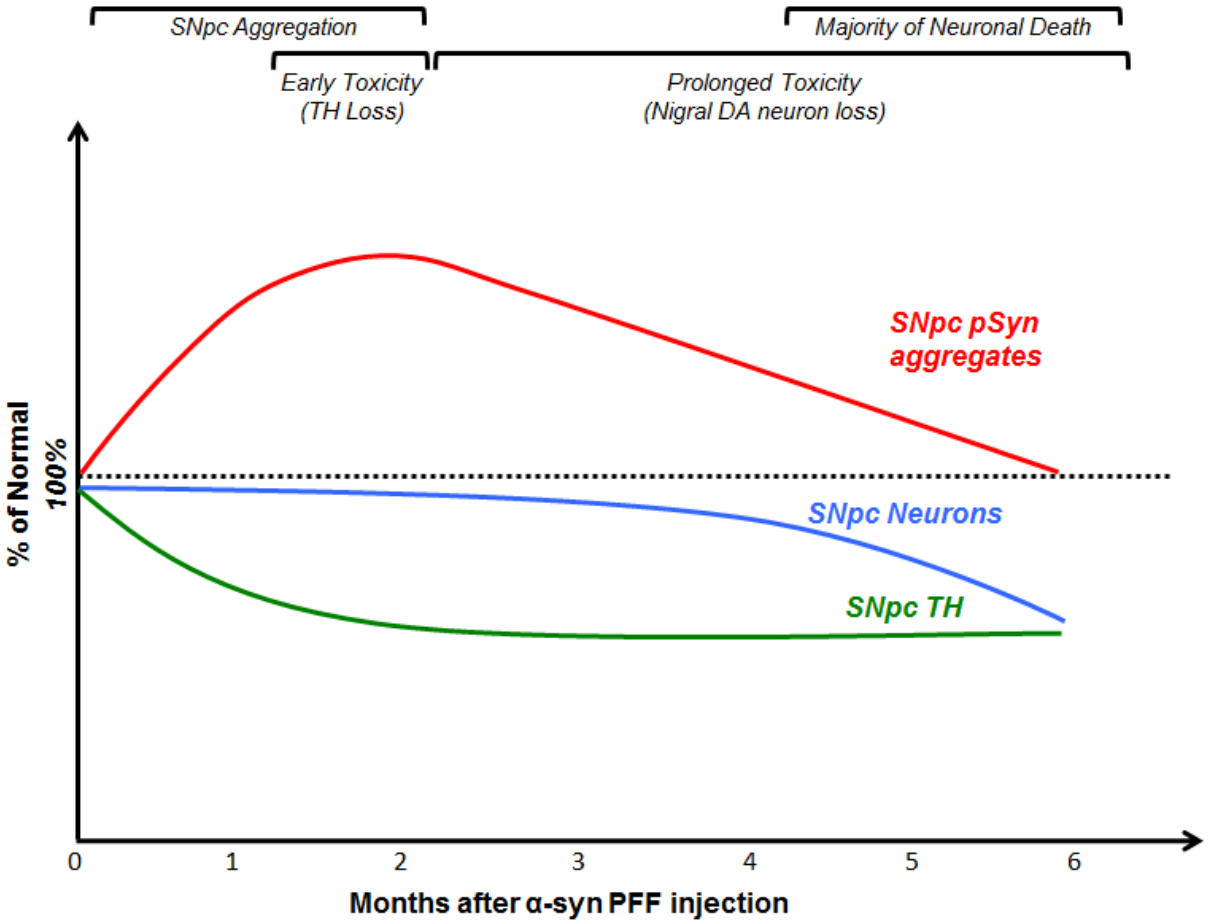

Figure 1.9 Timeline of events in α-syn PFF model

Goals of current study

This current study was based on the hypothesis that environmental exposures, in particular to the organochlorine pesticide dieldrin, alter PD risk by altering neuronal vulnerability to α-syn-mediated toxicity. Currently, it is difficult to model how environmental exposures affect risk of PD, despite a large body of research into specific targets of a variety of exposures. In Phase 1, we utilized the previously established developmental dieldrin exposure paradigm (129)

In Phase 2, we used the α-syn PFF model as a PD model to assess if developmental dieldrin exposure alters susceptibility in the model. Previous studies combined the developmental dieldrin exposure model with MPTP toxicity to model how environmental exposures affect risk of PD; however, the relevance of the MPTP model to PD pathophysiology has been questioned. The recent development of the α-syn PFF model provides a unique opportunity to test how environmental exposures affect PD. Thus, we explored how environmental risk factors alter susceptibility to PD by combining the developmental dieldrin exposure model with the α-syn PFF model. The sex-specific nature of the previously observed increased neuronal susceptibility to MPTP after developmental dieldrin exposure also provides an opportunity to study mechanisms underlying sex differences in sporadic PD. Here, we examined whether this sex specificity is also true in the α-syn PFF model.

The goals of this study were three-fold:

1) To study sex-specific effects of developmental dieldrin exposure on α-syn protein levels, expression of genes involved in inflammation, and striatal DA levels (Chapter 2)
2) To assess neuronal susceptibility to α-syn PFF-induced toxicity in male and female mice developmentally exposed to dieldrin (Chapter 3)
3) To characterize sex differences in the α-syn PFF model (Chapter 4)

Together, these experiments establish a novel approach for exploring the mechanisms by which environmental exposures modify the risk of developing PD and the mechanisms underlying sex differences in PD risk.

Chapter 2 Effects of developmental exposure to dieldrin in male and female mice

Abstract

Human and animal studies have shown that exposure to the organochlorine pesticide dieldrin is associated with increased risk of Parkinson's disease (PD). Despite previous work showing a link between developmental dieldrin exposure and increased neuronal susceptibility to 1-methyl-4-phenyl-1,2,3,6-tetrahydropyridine (MPTP) toxicity in male C57BL/6 mice, the mechanisms mediating this effects have not been identified. Here, we tested the hypothesis that developmental exposure to dieldrin induces changes in expression of α-synuclein (α-syn), dopamine transporter (DAT) or vesicular monoamine transporter 2(VMAT2), and/or neuroinflammation. Starting at 8 weeks of age and prior to mating, female C57BL/6 mice were exposed to 0.3 mg/kg dieldrin by feeding (every 3-4 days) throughout breeding, gestation, and lactation. At 12 weeks of age, F1 pups were sacrificed and dorsal striatum was dissected. Striatal tissue was assessed for expression of total α-syn, DAT and VMAT2 expression by western blotting, inflammation by TaqMan Mouse Immune Array, and levels of dopamine (DA) and DA metabolites by HPLC. While developmental dieldrin exposure had no effect on total α-syn, DAT or VMAT2 levels or on striatal DA levels in both male and female F1 pups, exposure produced distinct effects on the male and female inflammatory gene profile. Together, our data demonstrate that developmental dieldrin exposure leads to sex specific changes in genes involved in neuroinflammation that persist into adulthood. Such changes may underlie the sex specific sensitivity to subsequent parkinsonian toxicants, suggesting that exposures at critical stages of development may alter inflammatory pathways and contribute to late-life neurodegenerative disease, including PD.

Introduction

Dieldrin and relevance to PD

Dieldrin is a highly toxic organochlorine pesticide that was phased out of commercial use in the 1970s. Due to its high stability and lipophilicity, it has persisted in the environment and has been classified as a persistent organic pollutant (POP) (CDC, 2016). Because of these properties, dieldrin also accumulates in lipid-rich tissues like the brain (123,125,204). Despite being phased out in the 1970-1980s, the health effects of past dieldrin exposures will continue for decades as the aged population currently diagnosed with PD and those that will develop PD in the next 20-30 years were likely exposed to dieldrin before its phase out (123,204–206).

This project focuses on dieldrin as a representative toxicant because of its association with PD risk in epidemiological studies (99–114,120,123–126,207). While epidemiological studies alone cannot support a causal link, when combined with mechanistic studies and postmortem studies that show higher levels of organochlorine pesticides in brains from PD patients and mechanistic studies, a role for organochlorine pesticides generally and dieldrin specifically emerges (108,111,120). *In vitro* studies of dieldrin toxicity have demonstrated that dieldrin induces oxidative stress, is selectively toxic to dopaminergic cells, disrupts striatal dopamine (DA) activity, and may promote α-syn aggregation (120,123,171,173,175,208). Moreover, mechanistic animal research has shown that adult and developmental dieldrin exposures are associated with oxidative stress and disrupted expression of PD-related proteins (129,179).

The developmental model of dieldrin exposure as a model of increased PD susceptibility

The developmental dieldrin exposure model has previously been characterized as a model of increased PD susceptibility, and we have established this model in our lab (129,191). In this model, developmental exposure to dieldrin induces stable alterations in the DA system that increase susceptibility to subsequent exposure to MPTP in male mice (129). Specifically, male and female mice developmentally exposed to dieldrin showed increased dopamine transporter (DAT) and vesicular monoamine transporter 2 (VMAT2) protein levels, as well as increased *Nr4a2* expression (129). In male mice only, developmental exposure to dieldrin led to an increased DAT:VMAT2 ratio and exacerbated (MPTP) toxicity, which is a classic model of dopaminergic loss in PD (129). Vesicular integrity can impact vulnerability of dopaminergic neurons to neurotoxicants, and the DAT:VMAT2 ratio has been used to predict susceptibility of neurons to PD-related neurodegeneration (128,209,210). Based on this, the authors hypothesized that this change in DAT:VMAT2 ratio and the resulting changes in DA handling underlie the observed increase in MPTP-induced neurotoxicity (129). However, the biological mechanisms mediating these long-lasting effects of developmental dieldrin exposure on the dopaminergic system have not been identified.

Developmental dieldrin exposure induces changes in DNA methylation

The epigenome in general and DNA modifications specifically have been recognized as potential mediators of the relationship between developmental exposures and adult disease. Epigenetic marks are sensitive to the environment, established during cellular differentiation, and regulate gene expression throughout the lifespan (211,212). Thus, it is possible that developmental dieldrin exposure induces changes in the epigenome, creating a poised

epigenetic state in which developmental exposure has programmed a modified response to later-life challenges. In addition, evidence for epigenetic regulation playing a role in PD has been growing, particularly for DNA methylation (213–219). In a recent study, our lab identified distinct patterns of differential methylation in male and female offspring, suggesting that DNA methylation may play a role in mediating the long-lasting effects of developmental dieldrin exposure (191).

Developmental dieldrin exposure exacerbates the MPTP-induced immune response

Previous work has shown that the developmental dieldrin exposure alone does not affect the levels of glial fibrillary acidic protein (GFAP) in the striatum, yet it potentiates MPTP-induced increases in GFAP protein levels in striatum of male mice (129). GFAP is an intermediate filament that is expressed in numerous cell types of the central nervous system including astrocytes. Increased expression of GFAP is indicative of gliosis, the proliferation and hypertrophy of glial cells, and neuroinflammation (220). Taken together, these data suggest that developmental dieldrin exposure may induce changes in the neuroinflammatory systems that changes the sensitivity of these systems to a second-hit insult. Therefore, in this study, we screened expression of a panel of genes involved in immune and inflammatory responses assessing their differential expression before and after developmental dieldrin exposure in both sexes.

Developmental dieldrin exposure affects striatal expression of DAT and VMAT2 and exacerbates MPTP-induced increases in α-syn in the striatum

As discussed above, it was previously reported that developmental dieldrin exposure led to an increase in the DAT:VMAT2 ratio in adulthood and a corresponding increase in DA turnover (129). After MPTP, male mice exposed to dieldrin showed greater loss of striatal DA, as well as a potentiated MPTP-induced increase in monomeric α-syn protein levels in the striatum of male mice. Dieldrin alone had no effect on overall levels of α-syn in the striatum, but the authors did not assess if dieldrin induced any changes in α-syn oligomerization (129). In the current project, we aimed to replicate these findings and explore if dieldrin induces changes in α-syn oligomerization.

Methods

Animals

Male and female C57BL/6 mice were purchased from Jackson Laboratory (Bar Harbor, Maine). Female mice were 7 weeks old upon arrival. In contrast, male mice used for breeding were 11 weeks old upon arrival. After a week of habituation, mice were switched to and maintained on a 12:12 reverse light/dark cycle for the duration of the study. Mice were housed in Thoren ventilated caging systems with automatic water and 1/8-inch Bed-O-Cobs bedding with Enviro-Dri for enrichment. Food and water were available ad libitum. Mice were maintained on standard LabDiet 5021chow (LabDiet). Females were individually housed during dieldrin dosing, except during the mating phase. F1 pups were group housed by sex; with 2-4 animals per cage. All procedures were conducted in accordance with the National Institutes of Health Guide for Care and Use of Laboratory Animals and approved by the Institutional Animal Care and Use Committee at Michigan State University.

Dieldrin exposure paradigm

Dosing was carried out as previously described (191). Female mice were habituated to peanut butter feeding for three days. During this period, each mouse was fed a peanut butter pellet containing 6 µl vehicle (corn oil) and monitored to ensure peanut butter consumption. Following habituation, mice were administered 0.3 mg/kg dieldrin (ChemService) dissolved in corn oil vehicle and mixed with peanut butter pellets every 3 days (221). Control mice received an equivalent amount of corn oil vehicle in peanut butter. This dose was based on previous results showing low toxicity, but clear developmental effects on subsequent neurotoxicity (129). Consumption of peanut butter pellets was ensured via visual inspection and typically

occurred within minutes. Adult C57BL/6 (8-week-old) female animals were treated throughout breeding, gestation, and lactation (Figure 2.1). Four weeks into female exposure, unexposed C57BL/6 males (12 weeks old) were introduced for breeding. Mating was scheduled for a maximum age difference of 2 weeks, although the actual age difference was less than 1 week. Offspring were weaned at postnatal day 22 and separated by litter and by sex. At 12-14 weeks (for qPCR and Western blotting), 20 weeks (for HPLC) and 36 weeks of age (for HPLC), male and female offspring from independent litters were sacrificed (n=20 per treatment per sex). One set of animals was used for each endpoint. For qPCR and HPLC, both sexes were analyzed. For Western Blot experiments only male offspring were used.

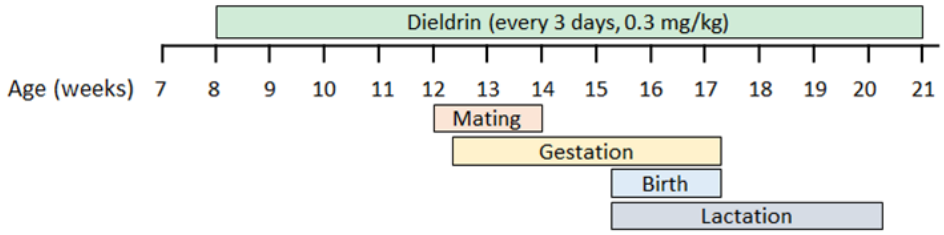

Figure 2.1 Experimental design for dieldrin dosing

Striatal dissections

For HPLC and qPCR, animals were euthanized by pentobarbital overdose until the pain response was absent to toe pinch and intracardially perfused with 0.9% saline. For western blot, animals were euthanized by cervical dislocation. Brains were extracted and flash frozen in 2-methylbutane on dry ice. Bilateral punches (1mm x 2mm) were collected from the dorsal striatum on a cryostat (Figure 2.2) Tissue punches for qPCR were immediately suspended in Trizol.

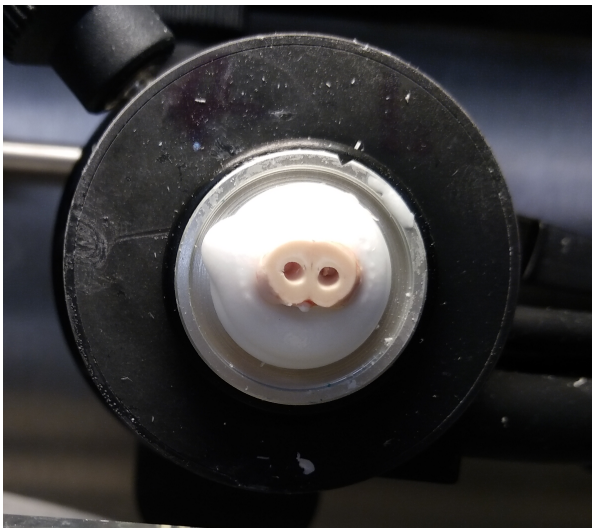

Figure 2.2 Striatal punches on a cryostat after bilateral dorsal striatum are removed.

Western blotting

Western blots for α-syn, DAT and VMAT2 were carried out as previously described (129,193,222–225). Striatal tissue punches were homogenized in tissue lysis buffer (Tris buffered saline with 1% SDS) and centrifuged at 1150 x g for 5 minutes at 4˚C. Protein levels were quantified by BCA protein assay. Samples were diluted with appropriate homogenization buffer, NuPage LDS sample buffer, and 100 mM DTT. For each sample, 10 µg of total protein for α-syn and 20 µg of total protein for DAT and VMAT2 was loaded onto a NuPage 10% Bis-Tris gel. Samples were co-blotted with dilution standards. Samples were subjected to PAGE and electrophoretically transferred to polyvinylidene difluoride membranes (ThermoFisher 88520). For α-syn detection only, immediately following the transfer, proteins were fixed to the membrane by incubating the membrane in 0.4% paraformaldehyde for 30 minutes at room temperature. After fixation, the membrane was incubated in REVERT staining solution (Li-Cor Biosciences, 926-11021) for 5 minutes and imaged on a Li-Cor Odyssey CLx for quantification of

total protein. Non-specific sites were blocked with Odyssey Blocking Buffer (LI-COR Biosciences, 927-50003), and membranes were then incubated overnight in the appropriate primary antibody: α-syn (BD 610787, 1:500), DAT (Millipore Sigma MAB369, 1:1000) or VMAT2 (Miller Lab, 1:10,000).(225) Primary antibody was prepared in 0.01% Tween in Odyssey Blocking Buffer. Primary antibody binding was detected with the appropriate secondary antibody (α-syn: IRDye 800CW Goat anti-Mouse, Li-Cor 926-32210; DAT: IRDye 800CW Goat anti-Rat, Li-Cor 926-32219, 1:10,000; VMAT2: IRDye 800CW Goat anti-Rabbit, Li-Core 926-32219) and imaged on a Li-Cor Odyssey CLx. Quantifications of both total protein and bands of interest were performed in Image Studio Lite Version 5.2. Intensities were calibrated to co-blotted dilutional standards and normalized to total protein.

HPLC

Striatal tissue punches were sonicated in 200 µl of an antioxidant solution (0.4 N perchlorate, 1.34 mm EDTA, and 0.53 mm sodium metabisulfite). A 10 µl aliquot of the homogenate was removed into 2% SDS for BCA protein assay (Pierce). Remaining samples were clarified by centrifugation at 10,000 rpm for 10 minutes. Deproteinized supernatants were analyzed for levels of DA, HVA and DOPAC using HPLC. Samples were separated on a Microsorb MV C8 100–5 column (Agilent Technologies) and detected using a CoulArray 5200 12-channel coulometric array detector (ESA) attached to a Waters 2695 Solvent Delivery System (Waters) using the following parameters: flow rate of 1 ml/min; detection potentials of 25, 85, 180, 420, and 480 mV; and scrubbing potential of 750 mV. The mobile phase consisted of 100 mm citric acid, 75 mM Na_2HPO_4, 80 µM heptanesulfonate monohydrate, pH 4.25, in 5% methanol.

Sample values were calculated based on a six-point standard curve of the analytes. Data were quantified as ng/mg protein.

Taqman Array Cards

RNA isolation was performed using the RNeasy Lipid Tissue Mini Kit (Qiagen), with minor modifications to improve RNA yield. First, tissue was homogenized in 200 µl cold Qiazol lysis reagent. Second, after homogenization, an additional 800 µl of Qiazol lysis reagent was added to each tissue sample followed by 200 µl of chloroform. Third, to facilitate separation of the RNA containing aqueous layer, samples were centrifuged in Phasemaker tubes. Finally, the optional DNase digestion step was included to improve purity of isolated RNA. RNA was eluted in 50 µl RNase-free water, and RNA yield and purity were both assessed using the Agilent RNA 6000 Pico Reagents with the Agilent 2100 Bioanalyzer System (Agilent Technologies). RIN scores were between 7.7 and 8.6 for all samples. Isolated RNA was stored at -80˚C.

cDNA synthesis was performed according to directions supplied with Superscript IV VILO master mix (Life Technologies). 750 ng of RNA input was used per reaction. Reactions also included 1 µl of RNaseOUT (ThermoFisher). cDNA was stored at -20°C until use. qPCR reactions were prepared according to the manufacturer's protocol using Taqman Fast Advanced Mastermix (ThermoFisher). The TaqMan Array Mouse Immune Panel (ThermoFisher) was run on a Viia7 Real-Time PCR instrument (ThermoFisher) according to kit instructions.

The $2^{-\Delta\Delta Ct}$ method was performed on the Taqman array data to estimate relative changes in gene expression by dieldrin exposure (226). ΔCt was calculated as follows: ΔCt = Ct (mean of target gene) – Ct (mean of housekeeping genes). Four housekeeping genes were used to calculate the housekeeping gene mean: *Actb*, *Gusb*, *Hprt1*, and *Gapdh*. We excluded *18S*

rRNA as a housekeeping gene because the assay failed in some samples. The ΔΔCt value for each gene was calculated as follows: ΔCt (dieldrin group) - ΔCt (control group). Fold change was calculated as follows: fold change = $2^{-\Delta\Delta Ct.}$ To test for differential gene expression between dieldrin and control brains, we ran Welch's two-sample t-tests comparing ΔCt values for each gene in the two experimental groups. Significance level for t-tests was set at $p< 0.05$. All gene expression analyses were stratified by sex. Lists of significant differentially expressed genes in male and female mouse brains were input into the STRING network tool to test for known protein-protein interactions. In STRING, the meaning of network edges was set to represent molecular action; otherwise, we used default settings.

Statistics

Welch's two-sample t-test was used to compare mean values between the two groups (vehicle vs. dieldrin) for western blot and neuroinflammation. For analysis of HPLC results, 2-way ANOVA followed by Sidak multiple comparisons test was used. Pregnant dams were the experimental unit for all analyses and all pups for each outcome came from independent litters.

Results

Dieldrin exposure does not alter striatal α-syn levels

Developmental dieldrin exposure (0.3 mg/kg) was previously shown to exacerbate the MPTP-induced increase in α-syn protein levels in striatum of male mice without a dieldrin-induced change in α-syn (129). Therefore, we sought to determine if there were dieldrin-induced changes in α-syn oligomerization. While were able to detect higher molecular α-syn species in samples of pure sonicated α-syn preformed fibrils, we were unable to detect any

higher molecular α-syn species in our PFF-injected animals, 1 to 2 months following PFF injections, even when maximizing protein loading and trying a variety of western blot protocols (data not shown; see Chapter 3 for PFF information). Thus, we were unable to test this hypothesis in dieldrin-exposed animals.

However, we were able to test whether developmental dieldrin exposure led to changes in α-syn levels in the striatum in adult male animals at 12 weeks of age (the age at which PFF injections were performed) by western blot. We were able to replicate the findings from the previous study (129) that dieldrin exposure on its own does not change total α-syn expression levels (Figure 2.3A,B).

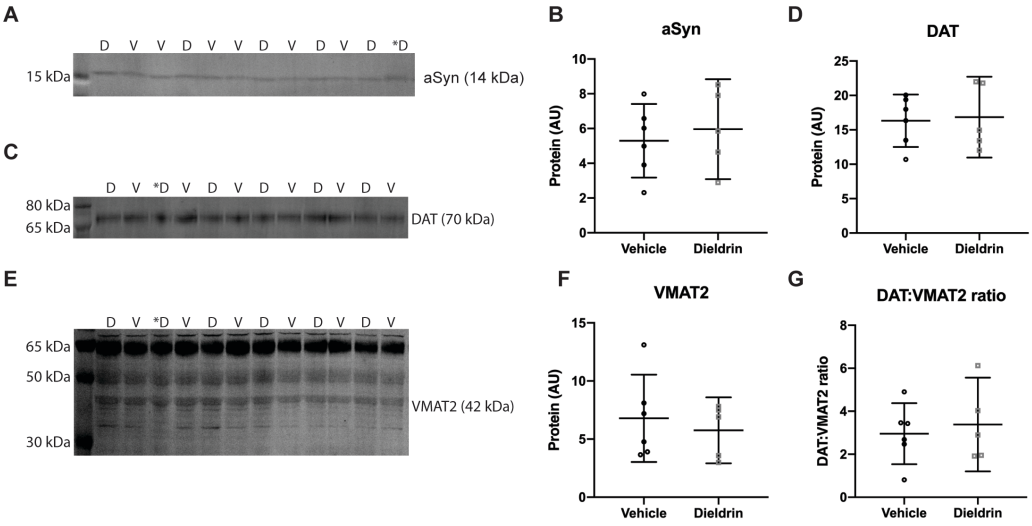

Figure 2.3 Effect of dieldrin exposure on levels of monomeric α-syn, DAT and VMAT2 in the striatum of male animals. α-syn Western Blots. Monomeric α-syn (A), DAT (C) and VMAT2 (E) were detected by western blot (vehicle: n = 6; dieldrin: n = 5). Samples are in mixed order for more accurate quantification. D= dieldrin, V=vehicle. Dieldrin sample with a * was excluded from all analysis. This sample was not stored properly and ran atypically on some blots. Full blots and total protein staining are shown in Figure 2.4. B) Quantification shows no effect of dieldrin on α-syn levels in the striatum (unpaired t-test with Welch's correction: p = 0.6279). D) Quantification shows no effect of dieldrin on DAT levels in the striatum (unpaired t-test with Welch's correction: p = 0.8469). F) Quantification of the 42 kDa band of dieldrin shows no effect of dieldrin on VMAT2 levels in the striatum (unpaired t-test with Welch's correction: p = 0.5764). G) Dieldrin shows no effect on DAT:VMAT2 ratio (unpaired t-test with Welch's correction: p = 0.6700). Data shown as mean +/- 95% CI.

Dieldrin exposure does not alter striatal DAT and VMAT2 levels

In the 2006 study showing that developmental dieldrin exposure exacerbated MPTP toxicity, the authors observed a dieldrin-induced increase in the DAT:VMAT2 ratio and a corresponding increase in DA turnover (129). To test if these findings were replicated in our experiment, we performed western blots for DAT and VMAT2 from striatum of male mice. In contrast to these previous results, we did not observe a dieldrin-induced change in DAT, VMAT2 or the DAT:VMAT2 ratio in our study (Figure 2.3 C-D). Full blots and total protein staining are shown in Figure 2.4.

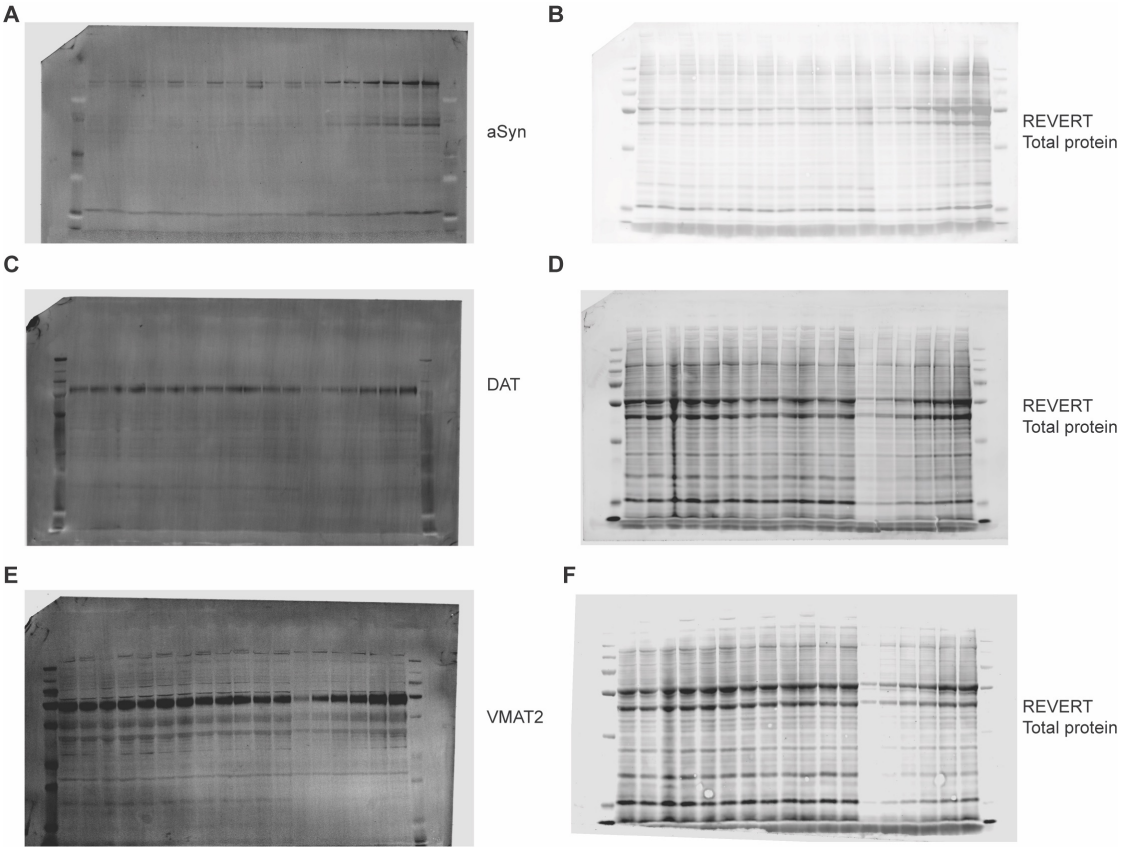

Figure 2.4 Western blots and total protein staining. α-synuclein (A) and corresponding REVERT total protein stain (B). DAT (C) and corresponding REVERT (D). VMAT2 (E) and corresponding REVERT (F). Co-blotted dilutions standards are also shown in the last six lanes on the right side of each blot.

Dieldrin exposure induces sex-specific patterns of expression in inflammatory genes in dorsal striatum

There is a growing recognition that neuroinflammation plays an important role in human PD and in the α-syn PFF model (202).In addition, previous results demonstrated that while dieldrin exposure did not affect glial fibrillary acidic protein (GFAP) levels in the striatum, it did exacerbate MPTP-induced increases in GFAP, suggesting that dieldrin exposure leads to a greater neuroinflammatory response to a second insult (129). Thus, we sought to determine whether developmental dieldrin exposure affects expression of neuroinflammatory genes in the striatum. For this experiment, we screened the expression of a targeted set of neuroinflammatory genes in striata from male and female mice developmentally exposed to dieldrin using the TaqMan Array Card Mouse Immune Panel. Analysis was stratified by sex to assess whether dieldrin has sex-specific effects on inflammatory gene expression. We observed distinct sex-specific effects on expression of neuroinflammatory genes, consistent with our previous results reporting sex-specific effects on DNA methylation and the transcriptome in the ventral midbrain (191). In male mice, nine genes were differentially expressed by dieldrin exposure ($p \leq 0.05$) (Table 2.1). In female mice, 18 genes were differentially expressed by dieldrin exposure (Table 2.2).

Gene	p-value	Fold	Expression in exposed group
Il15	0.0031	0.6944439	Downregulated
Stat1	0.0122	0.8447709	Downregulated
Fn1	0.0166	0.7328938	Downregulated
Nos2	0.0178	0.6984133	Downregulated
Ccl5	0.0198	0.4760219	Downregulated
Socs2	0.0333	0.7849496	Downregulated
Ikbkb	0.0368	0.7758577	Downregulated
H2-	0.0459	0.5142030	Downregulated
*Lrp2**	0.0466	0.2438510	Downregulated

Table 2.1 Differentially regulated genes in males. Genes that were differentially regulated between the dieldrin exposed group vs the control group in male mice (n=8 per treatment group, $p < 0.05$). One star (*) indicates the genes that do not cluster with other genes in STRING network analysis; two stars (**) indicates that the gene was not mapped to the STRING database.

Gene	p-value	Fold	Expression in exposed group
Csf1	0.0003	1.5955447	Upregulated
Tfrc	0.0024	1.2815964	Upregulated
Agtr2	0.0054	1.9362228	Upregulated
Stat4	0.0055	1.7925272	Upregulated
Cd68	0.0060	0.6350103	Downregulated
Socs1	0.0075	0.7602232	Downregulated
Ptprc	0.0078	1.3596591	Upregulated
Ikbkb	0.0140	0.7839894	Downregulated
Nfkb2	0.0198	1.2670066	Upregulated
Col4a	0.0222	1.4464285	Upregulated
Nfkb1	0.0238	1.2724289	Upregulated
Cxcl10	0.0337	2.0286149	Upregulated
Il1a	0.0351	0.8374558	Downregulated
Cd28	0.0382	0.4077085	Downregulated
Stat3	0.0419	1.1916636	Upregulated
Il5	0.0437	2.6215317	Upregulated
Socs2	0.0465	1.2408090	Upregulated
*Ski**	0.0482	1.2297090	Upregulated

Table 2.2 Differentially regulated genes in females. Genes that were differentially regulated between the dieldrin exposed group vs the control group in female mice (n=8 per treatment group, $p < 0.05$). One star (*) indicates the genes that do not cluster with other genes in STRING network analysis; two stars (**) indicates that the gene was not mapped to the STRING database.

To investigate whether the identified differentially expressed genes (DEGs) have known interactions, we performed STRING protein-protein network analysis. STRING analysis showed

that 7 of the 9 (77.8%) DEGs in males have known interactions between their encoded proteins (Figure 2.5A). Meanwhile, 16 of the 18 (88.8%) DEGs in females have known interactions between their encoded proteins (Figure 2.5B). Since this was a curated group of genes selected for function, we expected this high degree of connectivity and a high number of significantly enriched gene ontology terms. For both networks, the most enriched gene ontology terms were related to the cellular response to cytokines.

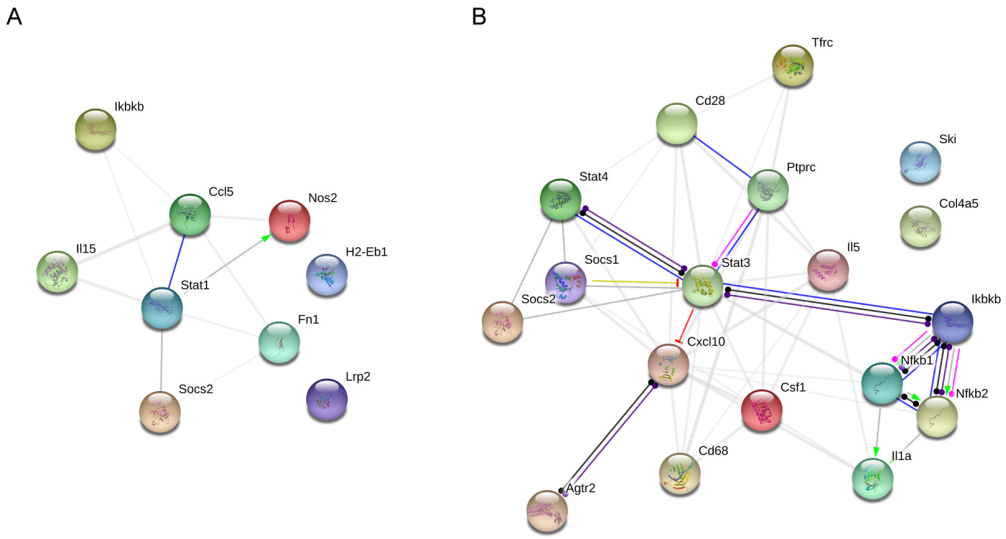

Figure 2.5 STRING interaction networks for male and female differentially expressed genes. Dieldrin-related differentially expressed genes (DEGs) for male and female animals were placed into the STRING network tool to investigate known interactions between the proteins encoded by the genes. We found a high degree of interconnectivity for both the male and female gene lists. A) In males, 7 of the 9 (77.8%) DEGs had known interactions. B) In females, 16 of the 18 (88.8%) DEGs had known interactions. Green line: activation, dark blue line: binding, black line: reaction, light blue line: phenotype, red line: inhibition, purple line: catalysis, pink line: posttranslational modification, yellow line: transcriptional regulation. Arrow cap: positive action, line cap: negative action, dot cap: unspecified action.

Levels of dopamine and dopamine metabolites of dopamine do not change with dieldrin exposure

Previous work showed that developmental dieldrin exposure (0.3 mg/kg) induced a male-specific increase in the striatal DOPAC:DA ratio, driven by an increase in DOPAC without a

concurrent change in DA (129). To replicate and expand on this finding, we measured the levels of DA, DOPAC, and HVA by HPLC in dorsal striatum of mice developmentally exposed to dieldrin or vehicle (n = 10 per group per sex). We were unable to replicate the previous results. Our results show that the level of DA, DOPAC, and HVA remain unchanged by developmental dieldrin exposure in both male and female mice at 20 weeks (Figure 2.6) and 36 weeks of age (Figure 2.7). Similarly, the DOPAC: DA and HVA:DA ratios were not significantly different by exposure group in either sex at any of the time points we investigated.

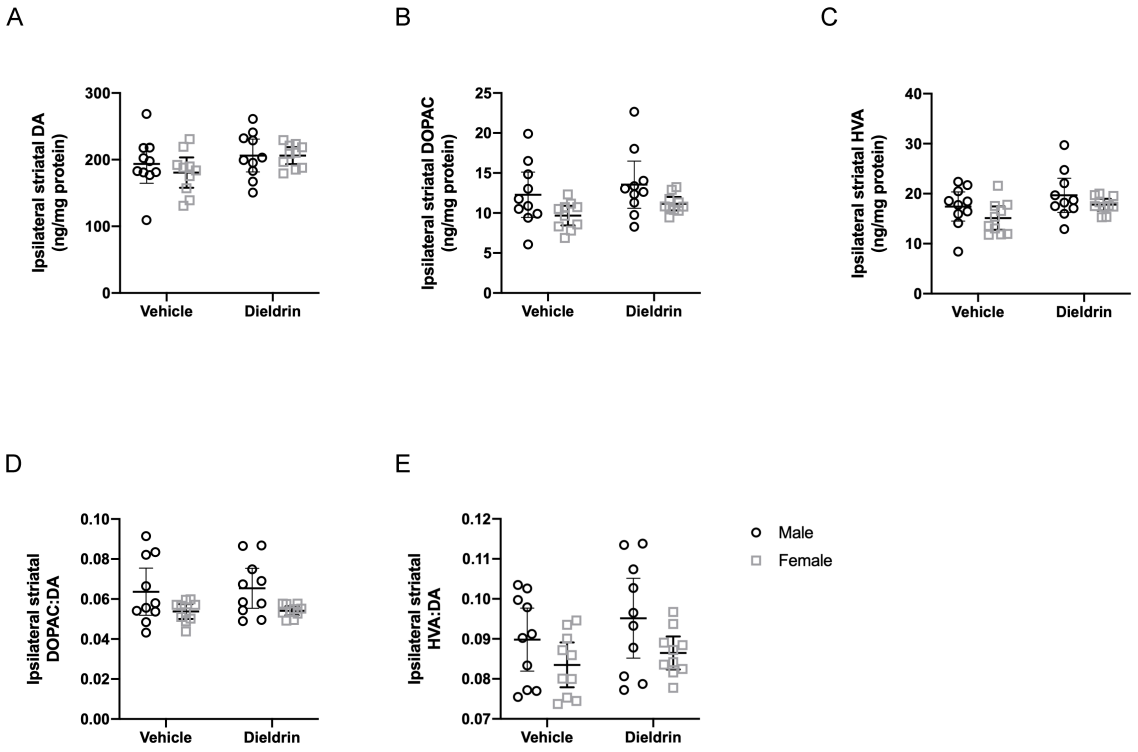

Figure 2.6 DA and DA metabolites at 20 weeks of age were measured by HPLC. Levels of (A) DA, (B) DOPAC, and (C) HVA remained unchanged between the male and female mice with dieldrin exposure. (D) DOPAC:DA and (E) HVA:DA ratios were also unaffected by dieldrin exposure and sex. Data shown as mean +/- 95% CI.

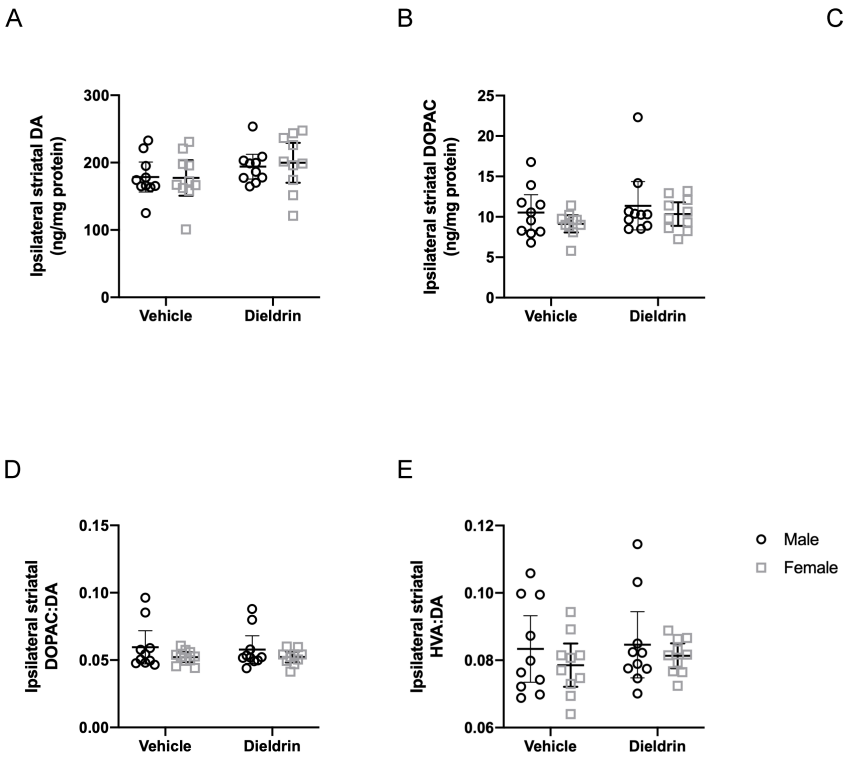

Figure 2.7 DA and DA metabolites at 36 weeks of age were measured by HPLC. Levels of (A) DA, (B) DOPAC, and (C) HVA remained unchanged between the male and female mice with dieldrin exposure. (D) DOPAC:DA and (E) HVA:DA ratios were also unaffected by dieldrin exposure and sex. Data shown as mean +/- 95% CI.

Discussion

This project has focused on characterizing dieldrin-induced changes in the DA system that may underlie this increase in susceptibility (191). In a previous study, we reported sex-specific, dieldrin-associated changes in DNA methylation and gene transcription in the ventral midbrain at genes related to dopamine neuron development and maintenance. These dieldrin-induced changes in gene regulation were identified at 12 weeks of age, which is when male-specific exacerbation of PFF- and MPTP-induced toxicity is observed (129). To complement those results, we explored additional dieldrin-induced changes in littermates in our study that did not receive PFF or saline injections.

Consistent with our finding that dieldrin did not exacerbate PFF-induced α-syn aggregation (Chapter 3), we also did not observe dieldrin-induced changes in overall levels of α-syn (Figure 2.3). This finding replicates previous results in this exposure paradigm (129). However, in contrast to the findings in Richardson et al, we did not observe dieldrin-induced changes in overall levels of DAT or VMAT2, or in the DAT:VMAT2 ratio in male animals (Figure 2.3). The previous report showed increased DAT and VMAT2 in both male and female animals exposed to the same dose of dieldrin used here, as well as a male-specific increase in DAT:VMAT2 ratio (129). Despite this difference in neurochemistry results, we observed a similar male-specific exacerbation of toxicity upon application of the second hit (PFFs in this study, MPTP in the previous study) (Chapter 3).

Next, we tested expression of a curated set of inflammatory genes in the striatum of dieldrin-exposed animals to determine if developmental dieldrin exposure caused long-lasting changes in the neuroinflammatory system in adulthood. Recognition of an important role of neuroinflammation in human PD and in the α-syn PFF model has been growing (30,202,227–234). In addition, previous results demonstrated that dieldrin exposure exacerbates MPTP-induced increases in expression of GFAP levels in the striatum, suggesting that dieldrin exposure leads to a greater neuroinflammatory response to a second insult. While we were unable to test expression of neuroinflammatory genes after the application of PFFs (Chapter 3), we did identify dieldrin-induced changes in the expression of neuroinflammatory genes. Consistent with our previous results showing sex-specific effects of dieldrin exposure on the nigral epigenome and transcriptome, we identified sex-specific effects of dieldrin on neuroinflammatory gene expression (n=9 in male mice; n=18 in female mice) (Table 2.1, Table

2.2). Since this was a curated set of genes, we also observed a very high degree of connectivity between these genes in STRING protein-protein network analysis (77.8% of male DEGs and 88.8% of female DEGs) (Figure 2.5). For both networks, the most enriched gene ontology terms were related to the cellular response to cytokines.

No single inflammatory pathway is apparent in the list of differentially regulated genes from either sex and these results are not consistent with canonical pro- or anti-inflammatory effects. In interpreting these results, it is critical to remember that gene expression was measured in developmentally exposed offspring at 12 weeks of age, when dieldrin is no longer detectable in the brain. Thus, these expression changes may not reflect a typical acute or even chronic inflammatory response. As with our previous epigenetic study, these observed changes likely reflect a persistent change in the baseline state of this system, such that the system responds differently to the second hit.

Despite the lack of a clear pro- or anti-inflammatory gene signature, a few patterns can be identified in the list of DEGs. Only one gene is differentially expressed in both sexes – *Ikbkb*, which encodes an NF-κB inhibitor. This gene is downregulated in both male and female animals, but only female animals show a corresponding increase in *Nkfb1* expression. The combination of increased *Nkfb1* expression and decreased *Ikbk* in the female animals suggests a state of microglial activation. Consistent with this idea, we observed increased expression of the microglial pro-inflammatory cytokine genes, *Cxcl10* and *Csf1*. However, we also observed dieldrin-induced decreased expression of *Il1a* and increased expression of *Socs1*, changes that are not consistent with a pro-inflammatory state. In males, the downregulation of *Ikbkb* is not accompanied by corresponding pro-inflammatory changes. Instead, we observed decreased

expression of four pro-inflammatory genes – *Il15, Stat1, Nos2, and Ccl5*. We also observed expression changes in genes involved in the adaptive immune response (upregulation of *Il5*, *Ptprc, Stat3,* and *Stat4*, and downregulation of *Cd28*) in female animals. When considered together, these gene expression results establish that developmental dieldrin exposure induces distinct sex-specific effects on neuroinflammatory pathways. While these changes are not consistent with canonical pro- or anti-inflammatory effects, they provide multiple avenues for follow-up studies. In particular, future studies will determine if these observed changes in gene expression correspond with activation or deactivation of microglia or the adaptive immune system in dieldrin-exposed animals. Furthermore, using our two-hit model, follow-up studies will test whether specific dieldrin-induced DEGs respond differently to a PFF second hit or if dieldrin exposure modifies PFF-induced microglial activation or immune response.

Lastly, Richardson et al proposed that the dieldrin-induced changes in the DAT:VMAT2 ratio and resulting increase in DA turnover as measured by increased DOPAC:DA ratio were the underlying cause of the observed increase in MPTP susceptibility. However, in our study, we were unable to replicate this finding, even though we replicated a male-specific increase in susceptibility in the α-syn PFF model (Chapter 3). The reason for this discrepancy is unclear, but may be due to technical differences in our protocol (we perfused mice with saline prior to HPLC) or the age at which we sacrificed these mice (20 and 26 weeks of age compared to 12 weeks of age).

Conclusion

The sex-specific nature of responses to developmental dieldrin exposure in neuroinflammation are likely not specific to the toxicants used here. A recent study demonstrated similar sex differences in response to rotenone, a commonly studied parkinsonian toxicant (235). These results are consistent with earlier work in our lab that demonstrated sex-specific epigenetic changes due to developmental exposure (129,191). Given the reduced incidence of PD and severity of disease course in human females, the sex differences in these models underscore the need to include female animals in toxicity studies (10–18,236).

Our work supports the DOHaD hypothesis that early life exposures produce changes that persist into adulthood and impact late life disease. Previous studies have shown that the developing brain is particularly sensitive to environmental perturbations, and that environmental chemicals can act as potent neurotoxicants during development (237–239). Such changes then may alter susceptibility to the future insults during adulthood.

Chapter 3 Effects of developmental exposure to dieldrin on a-synuclein preformed fibril- induced synucleinopathy in male mice

Abstract

Human and animal studies have shown that exposure to the organochlorine pesticide dieldrin is associated with increased risk of Parkinson's disease (PD). Previous work showed that developmental dieldrin exposure increased neuronal susceptibility to MPTP toxicity in male C57BL/6 mice, possibly via changes in dopamine (DA) packaging and turnover. However, the relevance of the MPTP model to PD pathophysiology has been questioned. We therefore studied dieldrin-induced neurotoxicity in the α-synuclein (α-syn)-preformed fibril (PFF) model, which better reflects the α-syn pathology and toxicity observed in PD pathogenesis. Specifically, we used a "two-hit" model to determine whether developmental dieldrin exposure increases susceptibility to α-syn PFF-induced synucleinopathy. Dams were fed either dieldrin (0.3 mg/kg, every 3-4 days) or vehicle corn oil starting 1 month prior to breeding and continuing through weaning of pups at postnatal day 22. At 12 weeks of age, male and female offspring received intrastriatal PFF or control saline injections. Consistent with the male-specific increased susceptibility to MPTP, our results demonstrate that developmental dieldrin exposure exacerbates PFF-induced toxicity in male mice only. Specifically, in male offspring, dieldrin exacerbated PFF-induced motor deficits on the challenging beam and increased DA turnover in the striatum 6 months after PFF injection. However, male offspring showed neither exacerbation of phosphorylated α-syn (p-syn) aggregation in the substantia nigra (SN) at 1 or 2 months post-PFF injection, nor exacerbation of PFF-induced TH and NeuN loss in the SN 6 months post-PFF injection. Collectively, these data indicate that developmental dieldrin exposure produces a male-specific exacerbation of synucleinopathy-induced behavioral and biochemical deficits. This sex-specific result is consistent with both previous work in the MPTP

model, our previously reported sex-specific effects of this exposure paradigm on the male and female epigenome, and the higher prevalence and more severe course of PD in males. The novel two-hit environmental toxicant/PFF exposure paradigm established in this project can be used to explore the mechanisms by which other PD-related exposures alter neuronal vulnerability to synucleinopathy in sporadic PD.

Introduction

Parkinson's disease (PD), the second most common neurodegenerative disorder in the United States, is characterized by progressive degeneration of dopaminergic neurons of the nigrostriatal pathway and the formation of alpha-synuclein (α-syn)-containing Lewy bodies. Several genes have been linked to inherited forms of PD; however, it is estimated that only 5-10% of PD cases are familial (240,241). The remaining ~90% of sporadic PD cases are likely due to a complex interaction between genes and environmental factors. Supporting this idea, epidemiologic studies have shown an association between exposure to persistent organic pollutants, including pesticides and industrial toxicants, and an increased risk of PD (99,101–115,119). When these data are combined with post-mortem analysis and mechanistic studies, a role for specific compounds in PD emerges (108,111,120).

Dieldrin is an organochlorine pesticide that has been associated with an increased risk of PD by both epidemiologic and mechanistic studies (111,120,123,124,126,127,170). Because dieldrin was phased out in the 1970s and 1980s, the potential for new, acute exposure to dieldrin is low. However, the health effects of past exposures will continue for decades as the population currently diagnosed with PD and those who will develop PD in the next 20-30 years were likely exposed to dieldrin prior to its phase out (123,204–206). Furthermore, well-established experimental models of dieldrin exposure have demonstrated that dieldrin induces oxidative stress, is selectively toxic to dopaminergic cells, disrupts striatal dopamine (DA) activity, and may promote α-syn aggregation (120,123,129,171–173,175,179).

Because of the established association of dieldrin with PD risk and well-characterized animal exposure dosing paradigms, our lab utilizes the developmental dieldrin exposure as a

representative model of increased PD susceptibility (129,179,191). According to the U.S. Public Health Service's Agency for Toxic Substances and Disease Registry, the most common forms of human exposure to dieldrin are oral through ingestion of contaminated food and inhalation for those individuals who live in homes that were treated with the pesticide (242). While dieldrin was phased out of commercial use several decades ago, many individuals who are now approaching the age of PD onset were exposed prior to the phase out. To understand how these types of early-life exposures affect adulthood risk for PD, we focused our efforts on a developmental oral exposure, one of the most common routes of exposure. In this model, developmental exposure to dieldrin induces persistent alterations in the DA system that cause a male-specific increase in susceptibility to subsequent exposure to MPTP (129). However, numerous therapeutics that protect against MPTP in preclinical studies have failed to translate to clinical benefit, suggesting that this model has limited utility for accurately predicting clinical translation or exploring toxicological mechanisms in PD (243). Moreover, MPTP is a fast-acting toxicant that induces rapid and extensive loss of striatal DA, which does not reflect the protracted course of loss of function and degeneration observed in disease. Finally, the failure of the MPTP model to develop widespread α-syn pathology calls into question its validity as a "second hit" for examining organochlorine-induced PD vulnerability (243,244). Instead, in the present study, we incorporated the α-syn pre-formed fibril (PFF) model to investigate dieldrin-induced parkinsonian susceptibility.

In 2012, Luk et al reported that intrastriatal injection of synthetic α-syn PFFs into wild-type mice seeded endogenous accumulation of Lewy Body (LB)-like intracellular α-syn inclusions and ultimately led to nigrostriatal degeneration (Figure 3.1) (194). These findings

have been replicated in transgenic mice, non-transgenic mice, rats, and monkeys (193,194,196,222,245–247). PFF-induced α-syn inclusions resemble LBs in that they are compact intracytoplasmic structures of hyperphosphorylated (ser129) α-syn (p-syn), co-localize with ubiquitin and p62, and are thioflavin-S-positive and proteinase-k resistant. Over time, the α-syn aggregates progressively compact and eventually lead to neuronal degeneration (193,194,248,249). Thus, the intrastriatal injection of α-syn PFFs can be used to model pathological synucleinopathy and nigrostriatal toxicity in mice. Here, we tested the hypothesis that developmental dieldrin exposure increases susceptibility to synucleinopathy and associated toxicity in the α-syn PFF model.

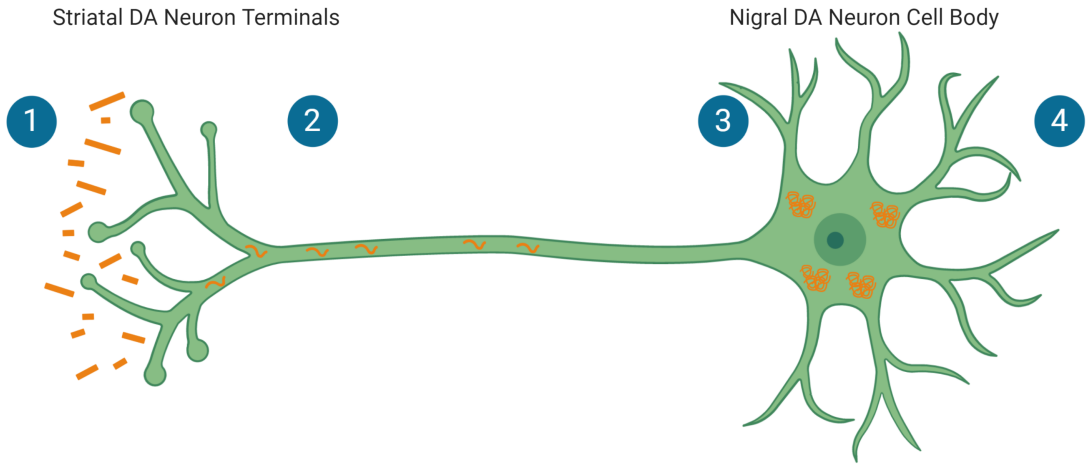

Figure 3.1 Uptake of exogenous α-syn PFFs and templating of endogenous α-synuclein following intrastriatal injection. 1) Sonicated mouse α-syn PFFs are taken up by neurons with axonal projections in the striatum, including dopaminergic terminals of the SNpc. 2) Once inside the neuron the α-syn PFFs trigger templating of endogenous soluble α-syn to accumulate into hyperphosphorylated inclusions. 3) These eventually become larger and compact into proteinase-K resistant, ubiquitin and thioflavin-T positive Lewy-like aggregates. 4) SNpc neurons possessing Lewy-like aggregates, downregulate their dopaminergic phenotype and eventually degenerate.

Methods

Animals: Male (11 weeks old) and female (7 weeks old) C57BL/6 mice were purchased from Jackson Laboratory (Bar Harbor, Maine). After a week of habituation, mice were switched to a 12:12 reverse light/dark cycle for the duration of the study. Mice were housed in Thoren ventilated caging systems with automatic water and 1/8-inch Bed-O-Cobs bedding with Enviro-Dri for enrichment. Food and water were available ad libitum. Mice were maintained on standard LabDiet 5021 chow (LabDiet). F0 females were individually housed during dieldrin dosing, except during the mating phase. F1 pups were group housed by sex; with 2-4 animals per cage. All procedures were conducted in accordance with the National Institutes of Health Guide for Care and Use of Laboratory Animals and approved by the Institutional Animal Care and Use Committee at Michigan State University.

Dieldrin exposure paradigm: Dosing was carried out as previously described (191). Female mice were habituated to peanut butter feeding for three days. During this period, each mouse was fed a peanut butter pellet containing 6 µl vehicle (corn oil) and monitored to ensure peanut butter consumption. Peanut butter pellets, which weigh about 0.13 g each, are only fed to mice twice a week. Consumption of this small amount of peanut butter does not impact weight gain in these animals. Thus, it appears that the peanut butter is merely replacing calories, not adding to total consumption, limiting concerns about the effects of increased caloric intake in this model. Following these three days of habituation, mice were administered 0.3 mg/kg dieldrin (ChemService) dissolved in corn oil vehicle and mixed with peanut butter pellets every 3 days (221). Control mice received an equivalent amount of corn oil vehicle in peanut butter. This dose was based on previous results showing low toxicity, but clear

developmental effects (129). Consumption of peanut butter pellets was ensured via visual inspection and typically occurred within minutes. Adult C57BL/6 (8-week-old) female animals were treated throughout breeding, gestation, and lactation (Figure 3.2). Four weeks into female exposure, unexposed C57BL/6 males (12 weeks old) were introduced for breeding. Mating was scheduled for a maximum age difference of 2 weeks, although all females were pregnant by the end of the first week. Offspring were weaned at postnatal day 22 and separated by litter and by sex. At 12-14 weeks of age, one set of male and female offspring from independent litters was sacrificed (n=10 per treatment per sex). An additional set of animals underwent saline or PFF injections at 12 weeks of age; these animals were sacrificed at 1, 2 and 6 months post-PFF injection (n = 10 per treatment per sex). Both sexes were assayed at the same time points. This produced 4 experimental groups (vehicle:saline, vehicle:PFF, dieldrin:saline, and dieldrin:PFF). Animals were singly housed following surgeries for the duration of the experiment.

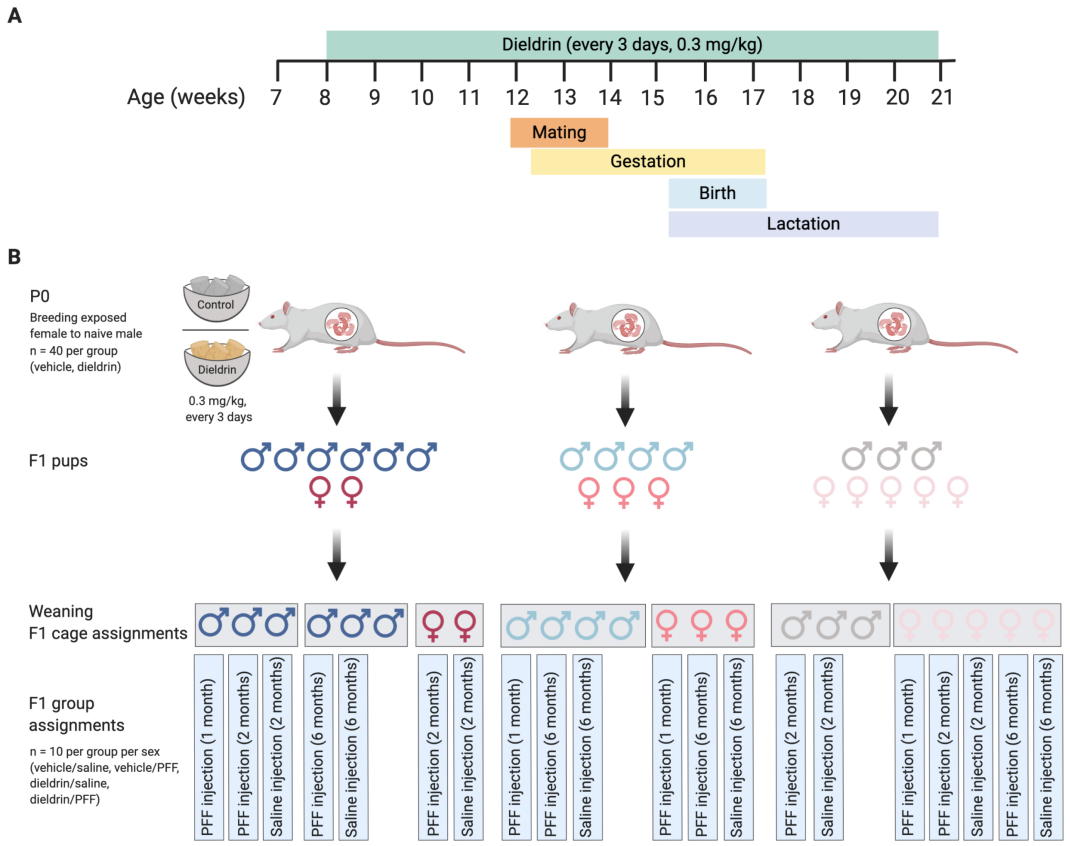

Figure 3.2 Dosing timeline, weaning strategy, cage and group assignments. A) Timeline of developmental dieldrin exposure model: In this paradigm, only female dams were fed dieldrin. Exposure began at 8 weeks of age with 0.3 mg/kg dieldrin dissolved in a corn oil vehicle and administered via peanut butter pellet. Males were introduced for mating when females were 12 weeks of age. Pregnancy was confirmed by monitoring weight. Dieldrin administration continued until pups (F1) were weaned at PND22. B) Weaning strategy, cage and group assignments for PFF injections: At weaning, pups (F1) were separated by sex and litter (colors represent different litters) with no more than 4 animals per cage (grey boxes represent cages). No animals that were singly housed were used in this study. Within each cage, animals were assigned to groups such that for every experimental group, all animals were from independent litters. Created in BioRender.

Preparation of α-syn PFFs and verification of fibril size: Fibrils were generated using wild-type, full-length, recombinant mouse α-syn monomers as previously described (194,196,197,200,250). Quality control was performed on full-length fibrils to confirm fibril formation (by transmission electron microscopy), amyloid structures within fibrils (by thioflavin T assay), a shift to higher molecular weight species compared to monomers (by sedimentation

assay), and low bacterial contamination (<0.5 endotoxin units mg^{-1} of total protein via a *Limulus* amebocyte lysate assay). On the day of surgery, PFFs were thawed to room temperature and diluted to 2 µg/µl in Dulbecco's phosphate buffered saline (PBS) (Gibco), and sonicated at room temperature using an ultrasonic homogenizer (300 VT; Biologics, Inc.) for 60 seconds, with 1 second pulses with the pulser set at 20% and power output set at 30%. Prior to surgeries, an aliquot of sonicated PFFs was analyzed using transmission electron microscopy.

Transmission electron microscopy (TEM): TEM was done as described previously (200). Samples were prepared on Formvar/carbon-coated copper grids (EMSDIASUM, FCF300-Cu). Grids were washed twice by floating grids on drops of distilled H_2O. Grids were floated for 1 min on 10 µl drops of sonicated PFFs diluted 1:50 in PBS, followed by 1 min on 10 µl drops of aqueous 2% uranyl acetate, wicking away liquid with filter paper after each step. Grids were allowed to dry before imaging with a JEOL JEM-1400+ transmission electron microscope. Pre-surgery, a brief assessment of fibril size was performed by measuring 20 representative fibrils to ensure fibril length was approximately 50 nm, a length known to produce optimal seeding (251,252). Prior to intrastriatal injections of the mouse α-syn PFFs, size of the sonicated α-syn PFFs were screened using transmission electron microscopy and the mean length of sonicated fibril size varied between 35-43.6 nm for each batch of PFFs prepared (Figure 3.3).

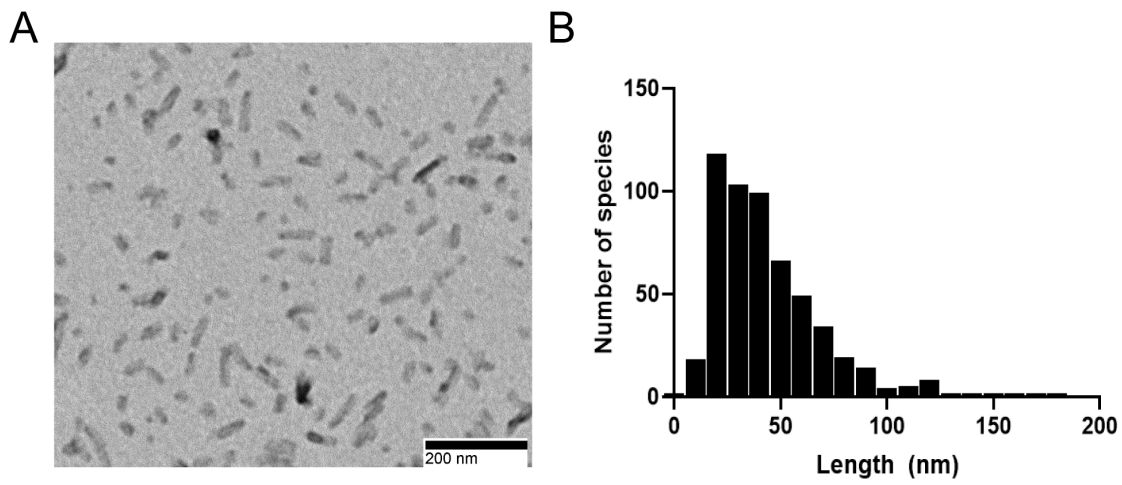

Figure 3.3 Sonicated α-syn PFFs (A) Representative TEM image of sonicated α-syn PFFs (B) Frequency distribution of fibril length

Intrastriatal injections of α-syn PFFs: Surgeries were performed as previously described, with slight modifications (194). Prior to surgery, mice were anesthetized with isoflurane. After anesthesia, 2.5 µl of liquid was unilaterally injected into the dorsal medial striatum using the following coordinates relative to bregma: anterior-posterior = 1.6 mm, medial-lateral = 2.0 mm, and dorsal ventral = -2.6mm. Injections were performed using pulled glass needles attached to 10 µl Hamilton syringes at a flow rate of 0.5 µl/minute. At the end of the injection, the needle was left in place for one minute, withdrawn 0.5 mm, left in place for an additional two minutes to avoid displacement of PFFs, and then completely retracted. Unilateral injections consisted of PBS (saline control) or 2 µg/µl α-syn PFFs (5 µg of total protein). During surgeries, PBS and PFFs were kept at room temperature. Post-surgery, animals received an analgesic (1 mg/kg of sustained release buprenorphine, subcutaneous administration) and were monitored closely until they recovered from anesthesia. In the three days following recovery, animals undergoing surgery were monitored daily for adverse outcomes.

Motor behavior assessment (challenging beam): The challenging beam was used to test motor performance and coordination. This test has been shown to be sensitive in detecting sensorimotor deficits in toxicant, α-syn, and genetic mouse models of PD with nigrostriatal dysfunction or neurodegeneration (253–257). Briefly, prior to beam training and testing, mice were acclimated to the behavior room for one hour. All behavioral experiments started at least one hour into the wake (dark) cycle of the mice. The plexiglass beam consisted of four 25 cm sections of gradually decreasing widths (3.5 cm, 2.5 cm, 2.0 cm, and 0.5 cm) and was assembled into a one-meter-long tapered beam. The home cage was placed at the end of the narrowest section to encourage mice to walk the length of the beam into their home cage. Mice were trained for two days on the tapered beam and received five trials each day. On the day of the test, the beam was made more challenging by placing a mesh grid (squares = 1 cm^2) over the beam. The grid corresponded to the width of each beam section and created an ~1 cm distance between the top of the grid and the beam. This allowed for the visualization of limb slips through the grid. On the day of the test, each mouse was videotaped for 5 trials. All mice were tested at baseline (prior to PFF injections) and at 4 and 6 months post-PFF injection. Videos were scored by trained raters blinded to experimental condition and with an inter-rater reliability of at least 90%. Raters scored the following outcome measures: time to traverse the beam, number of steps, and errors. An error was defined as a limb slip through the mesh grid during a forward movement (253). Each limb accounted for its own error (e.g. 2 slips in 1 forward movement = 2 errors). The mean of the 5 trials was used for analysis. For analysis, data were stratified by time point because experiments were not powered for longitudinal analysis.

Motor behavior assessment (rotarod): Rotarod testing was performed as previously described (194). Prior to rotarod training and testing, mice were acclimated to the behavior room for one hour. All behavioral experiments started at least one hour into the wake (dark) cycle of the mice. For training, each mouse received 3 practice trials with at least a 10-minute interval between each trial. For each trial, mice (n=10 per group) were placed on a rotarod with speed set at 5 rpm for 60 seconds. If an animal fell off, it was placed immediately back on the rotarod. Testing occurred 24 hours after training. For testing, the rotarod apparatus was set to accelerate from 4 to 40 rpm over 300 seconds and the acceleration was initiated immediately after an animal was placed on the rotarod. Each mouse underwent 3 trials with an inter-trial interval of at least 15 minutes. Males were always tested before the females, and the rods were cleaned between the trials to prevent cross-scents interfering with performance. All mice were tested at baseline (before receiving PFF injections) and at 4 and 6 months after PFF injections. The mean latency to fall in all 3 trials was used for analysis. For analysis, data were stratified by time point because experiments were not powered for longitudinal analysis.

Tissue collection: All animals were euthanized by pentobarbital overdose and intracardially perfused with 0.9% saline. At the 1-month time point, saline perfusion was followed by cold 4% paraformaldehyde perfusions and whole brains were extracted and post-fixed in 4% PFA for 24 hours and placed into 30% sucrose for IHC. For 2- and 6-months times point, brains were extracted after saline perfusion and rostral portions of each brain were flash frozen in 2-methylbutane on dry ice and stored at -80˚C until use for HPLC. The caudal portions of each brain were post-fixed in 4% PFA for 24 hours and placed into 30% sucrose for IHC.

HPLC: Striatal tissue punches (1mm x 2mm) were collected from the dorsal striatum on a cryostat and sonicated in 200 µl of an antioxidant solution (0.4 N perchlorate, 1.34 mm EDTA, and 0.53 mm sodium metabisulfite). A 10 µl aliquot of the sonicated homogenate was removed into 2% SDS for BCA protein assay (Pierce). Remaining samples were clarified by centrifugation at 10,000 rpm for 10 minutes. Deproteinized supernatants were analyzed for levels of DA, HVA and DOPAC using HPLC. Samples were separated on a Microsorb MV C18 100–5 column (Agilent Technologies) and detected using a CoulArray 5200 12-channel coulometric array detector (ESA) attached to a Waters 2695 Solvent Delivery System (Waters) using the following parameters: flow rate of 1 ml/min; detection potentials of 25, 85, 120, 180, 220, 340, 420 and 480 mV; and scrubbing potential of 750 mV. The mobile phase consisted of 100 mm citric acid, 75 mM Na2HPO4, and 80 µm heptanesulfonate monohydrate, pH 4.25, in 11% methanol. Sample values were calculated based on a six-point standard curve of the analytes. Data were quantified as ng/mg protein.

Immunohistochemistry: Fixed brains were frozen on a sliding microtome and sliced at 40 µm. Free-floating sections were stored in cryoprotectant (30%sucrose, 30% ethylene glycol, 0.05M PBS) at -20°C. A 1:4 series was used for staining. Nonspecific staining was blocked with 10% normal goat serum. Sections were then incubated overnight in appropriate primary antibody: p-syn (Abcam, Ab184674, 1:10,000) or TH (Millipore, MAB152, 1:4,000). Primary antibodies were prepared in TBS with 1% NGS/0.25% Triton X-100. Sections were incubated with appropriate biotinylated secondary antibodies at 1:500 (anti-mouse, Millipore AP124B or anti- Millipore AP132B), followed by Vector ABC standard detection kit (Vector Laboratories PK-6100). Visualization was performed using 0.5mg/ml 3,3’ diaminobenzidine (DAB, Sigma-Aldrich)

for 30 sec-1 minute at room temperature and enhanced with nickel. Slides stained for p-syn slides were counter-stained with Cresyl violet. Slides were dehydrated before coverslipping with Cytoseal (Richard-Allan Scientific) and imaged on a Nikon Eclipse 90i microscope with a QICAM camera (QImaging) and Nikon Elements AR (version 4.50.00).

Quantification of p-syn inclusion-bearing neurons in the SNpc: Total enumeration of neurons containing p-Syn was performed using StereoInvestigator (MBF Bioscience). The investigator was blinded to the treatment groups. Sections containing the SNpc (1:4 series) were used for all counts. Contours were drawn around the SNpc using the 4x objective. A 20x objective was used to identify the stained inclusions. All neurons containing p-syn within the contour were counted and total counts were multiplied by four to estimate the total number of neurons in each animal with inclusions. Samples injected with PFFs that did not have any p-syn pathology were excluded as missed injections.

Stereology: TH and NeuN neuron counts were estimated by unbiased stereology with StereoInvestigator (MBF Bioscience) using the optical fractionator probe as described previously (258–260). Briefly, sections containing the SNpc (1:4 series) were used for all counts. In all cases, the investigator was blinded to the treatment groups. Contours around the SNpc were drawn using the 4x objective and counting was done using a 60X oil immersion objective. The following settings were used: grid size (195 µm x 85 µm), counting frame (50 µm x 50 µm), guard zone (3 µm) and optical dissector height (23 µm). Section thickness was measured every third counting frame, with an average measured thickness of 29 µm. TH-labeled neurons within the counting frame were counted while optically dissecting the entire section through the z-axis. Variability was assessed with the Gundersen coefficient of error (≤0.1).

Data analysis and statistics: Statistical analysis of all data and graphing were performed using either GraphPad Prism or R (version 3.5.3). All analyses were stratified by sex. We did not include sex as an independent variable in our models because the required sample size to consider both exposure variables and sex as co-predictors was not feasible for this study. All two-group comparisons (total enumeration of p-syn, baseline behavior) were performed using an unpaired Welch's t-test. Stereology, HPLC results and post-PFF behavior were compared by two-way ANOVA followed by Sidak's multiple comparisons tests. Linear regression was performed to test for associations between HPLC results and behavioral outcomes using the lm() function in R. Pregnant dams were the experimental unit for all analyses and all pups for each outcome came from independent litters. All data are shown as mean +/- 95% CI. Results of two-way ANOVA are included in figure legends and significant results of Sidak post-tests are indicated on graphs.

Results

Dieldrin exposure exacerbates PFF-induced deficits in motor behavior

Animals were tested on challenging beam and rotarod prior to PFF injections (baseline), and at 4 months and 6 months post-PFF injections. On the rotarod, we observed no PFF- or dieldrin-induced deficits in the latency to fall at any time point (Figure 3.4). On challenging beam, a sensorimotor test that assesses fine motor coordination and balance in mice, the biggest differences were detected at the 6 month time point (Figure 3.5) (253–257). Deficits in motor performance and coordination manifest as a combination of changes in the three outcome measures reported, such that any one outcome measure on its own does not necessarily reflect the DA deficit. For example, mice with specific nigrostriatal DA neuron loss have displayed slower traversal times (bradykinesia), increased steps (shortened gait), and/or increased errors (postural instability) on the beam (254,257,261).

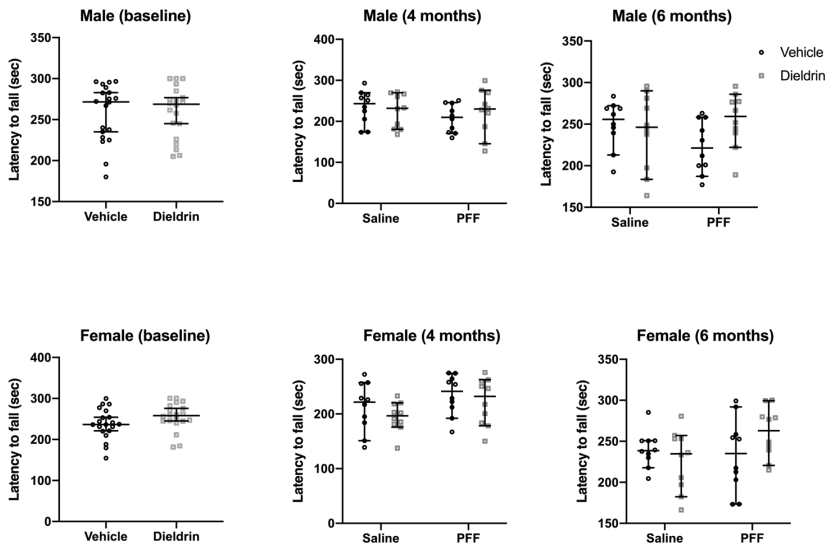

Figure 3.4 No PFF- or dieldrin-induced effects were observed on rotarod in male or female mice. Male and female mice (n = 20 per group at baseline, n = 10 per group at later time points) were tested on rotarod prior to PFF injections (Baseline) and at 4 and 6 months post-PFF injections. Latency to fall in both sexes at all time points, except females at 4 months, was unaffected by either PFF injection or dieldrin exposure. In females at 4 months, there was a significant PFF effect by two-way ANOVA (p = 0.0478), but no single comparison was significant by Sidak post-test. Data is shown as mean (95% CI)

Baseline: There were no significant differences in any of the outcome measures for either sex at baseline testing (Table 3.1).

Male	**Vehicle**	**Dieldrin**
Time to traverse	11.60 (10.45-12.74)	11.05 (9.892-12.21)
Steps	20.01 (18.89-21.13)	19.24 (18.82-19.66)
Errors/Step	0.047 (0.036-0.058)	0.050 (0.036-0.063)
Female		
Time to traverse	12.84 (11.52-14.16)	12.85 (11.45-14.25)
Steps	17.80 (17.43-18.17)	16.47 (15.37-17.57)
Errors/Step	0.0885 (0.07-0.10)	0.095 (0.073-0.117)

Table 3.1 Challenging beam performance in male and female mice at baseline. Male and female mice (n = 20 per group) were tested on challenging beam prior to PFF injections. Data shown as mean (95% CI). Results of Welch's t-tests to compare vehicle and dieldrin were all not significant.

4 months post PFF injection: In male animals, we observed no differences between the groups in time to traverse the beam (Table 3.2). However, dieldrin and PFF both showed a significant effect on steps across with beam, and there was a significant interaction effect. Post-

tests showed that dieldrin exposed animals (dieldrin:saline) made fewer steps across the beam than vehicle controls (vehicle:saline) and that PFFs had no effect on steps in vehicle exposed animals but caused an increase in steps in dieldrin exposed animals. In addition, there was a significant effect of PFF on errors per step at this time point. Post-tests identified a PFF-induced reduction in errors in dieldrin exposed animals.

In female animals, there were also no differences between the groups in time to traverse (Table 3.2). Dieldrin exposed animals (dieldrin:saline) made more steps across the beam than their vehicle control, while in PFF-injected animals, dieldrin exposed animals (dieldrin:PFF) made fewer steps than their vehicle control (vehicle:PFF). PFFs also induced a significant increase in steps in vehicle exposed animals. Control animals (vehicle:saline) made fewer errors per step than the other groups at this time point and fewer errors than they did at baseline; the other treatment groups made similar errors per step than they did at baseline (Table 3.2, Figure 3.6F).

	Saline		PFF	
Male	**Vehicle**	**Dieldrin**	**Vehicle**	**Dieldrin**
Time to traverse	11.136 (10.053-12.219)	9.462 (8.168-10.756)	10.849 (9.585-12.113)	10.863 (10.076-11.65)
Steps	16.84 (16.166-17.514)	11.760 (10.932-12.588)****	15.720 (14.933-16.507)	15.280 (14.625-15.935)
Errors/Step	0.080 (0.049-0.058)	0.116 (0.086-0.146)	0.057 (0.040-0.0674)	0.052 (0.034-0.070)
Female				
Time to traverse	11.273 (10.182-12.364)	10.765 (9.795-11.735)	11.974 (10.392-13.556)	11.001 (9.586-12.416)
Steps	15.020 (14.308-15.732)	16.280 (15.636-16.924)**	17.180 (16.481-17.879)	15.520 (14.992-16.048)***
Errors/Step	0.046 (0.026-0.066)	0.115 (0.093-0.137)***	0.113 (0.083-0.143)	0.114 (0.085-0.143)

Table 3.2 Challenging beam performance in male and female mice at 4 months post-PFF injection. Male and female mice (n = 10 per group) were tested on challenging beam 4 months after PFF injections. Two-way ANOVA with Sidak's multiple comparison tests were performed. Results of Sidak post-tests between dieldrin exposed animals and corresponding vehicle controls are indicated on the table. All significant post-test results are included in this legend. *Males:* There were no significant differences in males on time to traverse. On steps, PFF, dieldrin and the interaction were all statistically significant by two-way ANOVA (PFF: $p = 0.0008$; dieldrin, $p < 0.0001$; Interaction: $p < 0.0001$). Sidak post-tests shows a significant effect of dieldrin in saline-injected animals (vehicle:saline vs dieldrin:saline, $p < 0.0001$) but not in PFF-injected animals, as well as an effect of PFF in dieldrin exposed animals (dieldrin:saline vs dieldrin:PFF, $p <0.0001$), but no effect of PFF in vehicle animals. On errors/step, there was a significant effect of PFF by two-way ANOVA (PFF: $p = 0.003$; dieldrin, $p = 0.1657$; interaction, $p = 0.0695$). Sidak post-tests showed no significant effect of dieldrin but did identify a PFF effect in dieldrin exposed animals (dieldrin:saline vs dieldrin:PFF, $p = 0.0012$). *Females:* There were no significant differences in time to traverse. On steps, PFF and the interaction were statistically significant (PFF: $p = 0.0199$; dieldrin, $p = -.4907$; interaction: $p < 0.0001$). Sidak post-tests revealed a significant effect on dieldrin in both saline- and PFF-injected animals (vehicle:saline vs dieldrin:saline, $p = 0.0222$; vehicle:PFF vs dieldrin: PFF, $p = 0.0014$), as well as a PFF-effect in vehicle exposed animals but not dieldrin exposed animals (vehicle:saline vs vehicle:PFF, $p =< 0.0001$; dieldrin:saline vs dieldrin:PFF, $p =0.3510$) . On errors/step, PFF, dieldrin and the interaction were all statistically significant by two-way ANOVA (PFF: $p = 0.0061$; dieldrin, $p = 0.0038$; Interaction: $p = 0.0048$). Sidak post-tests revealed a significant effect of dieldrin in saline-injected animals (vehicle:saline vs dieldrin:saline, $p = 0.0007$), as well as a PFF-related increase in errors in vehicle animals (vehicle:saline vs vehicle:PFF, $p = 0.0011$).

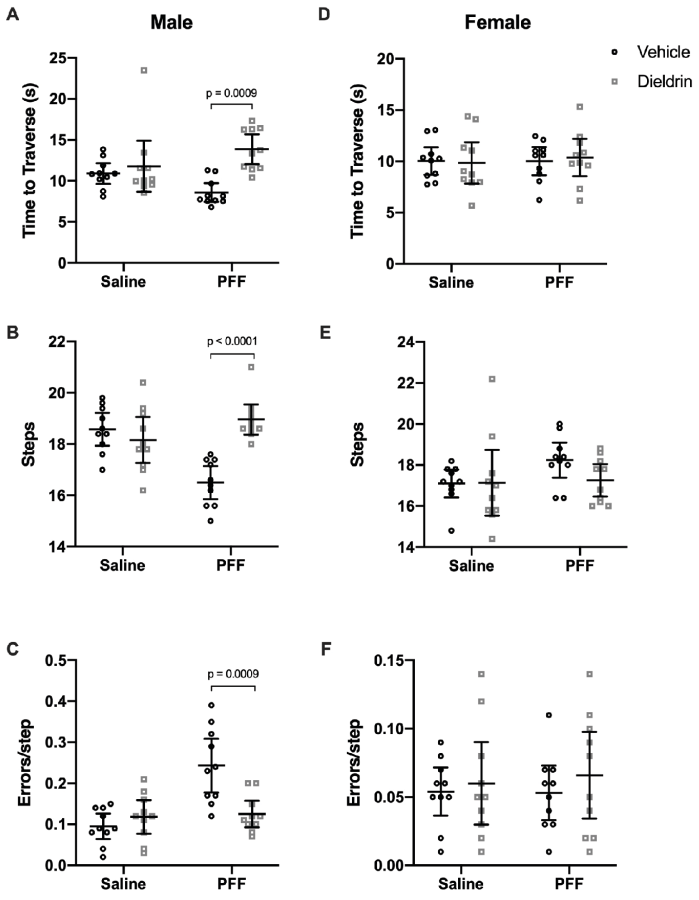

Figure 3.5 Dieldrin exacerbates PFF-induced motor deficits on challenging beam in male animals only. Six months after PFF-injection, motor behavior was assessed on challenging beam in male (A-C) and female (D-F) animals (n = 10 per group). Time to traverse (A,D), steps across the beam (B,E) and errors per step (C,F) were scored. A) Time to traverse at 6 months after PFF injection in male animals (two-way ANOVA: PFF, p = 0.8914; dieldrin, p = 0.0013; interaction, p = 0.0171). Sidak post-tests showed a significant dieldrin-related increase in time to traverse in PFF injected animals (vehicle:PFF vs dieldrin:PFF animals, p = 0.0009). B) Steps at 6 months after PFF injection in male animals (two-way ANOVA: PFF, p = 0.0023; dieldrin, p = 0.0469; interaction, p < 0.0001). Sidak post-tests showed a significant dieldrin-related increase in steps in PFF-injected animals (vehicle:PFF vs dieldrin:PFF animals, p < 0.0001), as well as a significant effect of PFF in vehicle exposed animals (vehicle:saline vs vehicle:PFF, p = 0.0002). C) Errors per step at 6 months post-PFF injection (two-way ANOVA: PFF, p = 0.0004; dieldrin, p = 0.0215; interaction, p = 0.0010). Sidak post-tests showed a significant dieldrin-related decrease in errors per step in PFF-injected animals (vehicle:PFF animals vs dieldrin:PFF animals, p=0.0009), as well as a significant effect of PFF in vehicle exposed animals (vehicle:saline vs vehicle:PFF, p < 0.001). D-F) In female animals, all results were non-significant. G) Summary diagram illustrating the progression of motor deficits as DA deficits become more severe. All data shown as mean +/- 95% CI with significant results of Sidak post-tests for dieldrin to vehicle comparisons indicated on graphs. All significant post-test results are reported in this legend.

6 months post PFF injection: In male animals, dieldrin exposure was associated with a 40% increase in time to traverse in PFF-injected animals, but we observed no effect of PFF alone in saline-injected animals (Figure 3.5A). For steps, PFF-injection alone caused a significant decrease in steps, and there was a significant dieldrin-associated increase in steps in the PFF-injected animals, with dieldrin exposed animals showing a 13% increase in steps (Figure 3.5B). For errors per step, there was a robust PFF-related increase in the vehicle exposed animals that was not observed in dieldrin exposed animals that received PFF injections (Figure 3.5C). In addition, while the dieldrin:PFF male animals did not make as many errors as the vehicle:PFF group, they did make more errors compared to their baseline performance (Figure 3.6C). While this result in errors per step alone would seem to suggest a lack of exacerbation of PFF-induced effects by dieldrin, this group shows deficits in more of the beam outcomes than vehicle:PFF mice. In contrast, at this timepoint in females, there were no differences between the groups in any of the outcomes (Figure 3.5D-F).

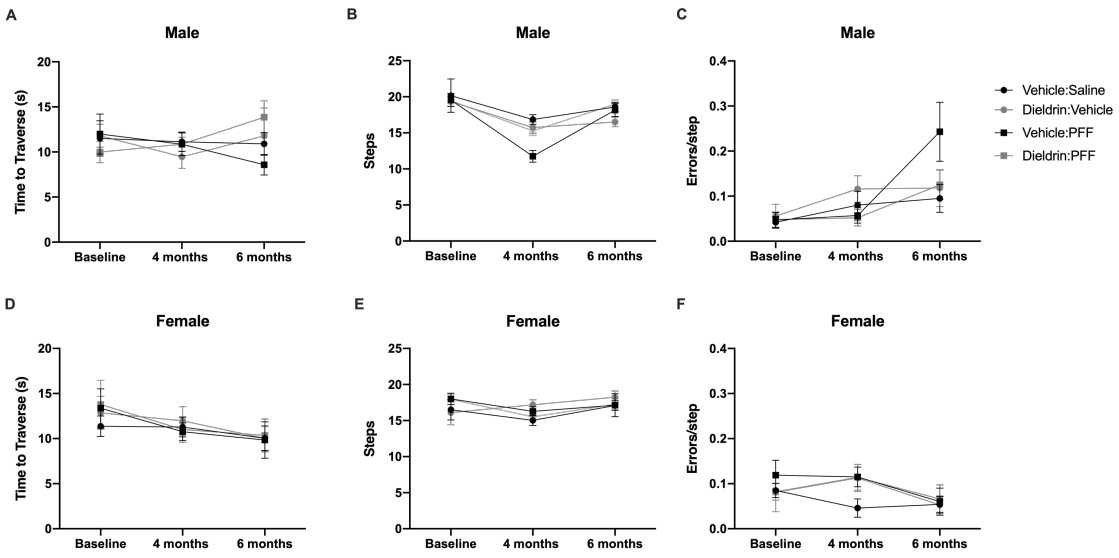

Figure 3.6 Behavioral data at all time points. All challenging beam data presented longitudinally to highlight changes over time. A-C) Male animals; D-F) Female animals; A,D) Time to traverse; B,D) Steps; C,F) Errors per step. Statistical analysis was stratified by time point since we lacked statistical power for a longitudinal analysis.

Dieldrin exposure does not increase PFF-induced p-syn aggregation

In mice, phosphorylated α-syn (p-syn) aggregates accumulate progressively until 2 months after PFF injections in the substantia nigra (SN) pars compacta, evolving from pale cytoplasmic inclusions 1 month post-PFF injection to dense perinuclear Lewy body-like inclusions by 3 and 6 months post-PFF injection (194). To determine whether developmental dieldrin exposure increases the propensity for α-syn to aggregate, we quantified the number of p-syn-containing neurons in the ipsilateral SN at 1 and 2 months post-PFF injection in mice developmentally exposed to dieldrin or vehicle. Our results showed that developmental dieldrin exposure had no effect on the number of p-syn-containing neurons in the ipsilateral nigra at 1 or 2 months post-PFF injection in male or female animals (Figure 3.7). The number of p-syn-

containing neurons was similar between males and females. Consistent with previous observations, we observed no neurons containing p-syn inclusions in the contralateral SN.

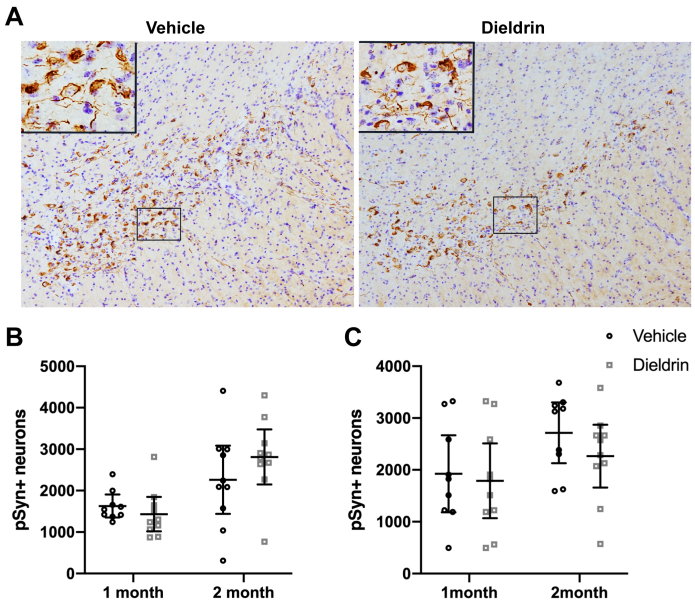

Figure 3.7 Developmental dieldrin exposure does not affect the propensity of p-syn to accumulate in the SN. A) Representative images of p-syn immunohistochemistry from the identical coronal levels through the ipsilateral SN in male animals 2 months after intrastriatal PFF injection. B) Total enumeration of p-syn-containing neurons in ipsilateral SN in male animals (n = 9 for 1-month vehicle due to seeding failure in 1 animal; n = 10 in all other groups; unpaired t-test with Welch's correction: 1 month, p = 0.1919; 2-month, p = 0.1272). C) Total enumeration of p-syn-containing neurons in ipsilateral SN in female animals (n = 9 for 1 month vehicle due to seeding failure in 1 animal; n = 10 in all other groups; unpaired t-test with Welch's correction: 1 month, p = 0.4712; 2 month, p = 0.1195). Data shown as mean +/- 95% CI.

Dieldrin exposure exacerbates PFF-induced increases in DA turnover

To test if dieldrin exacerbated PFF-induced decreases in striatal DA levels, we measured DA and two of its metabolites, DOPAC and HVA, in ipsilateral and contralateral dorsal striatum by HPLC at 2 and 6 months post-PFF injections. Consistent with previous results, we showed PFF-induced deficits in DA levels (~45% loss at 6 months) in the ipsilateral dorsal striatum of male animals at both time points, but this loss was not exacerbated by prior dieldrin exposure

(Figure 3.8A, Figure 3.9A) (194). We also showed, for the first time, that female mice exhibit a PFF-induced loss of striatal DA (~40% loss at 6 months) at both time points (Figure 3.8F, Figure 3.9F). In both male and female animals, we observed PFF-induced deficits in DOPAC and HVA at the two measured time points, but there was no exacerbation of this loss by dieldrin in either sex (Figure 3.8B,C,G,H, Figure 3.9B,C,G,H). These PFF-induced deficits were also seen at 2 months post-PFF injection (Figure 3.9A-C, F-H). Dieldrin had no effect on these outcome measures at 2 months in male animals. In female animals, dieldrin significantly reduced the PFF-induced loss of HVA levels, suggesting that the progression of striatal dysfunction is slower in female animals (Figure 3.9H).

To investigate the effects of dieldrin exposure and PFFs on DA turnover, we calculated ratios of DOPAC and HVA to DA. At both time points, in both sexes, we observed PFF-induced increases in both the DOPAC:DA and HVA:DA ratios, indicative of increased DA turnover and deficits in DA packaging. In male animals at 6 months post-PFF injection only, this increase in HVA:DA ratio was further exacerbated by prior dieldrin exposure (Figure 3.8E). This dieldrin-induced exacerbation was not observed in females animals at 6 months post-PFF injection or at 2 months post-PFF injection in either sex (Figure 3.8J, Figure 3.9E,J).

As expected, levels of DA and its metabolites remained unchanged following PFF injection in the contralateral striatum and dieldrin exposure alone had no effect on DA levels, DA metabolites, or DA turnover in the contralateral striatum (Figure 3.10).

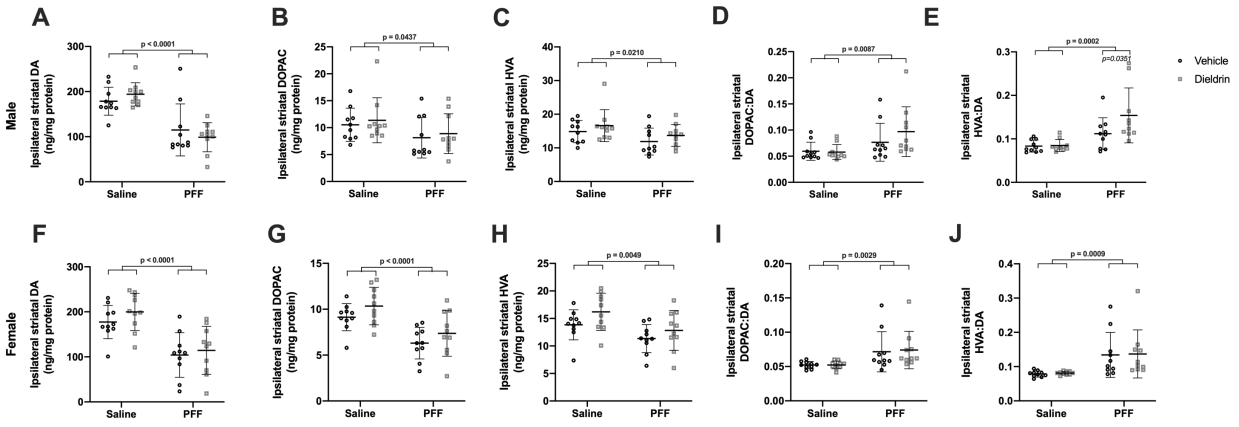

Figure 3.8 Developmental dieldrin exposure exacerbates PFF-induced increases in DA turnover in male animals only 6 months after PFF injection. Levels of DA, DOPAC, and HVA in the ipsilateral dorsal striatum were measured 6 months post-PFF injection by HPLC in male (A-E) and female (F-J) animals (n = 10 per group). A) PFF-induced loss of DA levels in ipsilateral dorsal striatum in male animals (two-way ANOVA: PFF, $p < 0.0001$; dieldrin, $p = 0.9788$, interaction, $p = 0.2052$). B) PFF-induced loss of DOPAC levels in ipsilateral dorsal striatum in male animals (two-way ANOVA: PFF, $p = 0.0437$; dieldrin, $p = 0.9671$; interaction, $p = 0.5027$). C) PFF-induced loss of HVA levels in ipsilateral dorsal striatum in male animals (two-way ANOVA: PFF, $p = 0.0210$; dieldrin, $p = 0.1558$; interaction, $p = 0.9847$). D) PFF-induced increase in DOPAC:DA ratio in ipsilateral dorsal stratum of male animals (two-way ANOVA: PFF, $p = 0.0087$; dieldrin, $p = 0.3607$; interaction, $p = 0.2814$). E) HVA:DA ratio in ipsilateral dorsal striatum of male animals (two-way ANOVA: PFF, $p = 0.0002$; dieldrin, $p = 0.0786$; interaction, $p = 0.0967$). Sidak post-tests showed a significant effect of dieldrin in PFF injected animals (vehicle:PFF vs. dieldrin:PFF, $p = 0.0351$), but not saline injected animals. F) PFF-induced loss of DA levels in ipsilateral dorsal striatum of female animals (two-way ANOVA: PFF, $p < 0.0001$; dieldrin, $p = 0.2667$; interaction, $p = 0.6746$). G) PFF-induced loss of DOPAC levels in ipsilateral dorsal striatum in female animals (two-way ANOVA: PFF, $p < 0.0001$; dieldrin, $p = 0.0654$; interaction, $p = 0.8994$). H) PFF-induced loss of HVA levels in ipsilateral dorsal striatum of female animals (two-way ANOVA: PFF, $p = 0.0049$; dieldrin, $p = 0.0565$; interaction, $p = 0.6614$). I) PFF-induced increase in DOPAC:DA ratio in ipsilateral dorsal striatum of female animals (two-way ANOVA: PFF, $p = 0.0029$; dieldrin, $p = 0.8397$; interaction, $p = 0.8502$). J) PFF-induced increase in HVA:DA ratio in ipsilateral dorsal striatum of female animals (two-way ANOVA: PFF, $p = 0.0009$; dieldrin, $p = 0.8577$; interaction, $p = 0.9994$). Data shown as mean +/- 95% CI with significant results of two-way ANOVA indicated on graphs in bold and of Sidak post-tests for dieldrin to vehicle comparisons indicated in italics. Except where indicated (E), all measures had significant PFF-induced deficits, but no significant effect of dieldrin.

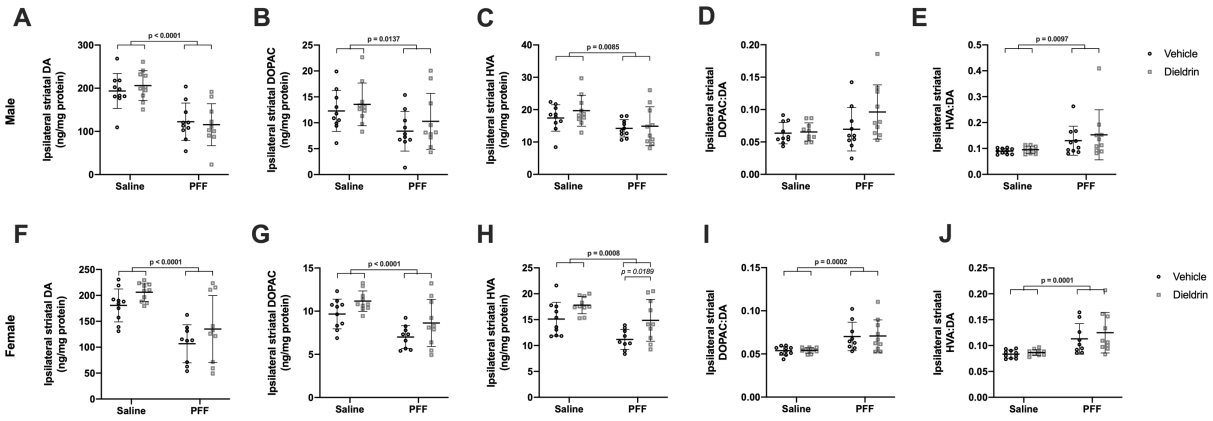

Figure 3.9 HPLC results at 2 months post-PFF injections. Levels of DA, DOPAC and HVA in ipsilateral dorsal striatum were measured 2 months post-PFF injection by HPLC in male (A-E) and female (F-J) animals (n = 10 per group; n = 9 for vehicle:PFF female group, one animal was excluded due to PFF seeding failure based on p-syn counts). A) PFF-induced loss of DA levels (two-way ANOVA: PFF, $p < 0.0001$; dieldrin, $p = 0.8310$; interaction, $p = 0.4696$). B) PFF-induced loss of DOPAC levels (two-way ANOVA: PFF, $p = 0.0137$; dieldrin, $p = 0.2607$; interaction, $p = 0.8189$). C) PFF-induced loss of HVA levels (two-way ANOVA: PFF, $p = 0.0085$; dieldrin, $p = 0.3247$; interaction, $p = 0.5916$). D) No significant effect of PFF or dieldrin on DOPAC:DA ratio (two-way ANOVA: PFF, $p = 0.0810$; dieldrin, $p = 0.1144$; interaction, $p=0.1597$). E) PFF-induced increase in HVA:DA ratio (two-way ANOVA: PFF, $p = 0.0097$; dieldrin, $p = 0.4414$; interaction, $p = 0.6346$). F) PFF-induced loss of DA levels (two-way ANOVA: PFF, $p < 0.0001$; dieldrin, $p = 0.0508$; interaction, $p = 0.9145$). G) PFF and dieldrin effects on DOPAC levels (two-way ANOVA: PFF, $p < 0.0001$; dieldrin, $p = 0.0129$; interaction, $p = 0.9125$). H) PFF and dieldrin effects on HVA levels (two-way ANOVA: PFF, $p = 0.0008$; dieldrin, $p = 0.0017$; interaction, $p = 0.6033$). Sidak post-tests show a dieldrin-induced increase in HVA in PFF-injected animals (vehicle:PFF vs dieldrin:PFF: $p = 0.0189$). I) PFF-induced increase in DOPAC:DA ratio (two-way ANOVA: PFF, $p = 0.0002$; dieldrin, $p = 0.9054$; interaction, $p=0.9842$). J) PFF-induced increase in HVA:DA ratio (two-way ANOVA: PFF, $p = 0.0001$; dieldrin, $p = 0.3585$; interaction, $p = 0.5825$). Data shown as mean +/- 95% CI with significant results of two-way ANOVA indicated on graphs in bold and of Sidak post-tests indicated in italics. Except where indicated (H), Sidak post-hoc tests showed no significant effect of dieldrin exposure.

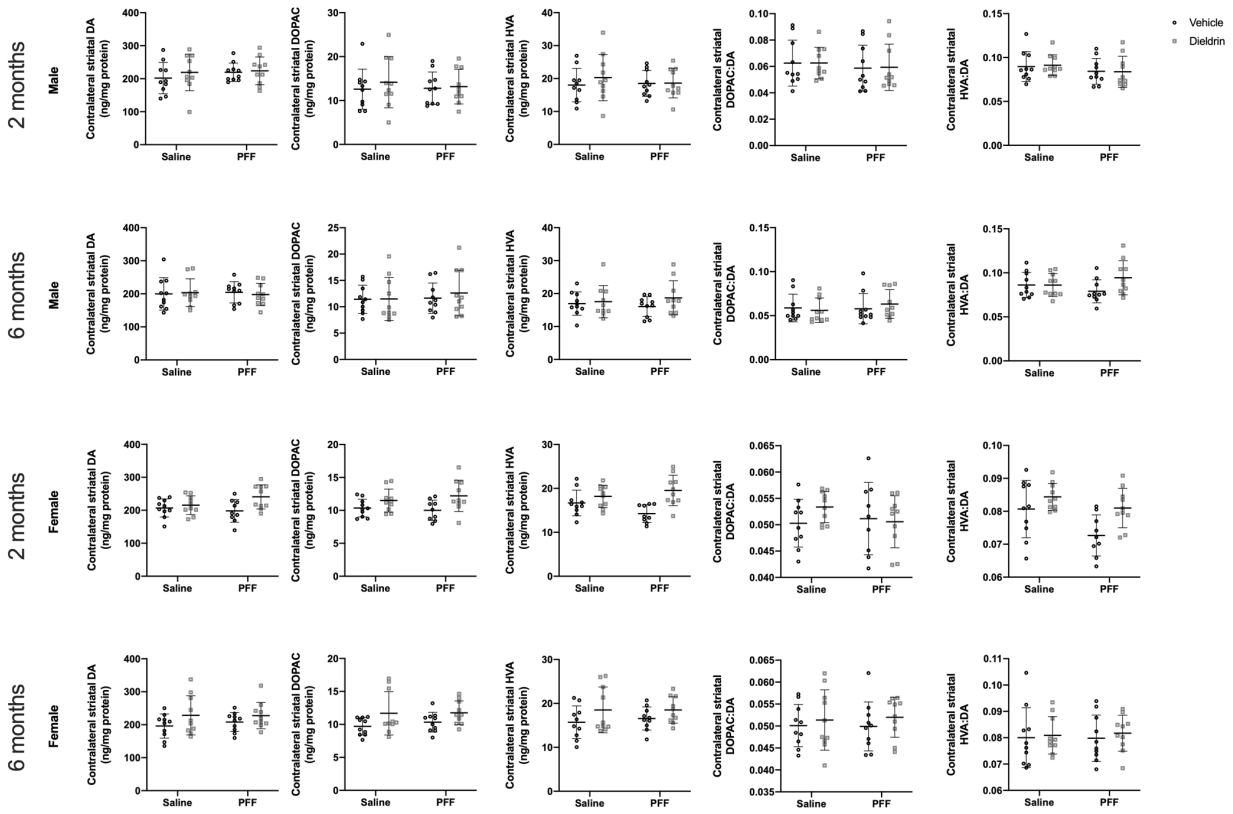

Figure 3.10 Contralateral HPLC at 2 and 6 months after PFF injections in male and female animals. As expected, there was no significant effect of PFF injection or dieldrin exposure on DA, DOPAC or HVA levels in male or female animals (n = 10 per group), at either timepoint. Data shown as mean +/- 95% CI.

The combination of male-specific deficits in motor behavior and DA turnover at 6 months post-PFF injection suggests that this dieldrin-induced exacerbation may be due to increased synaptic deficits in the striatum. To further explore this potential link between DA turnover and the observed behavioral phenotype, we carried out linear regression for all male PFF-injected animals, regardless of dieldrin status, to determine if there is an association between DA turnover and behavioral outcome measures. We found a statistically significant association between HVA:DA ratio and time to traverse: the more severe the deficit in DA turnover, the more severe the behavioral deficit on time to traverse (Figure 3.11). Although we

also observed a negative relationship between HVA:DA ratio and errors per step, this association was not statistically significant.

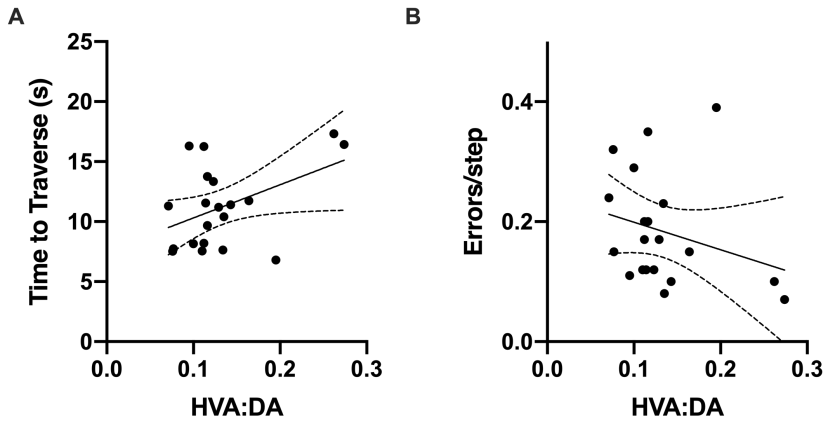

Figure 3.11 DA turnover is associated with behavioral phenotype. Linear regression was performed for all male PFF-injected animals with no additional covariates or interaction terms to explore associations between DA turnover and motor behavior outcomes. A) There was a significant positive association between DA turnover (HVA:DA) and time to traverse (beta coefficient = 27.651, p=0.0498). B) In contrast, the negative association between DA turnover (HVA:DA) and errors per step was not significant (beta coefficient = -0.46011, p-value = 0.248).

Dieldrin exposure does not exacerbate PFF-induced loss of TH phenotype or neuronal loss in the substantia nigra

To determine if developmental dieldrin exposure exacerbates the PFF-induced loss of TH phenotype, we performed IHC for TH and estimated the number of TH^+ neurons in the SN 6 months post-PFF injection by stereology. Consistent with prior results, we observed a ~35% loss of TH^+ neurons ipsilateral to the injection site in the SN 6 months after PFF injections (Figure 3.12A,D) (194). Developmental dieldrin exposure did not significantly affect PFF-induced loss of TH^+ neurons in male animals (Figure 3.12A,D).

In contrast, in female animals, there was a significant effect of PFF on number of TH^+ neurons, with a less than 20% loss of TH^+ neurons ipsilateral to the injection site in the SN 6

months after PFF injections (Figure 3.12C). However, post-tests revealed no significant effect of dieldrin or PFF alone. As expected, there was no loss of TH^+ neurons in the contralateral uninjected SN in either male or female animals (Figure 3.13).

To assess whether the loss of TH immunoreactivity in PFF-injected male animals was accompanied by degeneration of these neurons, we performed IHC for NeuN in male animals and estimated the number of $NeuN^+$ neurons in the SN by stereology. We observed a PFF-induced loss of $NeuN^+$ neurons (~20%) in the ipsilateral SN, with no effect of dieldrin on this loss (Figure 3.12B). Given the modest loss of ipsilateral TH^+ neurons in females, we did not estimate NeuN counts in female mice. Consistent with TH results, we did not observe any contralateral loss of $NeuN^+$ neurons in male mice (Figure 3.13).

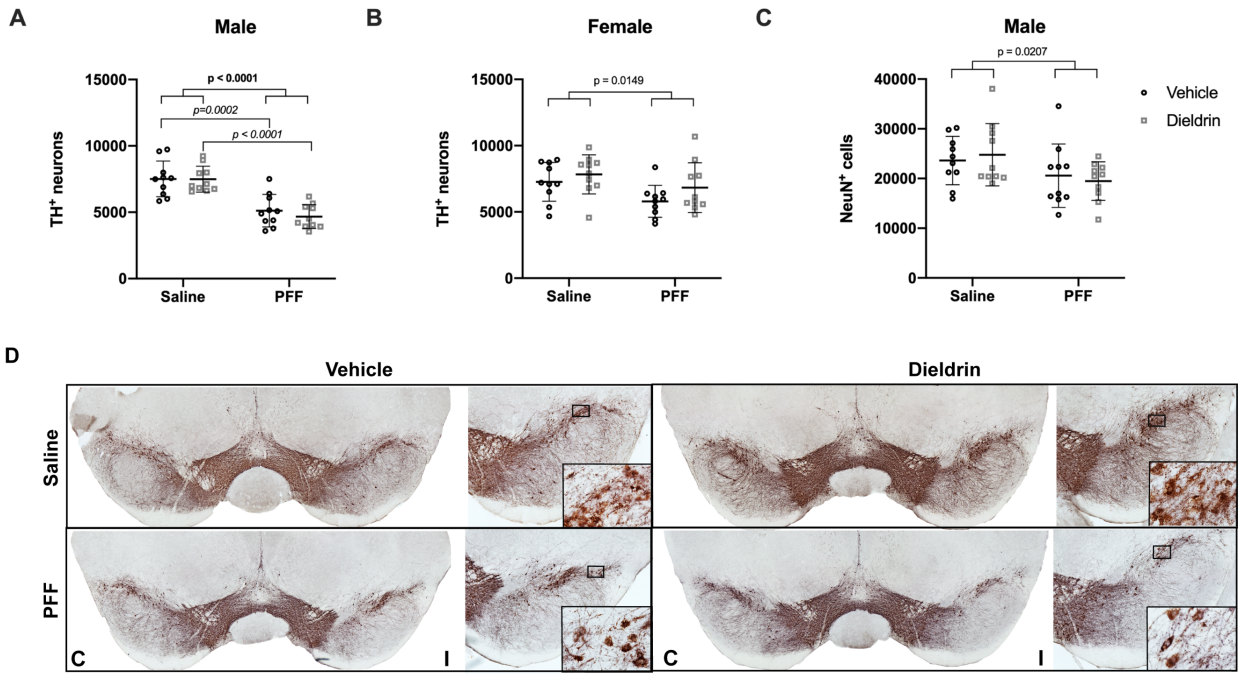

Figure 3.12 Dieldrin does not exacerbate the male-specific PFF-induced loss of ipsilateral nigral TH immunoreactive neurons. Number of TH^+ neurons in the ipsilateral nigra was estimated by unbiased stereology. A) Ipsilateral nigral TH neuron counts in male animals (n = 10 per group) show a PFF-induced loss of TH^+ neurons (two-way ANOVA: PFF, $p < 0.0001$; dieldrin, $p = 0.5215$; interaction, $p = 0.5444$). Sidak post-tests show no significant effect of dieldrin, but a significant effect of PFFs in vehicle and dieldrin exposed animals (vehicle:saline vs vehicle:PFF, $p = 0.0002$; dieldrin:saline vs dieldrin:PFF, $p < 0.0001$). B) Quantification of ipsilateral nigral NeuN counts in male animals (n = 10 per group) show a PFF-induced loss of NeuN (two-way ANOVA: PFF, $p = 0.0207$; dieldrin, $p = 0.9823$; interaction, $p = 0.5133$). Sidak post-tests show no significant effect in any individual comparison. C) Quantification of ipsilateral nigral TH counts in female animals (n = 10 per group) show a PFF effect (two-way ANOVA: PFF = 0.0149; dieldrin = 0.1061; interaction p = 0.6275). Sidak post-tests show no significant effect of PFFs or dieldrin. The only significant post-test was between dieldrin:saline and vehicle:PFF ($p = 0.0304$). D) Representative images from male animals of nigral TH immunohistochemistry. “C” and “I” indicate contralateral and ipsilateral sides. Data shown as mean +/- 95% CI with significant results of two-way ANOVA indicated on graphs in bold and of Sidak post-tests for dieldrin to vehicle comparisons indicated on graphs in italics. All significant post-test results are reported in this legend.

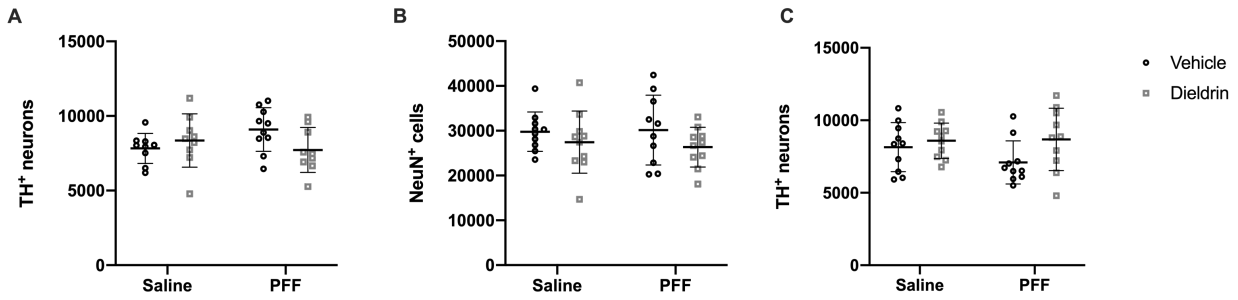

Figure 3.13 PFF injection and dieldrin show no effect on contralateral TH and NeuN immunoreactive neurons. A) Number of TH+ neurons in the contralateral nigra were estimated by unbiased stereology (n = 10 per group). A) There was no effect of dieldrin or PFF on contralateral nigral TH^+ neurons in male animals (two-way ANOVA: PFF, p = 0.5172; dieldrin, p = 0.3922; interaction = 0.0581). B) There was no effect of dieldrin or PFF on contralateral nigral $NeuN^+$ neurons in male animals (two-way ANOVA: PFF, p = 0.8462; dieldrin, p = 0.1186; interaction, p = 0.7063). C) There was no effect of dieldrin or PFF on contralateral nigral TH^+ neurons in female animals (two-way ANOVA: PFF, p = 0.3645; dieldrin, p = 0.0627; interaction = 0.2833). Data shown as mean +/- 95% CI.

Discussion

Male-specific exacerbation of synucleinopathy-induced deficits in motor behavior developmental dieldrin exposure

As an important validation, our results in the PFF-injected animals without dieldrin exposure replicated previous reports of PFF-induced pathology in mice (Chapter 4). Specifically, we observed comparable levels and timing of PFF-induced accumulation of p-syn-positive aggregates, loss of striatal DA, and loss of nigral TH^+ cells (Chapter 4) (194). Our new results in dieldrin-exposed animals demonstrate that developmental dieldrin exposure induces a male-specific exacerbation of PFF-induced behavioral and neurochemical deficits consistent with previous results in the MPTP model (129). However, dieldrin did not exacerbate the timing or extent of PFF-induced α-syn accumulation and aggregation into p-syn positive aggregates in the nigra (Figure 3.7), indicating that dieldrin does not affect the propensity of α-syn to aggregate, but instead may affect the response to aggregation. This exacerbated response manifests as increased PFF-induced motor deficits assessed on the challenging beam and deficits in striatal DA handling 6 months post-PFF injection in animals exposed to dieldrin in male mice (Figure 3.5, Figure 3.8).

Of note, we found that mice exposed to dieldrin and receiving PFFs showed deficits in all beam parameters (traversal time, steps, and errors) over time while PFF alone mice only showed changes in one beam outcome (errors). Nigrostriatal DA system dysfunction and loss lead to the deficits in fine motor coordination and balance, which manifest as a combination of changes in the three outcome measures reported as previously shown in 6-OHDA, MPTP, Pitx3-aphakia, and Thy1-α-syn overexpression models (253,254,257,261).

Consistent with these previous findings, the observed combination of changes in errors per step, total steps and time to traverse indicates that dieldrin exposed male mice have a greater PFF-induced behavioral deficit on challenging beam, which in turn indicates a greater decline in dopaminergic function, as shown in Figure 3.5G. Thus, these results support the hypothesis that dieldrin exposure exacerbates PFF-induced motor deficits. All of the observed impairments on challenging beam were specific to male mice, with female mice showing no effect of dieldrin exposure or PFF injection on their performance on challenging beam (Figure 3.5; see ***Sex differences in PFF-induced motor deficits*** in Chapter 4).

Specifically, PFF injection alone did not affect the speed of male mice on the challenging beam. Only PFF-injected animals previously exposed to dieldrin showed an effect on this outcome measure, displaying a longer time to traverse at 6 months post-PFF injection (Figure 3.5A). Importantly, slowness of movement on the beam is similar to bradykinesia, one of the cardinal motor symptoms observed in PD. This finding is similar to results in other mouse models of PD-related pathology, including the MPTP mouse model and the Pitx3-aphakia mouse (254,257). In the Pitx3-aphakia mouse this deficit was reversed with L-DOPA, highlighting the contribution of the DA system to the traversal time outcome measure. Consistent with previous results in other α-syn models including the Thy1-α-syn overexpression models, we also found that PFF injection alone induced a significant increase in errors per step made on the beam (Figure 3.5C) (253,261). Errors or slips on the beam are suggestive of postural instability, another cardinal motor symptom observed in PD. PFF-injected animals previously exposed to dieldrin did make more errors at 6 months compared to their own baseline; however, they did not make as many errors compared to the PFF-injected animals not

exposed to dieldrin (Figure 3.5C, Figure 3.6C). This seeming discrepancy in results on time to traverse and errors is actually consistent with our previous observations. In MPTP-treated mice, we have observed that this increase in time to traverse can be associated with a reduced number of errors (Fleming et al. unpublished observations). MPTP-treated mice move more slowly across the length of the beam and appear to be more "cautious" with their stepping, resulting in fewer mistakes.

Our failure to replicate the PFF-induced deficit on rotarod likely relates to known variability between labs, and even within labs, on this test in this model (Figure 3.4). The reason behind this inconsistency is not clear. Our own rotarod data has a high level of variability, making it difficult to identify changes. However, given our robust PFF-induced pathology and deficits in our biochemical readouts, we are confident that the PFF-model itself worked. Instead, the rotarod test may lack the sensitivity required to consistently detect PFF-induced deficits. Indeed, there are cases where toxicant and genetic PD mouse models do not shown deficits on the rotarod but do demonstrate deficits in other tests including the challenging beam (262,263). We included the challenging beam in our behavioral tests based on reports of this variability and the inconsistency in rotarod testing in the PFF model. The challenging beam is more sensitive to more subtle changes in fine motor coordination and balance than the rotarod and has been used in a range of PD genetic and toxicant models (253,254,257,261). The discrepancy between the rotarod and challenging beam results reported here may be a result of the differing sensitivities of these tests.

Male-specific exacerbation of synucleinopathy-induced deficits in DA turnover after developmental dieldrin exposure

Defects in DA handling are broadly indicative of DA neuron dysfunction; consistent with this, we observed PFF-induced deficits in the DOPAC:DA and HVA:DA ratios, measures of DA turnover and handling, in both male and female mice (Figure 3.8D,E,I,J). None of these outcome measures were exacerbated by dieldrin exposure except for HVA:DA in male mice at 6 months after PFF injections. This male-specific exacerbation of the PFF-induced increase in DA turnover is indicative of a greater stress on the DA system in male animals and consistent with the male-specific exacerbation of motor deficits discussed above. In addition, the male-specific deficit in DA turnover is consistent with a large body of evidence supporting a central role for cytosolic DA in PD pathogenesis (128). Critically, it is not only overall levels of DA that matter for disease etiology and progression, but also the ability of a neuron to maintain DA within synaptic vesicles to both protect against cytosolic degradation of DA and allow the cell to release enough DA into the synapse (151,153–155,183,264–269). Taken together, the behavioral and HPLC data suggest that developmental dieldrin exposure causes persistent changes to the nigrostriatal system that exacerbate the response to PFF-induced synucleinopathy through disruption of striatal synaptic terminals (Figure 3.11, Figure 3.14). These results suggest that a more detailed analysis of DA uptake, release and turnover in the striatum is warranted in this two-hit model.

In contrast to the neurochemical findings, we did not observe an exacerbation in loss of nigral TH phenotype or degeneration of nigral neurons at the same 6-month time point (Figure 3.12). The discrepancy between these striatal and nigral observations may be a byproduct of the time point chosen. Six months after PFF injections was the latest time point that we

assessed in this study, but also the earliest time point where we observed neurochemical or behavioral deficits. Therefore, it is possible that 6 month follow-up is still too early to observe the effects of exposure-induced exacerbation of degeneration, which typically lags behind striatal dysfunction and degeneration of the synaptic terminals. Thus, at later time points, animals with greater striatal synaptic deficits may eventually show greater nigral loss. Now that we have established the phenotype in this two-hit model, further studies will assess possible acceleration and/or exacerbation of these synaptic deficits in the striatum at later time points.

A model of dieldrin-induced increases in susceptibility to synucleinopathy

Based on the results reported here, our previous characterization of epigenetic changes induced by developmental dieldrin exposure, and the mechanisms of dieldrin toxicity, we propose a model for how developmental dieldrin exposure leads to increased susceptibility to synucleinopathy induced deficits in motor behavior (129,191). In this model, exposure to dieldrin occurs during prenatal and postnatal development. The half-life of dieldrin in mouse brain is less than a week, so no detectable dieldrin remains in the brain of F1 offspring by a few weeks after weaning (129,179,270). When dieldrin is present in the developing brain, it is thought to act on developing DA neurons by inhibiting $GABA_A$ receptor-mediated chloride flux, resulting in increased neuronal activity (Figure 3.14A) (184,185,187,189,271,272). Based on previous results, we propose that this net increase in neuronal activity modifies the dopamine system through persistent changes in epigenetic mechanisms, leading to dysregulation of genes important for dopamine neuron development and maintenance (Figure 3.14B,C) (191). We hypothesize that these changes then alter the response of this system to future insults, possibly via alterations in striatal dopamine synapses that manifest as increased DA turnover

upon application of PFFs (Figure 3.8, Figure 3.14C). In support of our proposed model, the present work reported here identified a dieldrin-induced, male-specific exacerbation of PFF-induced deficits in striatal DA handling (Figure 3.8, Figure 3.14D) and motor behavior (Figure 3.5, Figure 3.14E). Further studies in our lab will focus on exploring the synaptic mechanisms underlying this phenotype and will aim to connect the observed epigenetic changes with these mechanisms. In addition, in a current study, we are tracking the longitudinal patterns of dieldrin-induced epigenetic changes from birth to 12 weeks of age to determine if dieldrin-induced epigenetic changes are maintained from birth or if they represent an altered longitudinal trajectory of epigenetic changes.

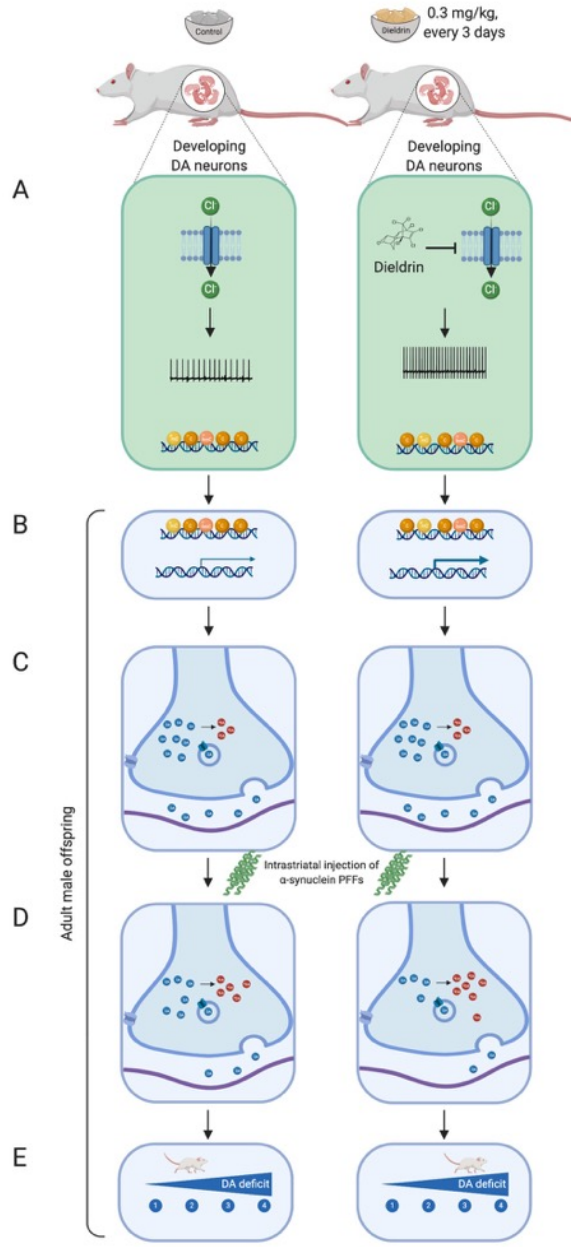

Figure 3.14 Proposed mechanism by which developmental dieldrin exposure leads to exacerbation of PFF-induced toxicity. Dams are fed vehicle or dieldrin containing food starting 1 month prior to mating and continuing through weaning of F1 pups. Dieldrin inhibits chloride influx through GABAA receptors resulting in increased neuronal activity (A). This change in activity produces epigenetic changes throughout the lifespan even when dieldrin is no longer present (B). These epigenetic changes affect dopamine neuron development and maintenance, producing stable changes in striatal dopamine synapse function (C). These synaptic changes lead to increased susceptibility to PFF-induced synucleinopathy (D, E). Created in BioRender.

Conclusion

In chapter of this dissertation, we demonstrated sex-specific effects of developmental dieldrin exposure on α-syn PFF-induced toxicity. Specifically, we showed that developmental dieldrin exposure increases α-syn-PFF-induced motor deficits and deficits in DA handling but does not affect PFF-induced loss of nigral TH^+ neurons. These results indicate that our two-hit exposure model represents a novel experimental paradigm for studying how environmental factors increase risk of PD.

Chapter 4 Sex-specific susceptibility in the α-syn PFF mouse model

Abstract

Parkinson's disease (PD) is more common in males and the disease course in males is more severe. While the exact mechanisms underlying these sex differences are unclear, and it has been hypothesized that higher estrogen in females leads to higher dopamine levels in the striatum, which protects against PD. Despite this known sex difference, most animal models of PD have only been characterized in male animals, with observations of female resilience in a variety of models largely ignored. Attempts to model sex differences have typically required surgical and pharmacological treatments to manipulate hormonal state. Here, we compared the response of male and female mice to α-syn PFF-induced synucleinopathy to test the hypothesis that male mice will show increased susceptibility compared to female mice, reflecting the sex difference in human PD. We found that female mice show PFF-induced pathology, but no PFF-induced motor deficits. Specifically, male mice, but not female mice, show PFF-induced motor deficits on the challenging beam 6 months after PFF injection. Male and female animals showed similar levels of PFF-induced phosphorylated α-syn (p-syn) aggregation, loss of DA, DOPAC and HVA levels and increases in DA turnover. While these data at first appear contradictory, our data suggest that female animals may show less loss of ipsilateral nigral TH immunoreactivity than male mice. Together, these results suggest a new hypothesis that female mice may have reduced or slower loss of nigral DA neurons and a resulting behavioral resilience to the same level of DA loss compared to their male counterparts. This is the first study to show sex differences in sensorimotor function in the PFF model and suggests that the PFF model may be a valuable tool to model sex-differences in PD

pathology and etiology that does not require any additional surgery or other treatments to manipulate hormonal state.

Introduction

Sex differences in Parkinson's disease

PD is more common in males than in females across all ages with twice as many men suffering from PD than women in any given age range (10). In males, the incidence rate rises from 3.59 per 100,000 persons at 40-49 years to 132.72 per 100,000 at 70-79 years (4). The corresponding incidence rate is lower in females: 2.94 per 100,000 at 40-49 years and 104.99 per 100,000 at 70-79 years (4). For both sexes, incidence declines after age 80, with peak incidence rates between 70-79 years (4). In addition, average age of onset is approximately 2 years earlier in men than women (11,12). In all nations studied, males are at greater risk for developing PD at all ages, with twice as many men diagnosed with PD than women (10,13–17,19,273,274). Furthermore, the age of onset for PD is approximately 2 years earlier in men than women (11,12), and the disease course tends to be more severe in males (10–19). Specifically, women present more often with tremor-dominant PD, which is associated with milder motor deterioration and striatal degeneration (11). While the mechanisms underlying these sex differences are unclear, it has been hypothesized that higher estrogen in females leads to higher dopamine levels in the striatum, which protects against PD (11). Despite the well-known effects of sex in human PD, studies investigating sex differences in animal models of PD remain scarce, with most studies exclusively using male animals.

Sex differences in parkinsonian susceptibility in developmental dieldrin models

In our developmental dieldrin model of parkinsonian susceptibility, we and others have demonstrated a sex-specific effect on the epigenome, inflammation pathways and susceptibility to both MPTP and α-syn PFFs (129,190,191) (Chapter 2, Chapter 3). In our lab, we previously

reported distinct patterns of differential DNA methylation in male and female offspring induced by developmental dieldrin (191). Previous studies have also shown that developmental dieldrin exposure has specific phenotypic effects in male and female mice, including male-specific changes in dopamine turnover and a male-specific increased susceptibility of dopaminergic neurons to MPTP (129). In earlier chapters of this dissertation we demonstrated the sex-specific effects of developmental dieldrin exposure on α-syn PFF-induced toxicity. Specifically, we showed that developmental dieldrin exposure increases α-syn-PFF-induced motor deficits and deficits in DA handling but does not affect PFF-induced loss of nigral TH^+ neurons (190). Moreover, we observed sex-specific effects of developmental dieldrin exposure on neuroinflammation (190). Despite this known sex differences in PD, most animal models of PD have only been characterized in male animals, with observations of female resilience in a variety of models largely ignored (10–18,235,236). In addition, attempts to model sex differences have typically required surgical and pharmacological treatments to manipulate hormonal state.

While the observed male-specific exacerbation of PFF toxicity after dieldrin exposure reported in Chapter 3 was expected, the finding that PFFs alone did not induce motor deficits in female animals was quite surprising. While this study was not designed to look at sex differences specifically, when analyses were stratified by sex in Chapter 3, we identified novel sex differences in sensorimotor function in the PFF model. Therefore, in this chapter, we have highlighted the sex specific differences we observed in the α-syn PFF model in unexposed group of animals.

While L-DOPA and related dopaminergic therapies help to manage motor symptoms in PD, there are no current therapies to slow or stop nigrostriatal degeneration in PD. This is partly due to the failure of animal models to recapitulate critical aspects of human disease such as Lewy Body formation and typical PD behavioral deficits in animal models (192). MPTP is the gold standard for pre-clinical testing, this model does not replicate specific key aspects of PD pathogenesis such as α-syn pathology, the progressive disease course, and behavioral deficits (192). Previous α-syn-based models do show some of these missing characteristics (i.e. α-syn pathology), but many rely on overexpression and super-physiological α-syn levels that are never seen in human brain. The α-syn preformed fibril (PFF) model of synucleinopathy was developed in rats and mice in order to address these limitations (193,194). This model shows protracted course of synuclein pathology and nigrostriatal degeneration, produces motor deficits without supraphysiological levels of α-syn protein, and progressive neuropathological and behavioral phenotypes (193–195).

In the PFF model, α-syn fibrils are generated from recombinant α-syn monomers and sonicated into small fragments that are about 50 nm in length. When applied to cells in cultures or injected directly in the brain of mice or rats, these fragments are taken into the synaptic terminals where they seed the formation of endogenous α-syn into insoluble phosphorylated α-syn (p-syn) inclusions. This eventually leads to neuronal dysfunction and degeneration while maintaining the context of normal physiological levels of endogenous α-syn. Supporting the idea that α-syn PFF-induce toxicity depends on the recruitment of the endogenous α-syn, introduction of PFFs to primary neurons that lack α-syn or in α-syn knockout mice do not induce toxicity (193,195–198).

The PFF model, first reported in male mice in a seminal 2012 paper, was later replicated in male rats (193,199–202). In male mice, intrastriatal injection of α-syn PFFs leads to deposits of hyperphosphorylated p-syn in regions that innervate the injection site. These p-syn deposits can be detected at the injection site in striatum, in cortical layers 4 & 5, and in the olfactory bulb ipsilateral to the injection site within the first 30 days after PFF injections. p-syn containing inclusions develop progressively, evolving from pale cytoplasmic accumulations at 1 month post PFF to dense perinuclear inclusion at 3 month post PFF in mice (194). The amygdala shows bilateral p-syn deposits consistent with its bilateral connections to the striatum. By 180 days post injection, p-syn immunoreactivity increases in affected regions and extends into contralateral neocortex, ventral striatum, thalamus, occipital cortex, commissural and brainstem fibers. Particularly relevant for studies of PD, p-syn aggregates also form in the SNc, with a peak at 2-3 months post-injection (194). Furthermore, striatal DA levels are reduced 3 months following PFF injections, and significant loss of TH and motor deficits are seen 6 months after the PFF injections (194). Though these events have been validated across multiple studies, they have only been characterized in male animals.

The α-syn PFF model was also replicated and optimized in male rats (193,200,202,203). The timeline of events is slightly different in rat, but the overall effect is similar. As in mice, actual neurodegeneration lags behind loss of TH phenotype (193). Unlike in mice, rats show contralateral degeneration at 6 months post-PFF injection. However, this may be seen at later time points in mice, as they have a slower time course of degeneration than rats in this model (193,199).

Methods

Animals

Male and female C57BL/6 mice were purchased from Jackson Laboratory (Bar Harbor, Maine). Female mice were 7 weeks old upon arrival. In contrast, male mice used for breeding were 11 weeks old upon arrival. After a week of habituation, mice were switched and maintained on a 12:12 reverse light/dark cycle for the duration of the study. Mice were housed in Thoren ventilated caging systems with automatic water and 1/8-inch Bed-O-Cobs bedding with Enviro-Dri for enrichment. Food and water were available ad libitum. Mice were maintained on standard LabDiet 5021chow (LabDiet). F0 females were individually housed except during the mating phase. F1 pups were group housed by sex; with 2-4 animals per cage. All procedures were conducted in accordance with the National Institutes of Health Guide for Care and Use of Laboratory Animals and approved by the Institutional Animal Care and Use Committee at Michigan State University.

Preparation of α-syn PFFs and verification of fibril size

Fibrils were generated using wild-type, full-length, recombinant mouse α-syn monomers as previously described (194,196,197,200,250). Quality control was performed on full length fibrils to confirm fibril formation (by transmission electron microscopy), amyloid structures within fibrils (by thioflavin T assay), a shift to higher molecular weight species compared to monomers (by sedimentation assay), and low bacterial contamination (<0.5 endotoxin units mg^{-1} of total protein via a *Limulus* amebocyte lysate assay). On the day of surgery, PFFs were thawed to room temperature and diluted to 2 µg/µl in Dulbecco's phosphate buffered saline (PBS) (Gibco), and sonicated at room temperature using an ultrasonic homogenizer (300 VT;

Biologics, Inc.) for 60 seconds, with 1 second pulses with the pulser set at 20% and power output set at 30%. Prior to surgeries, an aliquot of sonicated PFFs was analyzed using transmission electron microscopy.

Transmission electron microscopy

Transmission electron microscopy was performed as previously described (200). Samples were prepared on Formvar/carbon-coated copper grids (EMSDIASUM, FCF300-Cu). Grids were washed twice by floating grids on drops of distilled H_2O. Grids were floated for 1 min on 10 µl drops of sonicated PFFs diluted 1:50 in PBS, followed by 1 min on 10 µl drops of aqueous 2% uranyl acetate, wicking away liquid with filter paper after each step. Grids were allowed to dry before imaging with a JEOL JEM-1400+ transmission electron microscope. Pre-surgery, a brief assessment of fibril size was performed by measuring 20 representative fibrils to ensure fibril length was approximately 50 nm, a length known to produce optimal seeding (251,252). Post-surgery, the length of over 500 fibrils per sample was measured, and the average length and the size distribution plotted (Figure 4.1).

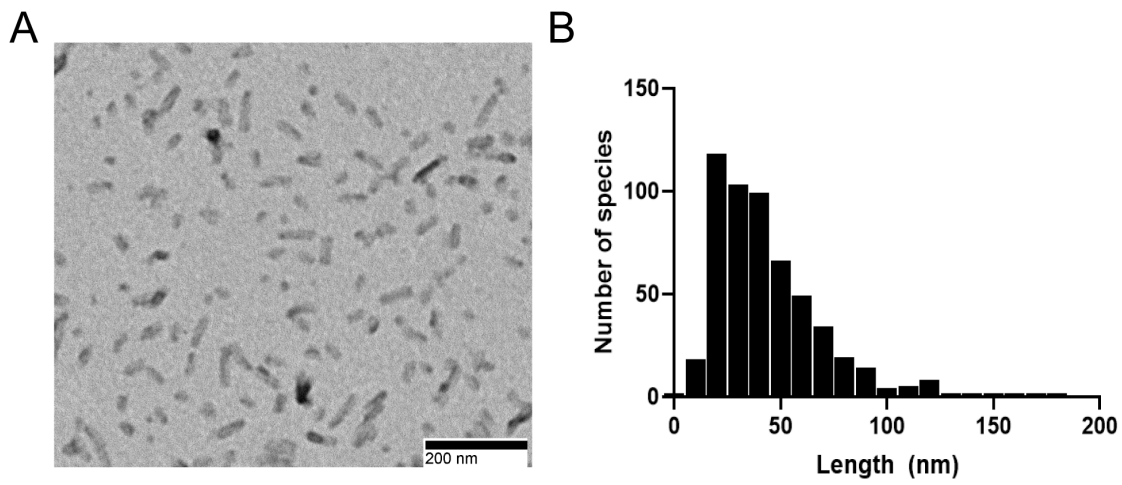

Figure 4.1 Confirmation of α-syn PFFs size (A) Representative TEM image of PFFs (B) Frequency distribution of estimated fibril size.

Intrastriatal injections of α-syn PFFs

Surgeries were performed as previously described, with slight modifications (194). Prior to surgery, mice were anesthetized with isoflurane. After anesthesia, 2.5µl of liquid was unilaterally injected into the dorsal medial striatum using the following coordinates relative to bregma: anterior-posterior = 1.6 mm, medial-lateral = 2.0 mm, and dorsal ventral = -2.6mm. Injections were performed using pulled glass needles attached to 10µl Hamilton syringes at a flow rate of 0.5µl/minute. At the end of the injection, the needle was left in place for one-minute, withdrawn 0.5 mm, left in place for an additional two minutes to avoid displacement of PFFs, and then completely retracted. Unilateral injections consisted of PBS (saline control) or 2µg/µl α-syn PFFs (5µg of total protein). During surgeries, PBS and PFFs were kept at room temperature. Post-surgery, animals received an analgesic (1mg/kg of sustained release buprenorphine, subcutaneous administration) and were monitored closely until they recovered

from anesthesia. In the three days following recovery, animals undergoing surgery were monitored daily for adverse outcomes.

Motor behavior assessment (challenging beam)

The challenging beam was used to test motor performance and coordination. This test has been shown to be sensitive in detecting sensorimotor deficits in toxicant, α-syn, and genetic mouse models of PD with nigrostriatal dysfunction or neurodegeneration (253–257). Briefly, prior to beam training and testing, mice were acclimated to the behavior room for one hour. All behavioral experiments started at least one hour into the wake (dark) cycle of the mice. The plexiglass beam consisted of four 25 cm sections of gradually decreasing widths (3.5 cm, 2.5 cm, 2.0 cm, and 0.5 cm) and was assembled into a one-meter-long tapered beam. The home cage was placed at the end of the narrowest section to encourage mice to walk the length of the beam into their home cage. Mice were trained for two days on the tapered beam and received five trials each day. On the day of the test, the beam was made more challenging by placing a mesh grid (squares = 1 cm^2) over the beam. The grid corresponded to the width of each beam section and created an ~1 cm distance between the top of the grid and the beam. This allowed for the visualization of limb slips through the grid. On the day of the test, each mouse was videotaped for 5 trials. All mice were tested at baseline (prior to PFF injections) and at 4 and 6 months post-PFF injection. Videos were scored by trained raters blinded to experimental condition and with an inter-rater reliability of at least 90%. Raters scored the following outcome measures: time to traverse the beam, number of steps, and errors. An error was defined as a limb slip through the mesh grid during a forward movement (253). Each limb accounted for its own error (e.g. 2 slips in 1 forward movement = 2 errors). The mean of the 5

trials was used for analysis. For analysis, data were stratified by time point because experiments were not powered for longitudinal analysis.

Motor behavior assessment (rotarod)

Rotarod testing was performed as previously described (194). Prior to rotarod training and testing, mice were acclimated to the behavior room for one hour. All behavioral experiments started at least one hour into the wake (dark) cycle of the mice. For training, each mouse received 3 practice trials with at least a 10-minute interval between each trial. For each trial, mice (n=10 per group) were placed on a rotarod with speed set at 5 rpm for 60 seconds. If an animal fell off, it was placed immediately back on the rotarod. Testing occurred 24 hours after training. For testing, the rotarod apparatus was set to accelerate from 4 to 40 rpm over 300 seconds and the acceleration was initiated immediately after an animal was placed on the rotarod. Each mouse underwent 3 trials with an inter-trial interval of at least 15 minutes. Males were always tested before the females, and the rods were cleaned between the trials to prevent cross-scents interfering with performance. All mice were tested at baseline (before receiving PFF injections) and at 4 and 6 months after PFF injections. The mean latency to fall in all 3 trials was used for analysis. For analysis, data were stratified by time point because experiments were not powered for longitudinal analysis.

Tissue collection

All animals were euthanized by pentobarbital overdose and intracardially perfused with 0.9% saline. At the 1-month time point, saline perfusion was followed by cold 4% paraformaldehyde perfusions and whole brains were extracted and post-fixed in 4% PFA for 24 hours and placed into 30% sucrose for IHC. For 2- and 6-months times point, brains were

extracted after saline perfusion and rostral portions of each brain were flash frozen in 2-methylbutane on dry ice and stored at -80˚C until use for HPLC. The caudal portions of each brain were post-fixed in 4% PFA for 24 hours and placed into 30% sucrose for IHC.

HPLC

Striatal tissue punches (1mm x 2mm) were collected from the dorsal striatum on a cryostat and sonicated in 200 µl of an antioxidant solution (0.4 N perchlorate, 1.34 mm EDTA, and 0.53 mm sodium metabisulfite). A 10 µl aliquot of the sonicated homogenate was removed into 2% SDS for BCA protein assay (Pierce). Remaining samples were clarified by centrifugation at 10,000 rpm for 10 minutes. Deproteinized supernatants were analyzed for levels of DA, HVA and DOPAC using HPLC. Samples were separated on a Microsorb MV C18 100–5 column (Agilent Technologies) and detected using a CoulArray 5200 12-channel coulometric array detector (ESA) attached to a Waters 2695 Solvent Delivery System (Waters) using the following parameters: flow rate of 1 ml/min; detection potentials of 25, 85, 120, 180, 220, 340, 420 and 480 mV; and scrubbing potential of 750 mV. The mobile phase consisted of 100 mm citric acid, 75 mM Na_2HPO_4, and 80 µm heptanesulfonate monohydrate, pH 4.25, in 11% methanol. Sample values were calculated based on a six-point standard curve of the analytes. Data were quantified as ng/mg protein.

Immunohistochemistry

Fixed brains were frozen on a sliding microtome and sliced at 40 µm. Free-floating sections were stored in cryoprotectant (30% sucrose, 30% ethylene glycol, 0.05M PBS) at -20°C. A 1:4 series was used for staining. Nonspecific staining was blocked with 10% normal goat serum. Sections were then incubated overnight in appropriate primary antibody: p-syn (Abcam,

Ab184674, 1:10,000), TH (Millipore, MAB152, 1:4,000). Primary antibodies were prepared in TBS with 1% NGS/0.25% Triton X-100. Sections were incubated with appropriate biotinylated secondary antibodies at 1:500 (anti-mouse, Millipore AP124B or anti- Millipore AP132B), followed by Vector ABC standard detection kit (Vector Laboratories PK-6100). Visualization was performed using 0.5mg/ml 3,3' diaminobenzidine (DAB, Sigma-Aldrich) for 30sec-1minute at room temperature and enhanced with nickel. Slides stained for p-syn slides were counter-stained with Cresyl violet. Slides were dehydrated before coverslipping with Cytoseal (Richard-Allan Scientific) and imaged on a Nikon Eclipse 90i microscope with a QICAM camera (QImaging) and Nikon Elements AR (version 4.50.00).

Quantification of p-syn inclusion-bearing neurons in the SNpc

Total enumeration of neurons containing p-Syn was performed using StereoInvestigator (MBF Bioscience). The investigator was blinded to the treatment groups. Sections containing the SNpc (1:4 series) were used for all counts. Contours were drawn around the SNpc using the 4x objective. A 20x objective was used to identify the stained inclusions. All neurons containing p-syn within the contour were counted and total counts were multiplied by four to estimate the total number of neurons in each animal with inclusions. Samples injected with PFFs that did not have any p-syn pathology were excluded as missed injections.

Stereology

TH immunoreactive neuronal counts were estimated by unbiased stereology with StereoInvestigator (MBF Bioscience) using the optical fractionator probe as described previously (258–260). Briefly, sections containing the SNpc (1:4 series) were used for all counts. In all cases, the investigator was blinded to the treatment groups. Contours around the SNpc

were drawn using the 4x objective and counting was done using a 60X oil immersion objective. The following settings were used: grid size (195 µm x 85 µm), counting frame (50 µm x 50 µm), guard zone (3 µm) and optical dissector height (23 µm). Section thickness was measured every third counting frame, with an average measured thickness of 29 µm. TH labeled neurons within the counting frame were counted while optically dissecting the entire section through the z-axis. Variability was assessed with the Gundersen coefficient of error (≤0.1).

Data analysis and statistics

Statistical analysis of all data and graphing were performed using either GraphPad Prism or R (version 3.5.3). This study was not designed to look at sex differences specifically, so all analyses were stratified by sex. All two-group comparisons were performed using an unpaired Welch's t-test. Stereology, HPLC results and post-PFF behavior were compared by two-way ANOVA followed by Sidak's multiple comparisons tests. Pregnant dams were the experimental unit for all analyses and all pups for each outcome came from independent litters. Here, Sidak's multiple comparisons tests are reported if and when they are significant following two-way ANOVA in Chapter 3. The comparison between sexes for this chapter is qualitative and suggestive of a need for experiments designed to test this hypothesis.

Results

Female mice do not show PFF-induced motor deficits

Animals were tested on challenging beam and rotarod prior to PFF injections (baseline), and at 4 months and 6 months post-PFF injections. Rotarod measures motor coordination and motor impairment (177,275). On the rotarod, we observed no PFF-induced deficits in the latency to fall at any time point in either sex (Figure 4.2). On challenging beam, a sensorimotor test that assesses fine motor coordination and balance in mice, the biggest differences were detected at the 6 month time point (Figure 4.3) (253–257). Results from each timepoint are described below.

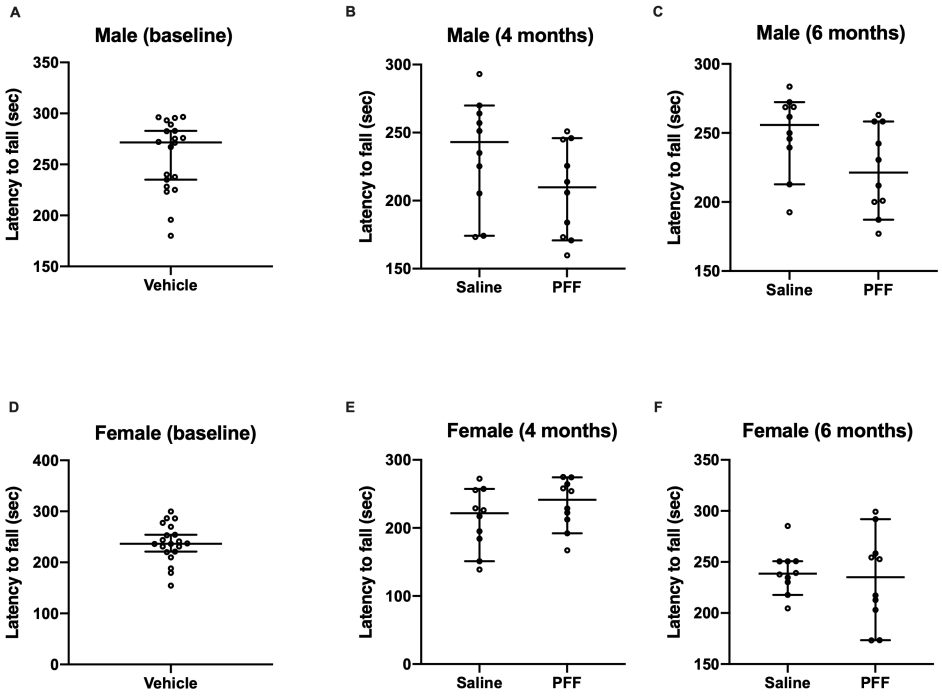

Figure 4.2 No PFF induced effects were observed on rotarod in male or female mice. Male and female mice (n = 20 per group at baseline, n = 10 per group at later time points) were tested on rotarod prior to PFF injections (Baseline) and at 4 and 6 months post-PFF injections. Latency to fall in both sexes at all time points was unaffected by PFF injection. All data shown as mean +/- 95% CI.

Baseline: At baseline, our results in vehicle exposed animals suggest that males and females may perform differently on the challenging beam with no treatment. While we did not specifically design the experiments to test for sex differences, these results suggest that while males and females traverse the beam in a similar amount of time, males may take more, smaller steps and make fewer errors at 12 weeks of age (Table 4.1).

	Male	***Female***
Time to traverse	11.60 (10.45-12.74)	12.84 (11.52-14.16)
Steps	20.01 (18.89-21.13)	17.80 (17.43-18.17)
Errors/Step	0.047 (0.036-0.058)	0.0885 (0.07-0.10)

Table 4.1 Challenging beam performance in male and female mice at baseline. Male and female mice (n = 20 per group) were tested on challenging beam prior to PFF injections. Data are shown as mean (95% CI).

4 months post PFF injection: In male animals, we observed no differences between saline and PFF injected animals in time to traverse the beam, steps and errors per step at this time point (Table 4.2).

In female animals, there were also no differences between saline and PFF injected in time to traverse (Table 4.2). PFFs induced a significant increase in steps and errors/steps. Saline injected animals made fewer steps and fewer errors per step at time point than they did at baseline (Figure 4.4).

Male	**Saline**	**PFF**
Time to traverse	11.136 (10.053-12.219)	10.849 (9.585-12.113)
Steps	16.84 (16.166-17.514)	15.720 (14.933-16.507)
Errors/Step	0.080 (0.049-0.058)	0.057 (0.040-0.0674)
Female		
Time to traverse	11.273 (10.182-12.364)	11.974 (10.392-13.556)
Steps	15.020 (14.308-15.732)	17.180 (16.481-17.879)
Errors/Step	0.046 (0.026-0.066)	0.113 (0.083-0.143)

Table 4.2 Challenging beam performance in male and female mice at 4 months post-PFF injection. Male and female mice (n = 10 per group) were tested on challenging beam 4 months after PFF injections. Two-way ANOVA with Sidak's multiple comparison tests were performed among 4 groups in Chapter 3. *Males:* Sidak's multiple comparison tests showed that there were no effects of PFFs on time to traverse, steps, and errors/step. *Females:* There were no significant differences in time to traverse. Sidak post-tests revealed a significant effect of PFFs on steps (vehicle:saline vs vehicle:PFF, $p<0.0001$) and on errors/step (vehicle:saline vs vehicle:PFF, $p = 0.0011$). Data are shown as mean (95% CI)

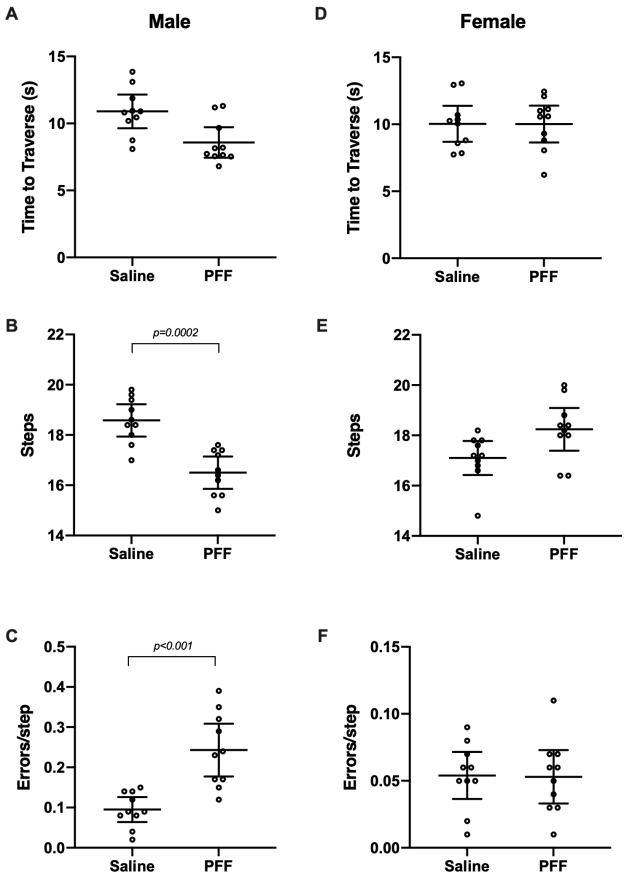

Figure 4.3 Dieldrin exacerbates PFF-induced motor deficits on challenging beam in male animals only. Six months after PFF-injection, motor behavior was assessed on challenging beam in male (A-C) and female (D-F) animals (n = 10 per group). Time to traverse (A,D), steps across the beam (B,E) and errors per step (C,F) were scored. A) Time to traverse at 6 months after PFF injection in male animals B) Steps at 6 months after PFF injection in male animals. Sidak post-tests showed significant effect of PFF vehicle:saline vs vehicle:PFF, p = 0.0002). C) Errors per step at 6 months post-PFF injection. Sidak post-tests showed a significant effect of PFF (vehicle:saline vs vehicle:PFF, p < 0.001). D-F) In female animals, all results were non-significant. All data shown as mean +/- 95% CI with significant results of Sidak post-tests for PFF to saline comparisons indicated on graphs. All significant post-test results are reported in this legend.

6 months post PFF injection: In male animals, we observed no effect of PFF in time to traverse (Figure 4.3A). For steps, PFF-injection caused a significant decrease in steps (Figure 4.3B). Meanwhile, there was a robust PFF-related increase in errors per step (Figure 4.3C). In contrast, at this timepoint in females, there was no effect of PFFs in any of the outcomes (Figure 4.3D-F).

Overall, time to traverse and total steps were fairly constant in both male and female mice across all time points tested (Figure 4.4A,D). In males, PFFs had significant effect on errors/step at 6-month time point in comparison to prior time points (Figure 4.4B,C). In contrast, PFFs had no effect on errors/step in female animals (Figure 4.4E,F).

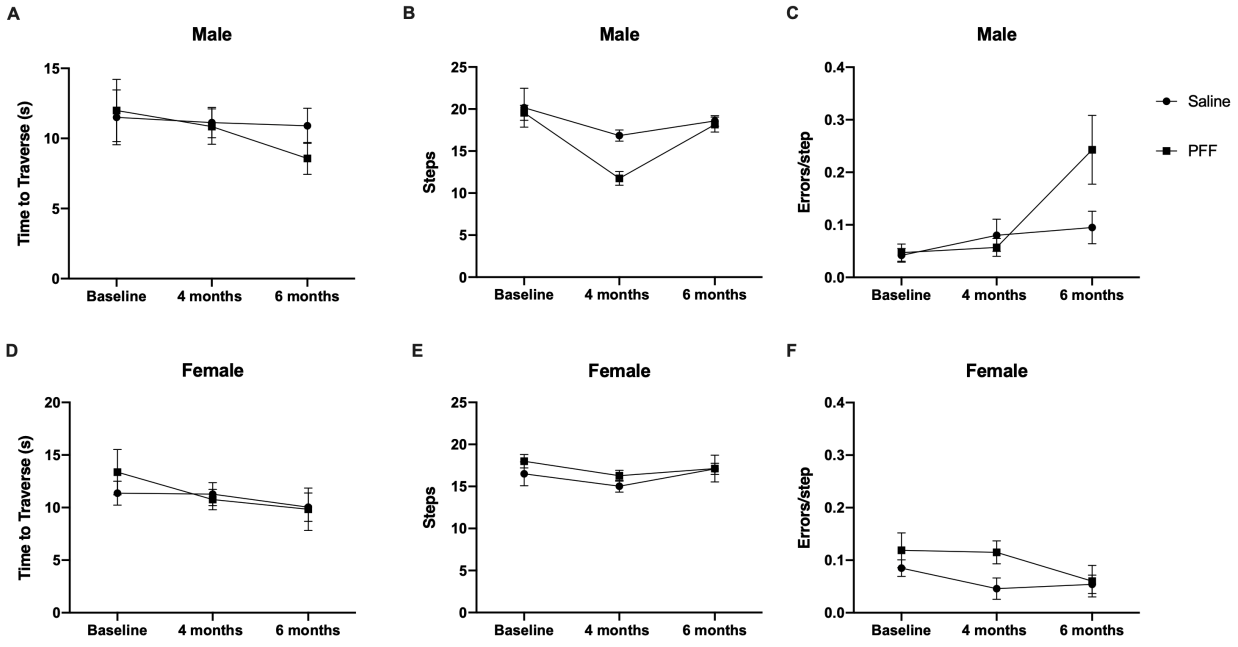

Figure 4.4 Behavioral data at all time points. All challenging beam data presented longitudinally to highlight changes over time. A-C) Male animals; D-F) Female animals; A,D) Time to traverse; B,D) Steps; C,F) Errors per step. Statistical analysis was stratified by time point since we lacked statistical power for a longitudinal analysis. All data shown as mean +/- 95% CI.

Male and female mice show similar levels of PFF-induced α-syn aggregation

In mice, p-syn aggregates accumulate progressively until 2 months after PFF injections in the substantia nigra (SN) pars compacta, evolving from pale cytoplasmic inclusions 1 month post-PFF injection to dense perinuclear Lewy body-like inclusions by 3 and 6 months post-PFF injection (194). Here, we quantified the number of p-syn-containing neurons in the ipsilateral SN at 1 and 2 months post-PFF injection in male and female mice.

Our results showed that the α-syn PFFs seed the formation of p-syn-positive aggregates in nigral neurons to a similar degree in male and female mice at both the 1 month and 2 month time points (Figure 4.5). Consistent with previous observations, there were no p-syn-containing inclusions in the contralateral SN in either male or female mice. Taken together, these data demonstrate that PFF-induced seeding of p-syn-positive aggregates proceeds on a similar timeline and to a similar degree in male and female mice.

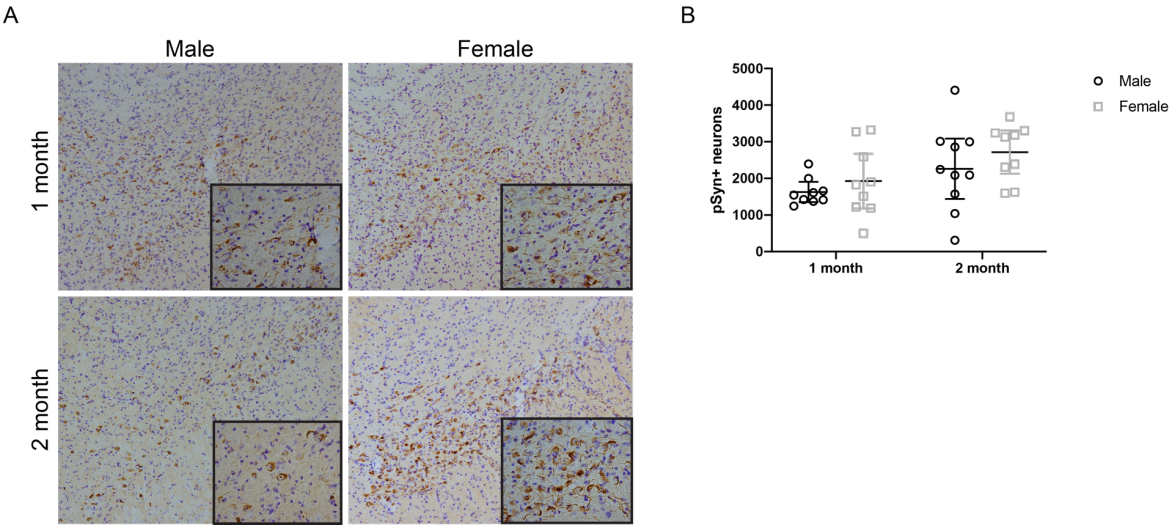

Figure 4.5 Developmental dieldrin exposure does not affect the propensity of p-syn to accumulate in the SN. A) Representative images of p-syn immunohistochemistry from the identical coronal levels through the ipsilateral SN in male and female animals 1 and 2 months after intrastriatal PFF injection. B) Total enumeration of p-syn-containing neurons in ipsilateral SN in male animals (n = 9 for 1-month n= 10 for 2 month). C) Total enumeration of p-syn-containing neurons in ipsilateral SN in female animals (n = 9). Data shown as mean +/- 95% CI.

Male and female mice have similar levels of PFF-induced striatal DA turnover

We also tested PFF-induced effects on levels of DA and two of its metabolites, DOPAC and HVA, in ipsilateral and contralateral dorsal striatum by HPLC at 2 and 6 months post-PFF injections in male and female mice.

At 2 months, we showed PFF-induced deficits in DA levels in the ipsilateral dorsal striatum of male animals (Figure 4.6A). Female mice also exhibit a PFF-induced loss of striatal

DA (Figure 4.6F). In both male and female animals, we observed PFF-induced deficits in DOPAC and HVA by 2-way ANOVA on 4 groups we tested in Chapter 3 (Figure 4.6B,C,G,H). These were significant by Sidak post-tests in female animals, yet they were not significant in male animals. To investigate the effects of PFFs on DA turnover, we calculated ratios of DOPAC and HVA to DA. In both sexes, we observed PFF-induced increases in the DOPAC:DA and HVA:DA ratios by 2-way ANOVA on 4 groups tested in Chapter 3, indicative of increased DA turnover and deficits in DA packaging (Figure 4.6D,E,I,J). These changes were not significant by Sidak post-tests except for DOPAC:DA ratio in female mice

At 6 months, consistent with previous results, we showed PFF-induced deficits in DA levels (~45% loss at 6 months) in the ipsilateral dorsal striatum of male animals (Figure 4.7A)(194). Female mice also exhibit a PFF-induced loss of striatal DA (~40% loss at 6 months) at both time points (Figure 4.7F). In both male and female animals, we observed PFF-induced deficits in DOPAC and HVA by 2-way ANOVA on 4 groups we tested in Chapter 3 but these were not significant by Sidak post-tests except for DOPAC levels in female mice (Figure 4.7B,C,G,H). In both sexes, we observed PFF-induced increases in the DOPAC:DA and HVA:DA ratios by 2-way ANOVA on 4 groups tested in Chapter 3, indicative of increased DA turnover and deficits in DA packaging similar to what was observed in 2 month time point (Figure 4.7D,E,I,J). These changes were not significant by Sidak post-tests.

As expected, levels of DA and its metabolites remained unchanged following PFF injection in the contralateral striatum and dieldrin exposure alone had no effect on DA levels, DA metabolites, or DA turnover in the contralateral striatum (Figure 4.8).

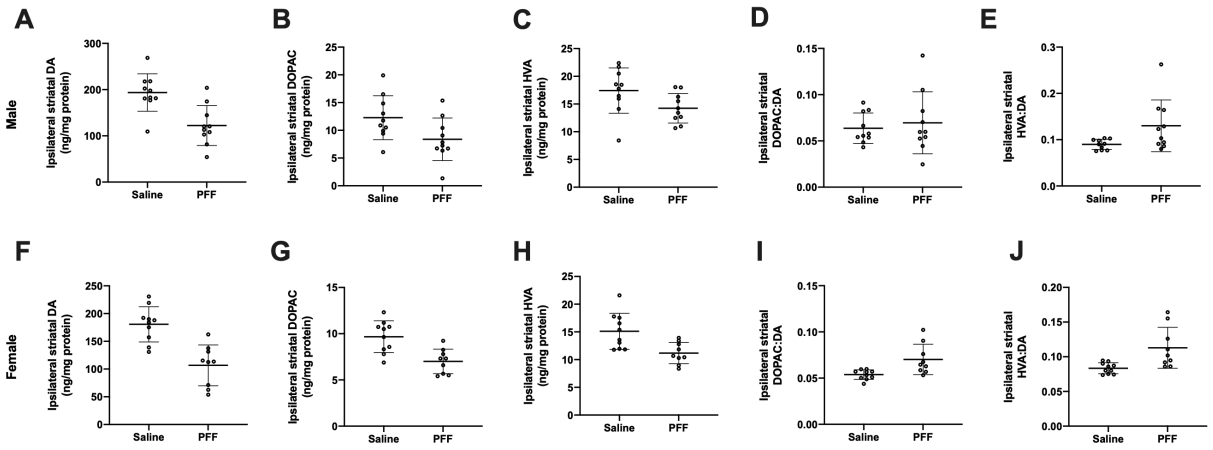

Figure 4.6 HPLC results at 2 months post-PFF injections. Levels of DA, DOPAC and HVA in ipsilateral dorsal striatum were measured 2 months post-PFF injection by HPLC in male (A-E) and female (F-J) animals (n = 10 per group; n = 9 for vehicle:PFF female group, one animal was excluded due to PFF seeding failure based on p-syn counts). A) PFF-induced loss of DA levels Sidak post-tests showed significant effect of PFF (vehicle:saline vs vehicle:PFF, p = 0.0033). B-E) No effect of PFF on DOPAC levels (B), HVA levels (C), DOPAC:DA ratio (D) and HVA:DA ratio (E) in ipsilateral dorsal striatum in male mice. F) PFF-induced loss of DA levels Sidak post-tests showed significant effect of PFF (vehicle:saline vs vehicle:PFF, p = 0.0027). G) PFF effects on DOPAC levels Sidak post-tests showed significant effect of PFF (vehicle:saline vs vehicle:PFF, p = 0.0214). H) PFF effects on HVA levels. Sidak post-tests showed significant effect of PFF (vehicle:saline vs vehicle:PFF, p = 0.0354) I) PFF-induced increase in DOPAC:DA ratio Sidak post-tests showed significant effect of PFF (vehicle:saline vs vehicle:PFF, p = 0.0450). J) No effect of PFF on HVA:DA ratio in ipsilateral dorsal striatum in female mice. Data shown as mean +/- 95% CI.

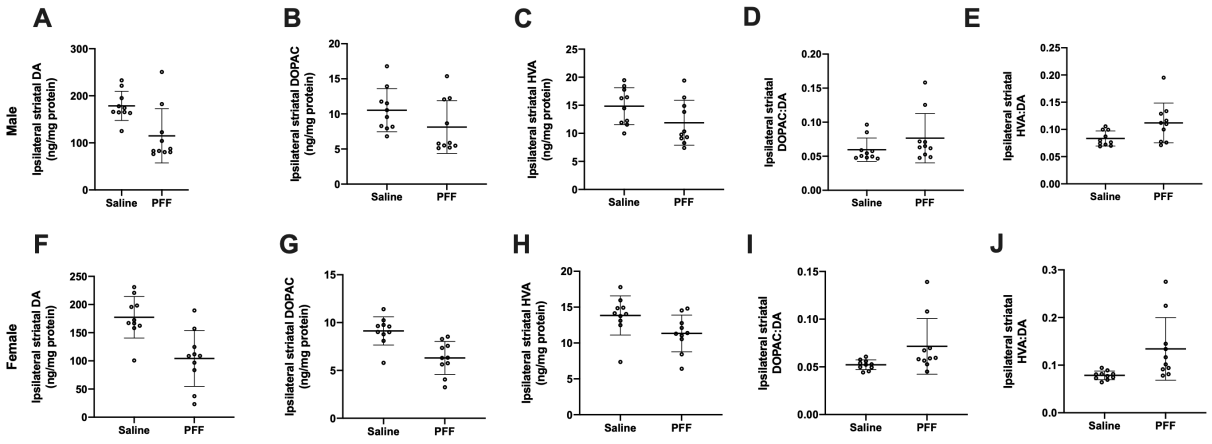

Figure 4.7 PFF-induced increases in DA turnover in male and female animals 6 months after PFF injection. Levels of DA, DOPAC, and HVA in the ipsilateral dorsal striatum were measured 6 months post-PFF injection by HPLC in male (A-E) and female (F-J) animals (n = 10 per group). A) PFF-induced loss of DA levels in ipsilateral dorsal striatum in male animals. Sidak post-tests showed significant effect of PFF (vehicle:saline vs vehicle:PFF, p = 0.0046). B-E) No effect of PFF on DOPAC levels (B), HVA levels (C), DOPAC:DA ratio (D) and HVA:DA ratio (E) in ipsilateral dorsal striatum in male mice. F) PFF-induced loss of DA levels in ipsilateral dorsal striatum of female animals. Sidak post-tests showed significant effect of PFF (vehicle:saline vs vehicle:PFF, p = 0.0061) G) PFF-induced loss of DOPAC levels in ipsilateral dorsal striatum in female animals. Sidak post-tests showed significant effect of PFF (vehicle:saline vs vehicle:PFF, p = 0.0165). H-I) No significant effect of PFF on HVA levels (H), DOPAC:DA ratio (I) and HVA:DA ratio (J) in ipsilateral dorsal striatum of female animals Data shown as mean +/- 95% CI.

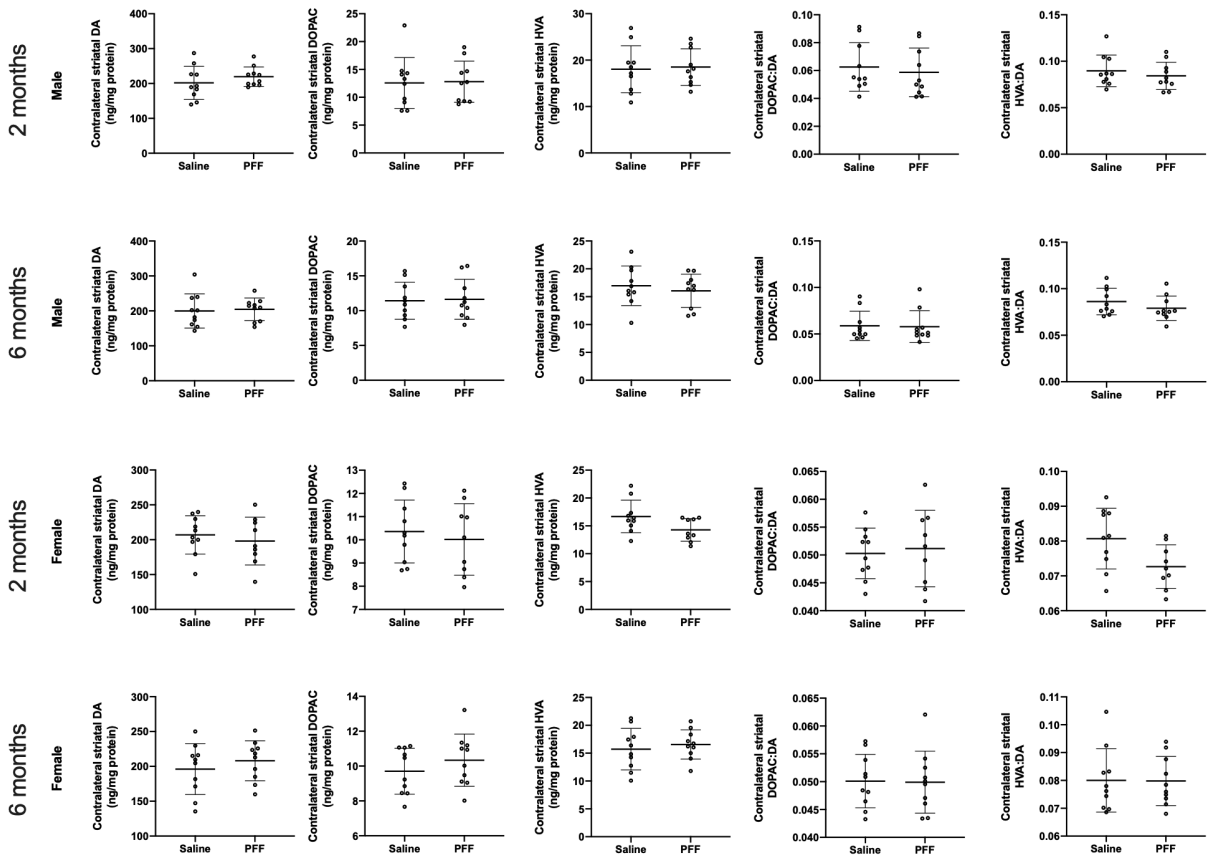

Figure 4.8 Contralateral HPLC at 2 and 6 months after PFF injections in male and female animals. As expected, there was no significant effect of PFF injection on contralateral DA, DOPAC or HVA levels in male or female animals (n = 10 per group), at either timepoint. Data shown as mean +/- 95% CI.

PFFs do not cause loss of TH phenotype or neuronal loss in the substantia nigra in female mice

We performed IHC for TH and estimated the number of TH^+ neurons in the SN 6 months post-PFF injection by stereology. Consistent with prior results, we observed a ~35% loss of TH^+ ipsilateral TH^+ neurons in the SN 6 months after PFF injections in male mice (Figure 4.9A,D) (194). There was a also a significant PFF-induced loss effect of ipsilateral TH^+ neurons in female animals at the same time point, but this loss was less than 20% (Figure 4.9C). As expected, there was no loss of TH^+ neurons in the contralateral, un-injected SN in either male or female animals (Figure 4.10A,B).

To assess whether the loss of TH immunoreactivity in PFF-injected male animals was accompanied by degeneration of these neurons, we performed IHC for NeuN in male animals and estimated the number of NeuN$^+$ neurons in the SN by stereology. We observed a PFF-induced loss of NeuN$^+$ neurons (~20%) in the ipsilateral SN (Figure 4.9C). Given that we observed a significant, but modest loss of ipsilateral TH$^+$ neurons in females, we did not estimate NeuN in female mice, as NeuN counts are more variable and we were not powered to detect a difference this small. Consistent with TH results, we did not observe any contralateral loss of NeuN$^+$ neurons in male mice (Figure 4.10C).

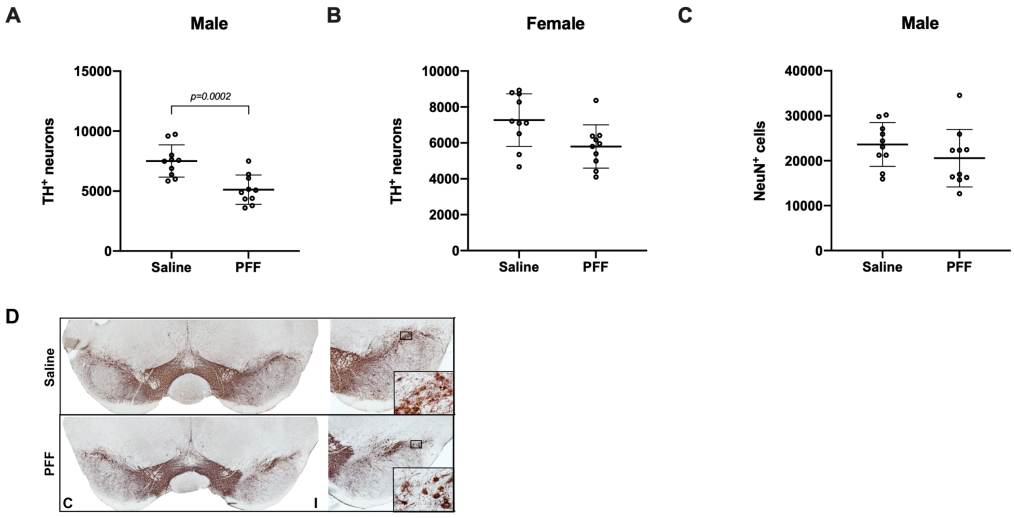

Figure 4.9 PFF-induced loss of ipsilateral nigral TH and NeuN immunoreactive neurons. Number of TH$^+$ neurons in the ipsilateral nigra was estimated by unbiased stereology. A) Ipsilateral nigral TH neuron counts in male animals (n = 10 per group) show a PFF-induced loss of TH$^+$ neurons. Sidak post-tests show a significant effect of PFFs in vehicle and dieldrin exposed animals (vehicle:saline vs vehicle:PFF, p = 0.0002). B) Quantification of ipsilateral nigral TH counts in female animals. Sidak post-tests show no significant effect of PFFs C) Quantification of ipsilateral nigral NeuN counts in male animals (n = 10 per group) D) Representative images from male animals of nigral TH immunohistochemistry. “C” and “I” indicate contralateral and ipsilateral sides. Data shown as mean +/- 95% CI. All significant post-test results are reported in this legend and on the graphs.

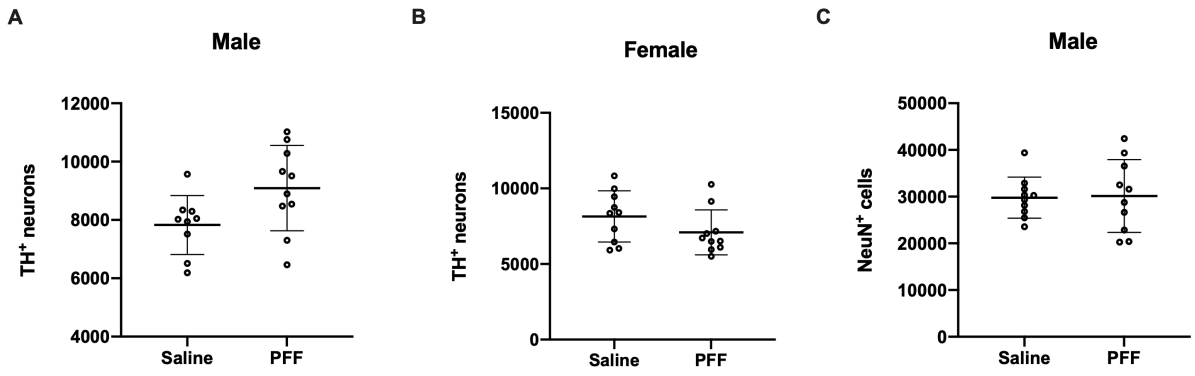

Figure 4.10 PFF injection and dieldrin show no effect on contralateral TH and NeuN immunoreactive neurons. A) Number of TH+ neurons in the contralateral nigra were estimated by unbiased stereology (n = 10 per group). A) There was no effect of dieldrin or PFF on contralateral nigral TH^+ neurons in male animals (two-way ANOVA: PFF, p = 0.5172; dieldrin, p = 0.3922; interaction = 0.0581). B) There was no effect of dieldrin or PFF on contralateral nigral $NeuN^+$ neurons in male animals (two-way ANOVA: PFF, p = 0.8462; dieldrin, p = 0.1186; interaction, p = 0.7063). C) There was no effect of dieldrin or PFF on contralateral nigral TH^+ neurons in female animals (two-way ANOVA: PFF, p = 0.3645; dieldrin, p = 0.0627; interaction = 0.2833). Data shown as mean +/- 95% CI.

Discussion

Sex differences in PFF-induced motor deficits

While we expected to see a male-specific exacerbation of PFF-induced toxicity by developmental dieldrin exposure in Chapter 3, the finding that PFFs alone did not induce motor deficits in female animals was quite surprising. Indeed, this is the first study to show sex differences in sensorimotor function in the PFF model. Despite male and female animals showing similar levels of PFF-induced p-syn aggregation (Figure 4.5), loss of DA, DOPAC and HVA levels and increases in DA turnover (Figure 4.6, Figure 4.7), female mice showed no motor behavior deficits (Figure 4.3). While these data at first appear contradictory, we found that female animals show less than 20% loss of ipsilateral nigral TH immunoreactivity between saline- and PFF-injected groups, whereas males showed a ~35% PFF-induced loss of TH immunoreactivity (Figure 4.9). Together, these data suggest that female mice may have reduced or slower loss of nigral DA neurons that manifests as a behavioral resilience compared to their male counterparts. This is consistent with the reduced incidence of PD and severity of disease course in human females (10–18,236).

Collecting tissue at a later time point (e.g. 9 months post-PFF injection) would reveal if the female-specific resilience is complete or simply reflects a slower progression of the effects of the observed neuropathology. This unanticipated finding is particularly important as it suggests that the PFF model may be a valuable tool to model sex-differences in PD pathology and etiology that does not require any additional surgery or other treatments to manipulate hormonal state. Although this study was not designed to directly compare male and female animals, these results warrant further investigation into sex differences in the PFF model.

The mechanisms underlying sex differences in PD remain unclear but many hypotheses have been proposed (reviewed in (19)). There is evidence suggesting that estrogen may be neuroprotective as estrogen-based hormone therapy can relieve PD symptoms when given in the early stages of the disease and may decrease the risk of developing PD (276–280). Furthermore, evidence in humans and other species suggest that the sex chromosomes themselves are likely contributors to biological sex differences and could potentially influence sex bias in many common complex diseases, including PD (19,281). As an example, *SRY* is a gene located on the Y chromosome that may be important for dopaminergic neuronal function in the SN. In post mortem brain specimens, SRY was found to be co-localized with the subpopulation of SN neurons that express TH (282). In addition, in an *in vitro* study using the M17 cell line, SRY was shown to positively regulate the expression of TH, DOPA decarboxylase and dopamine beta hydroxylase, enzymes involved in DA and norepinephrine synthesis (19,282). Furthermore, gene expression profiles in normal SN DA neurons are sex dependent, which may explain differential sensitivity of these neurons in males and females (283,284). In the normal brain, genes involved in signal transduction and neuronal maturation are expressed more highly in women, whereas genes implicated in PD pathogenesis, when harboring specific mutations such as α-syn and PINK-1, are expressed more highly in men (283,284). Future studies to explore how sex-specific factors interact with pathogenesis of disease are warranted. The sex differences in the α-syn PFF model are an opportunity to explore these in a model that has clear, inherent sex differences.

Conclusions

Importantly, this is the first study to characterize the α-syn PFF model in female mice. Our results underscore the importance of including both sexes in disease models, especially when here is a known sex difference in the human disease as there is with PD. Given the inherent sex-specific sensitivity in this model without surgical or pharmacological intervention, the α-syn PFF model could be a powerful system for exploring mechanisms underlying sex differences in PD, related to both disease pathogenesis and development of treatments and interventions.

Chapter 5 Conclusions

Conclusions

Developmental exposure to dieldrin induces persistent alterations in the DA system that cause a male-specific increase in susceptibility to subsequent exposure to MPTP, a parkinsonian toxicant (129). However, numerous therapeutics that protect against MPTP in preclinical studies have failed to translate to clinical benefit, suggesting that this model has limited utility for accurately predicting clinical translation or exploring toxicological mechanisms in PD (243). Moreover, MPTP is a fast-acting toxicant that induces rapid and extensive loss of striatal DA, which does not reflect the protracted course of loss of function and degeneration observed in disease. Finally, the failure of the MPTP model to develop widespread α-syn pathology calls into question its validity as a "second hit" for examining organochlorine-induced PD vulnerability (243,244). To address these limitations, in the present study, we incorporated the α-syn pre-formed fibril (PFF) model to investigate dieldrin-induced parkinsonian susceptibility.

In 2012, Luk et al reported that intrastriatal injection of synthetic α-syn PFFs into wild-type mice seeded endogenous accumulation of Lewy Body (LB)-like intracellular α-syn inclusions and ultimately led to nigrostriatal degeneration (194). These findings have been replicated in transgenic mice, non-transgenic mice, rats, and monkeys (193,194,196,222,245–247). PFF-induced α-syn inclusions resemble LBs in that they are compact intracytoplasmic structures of hyperphosphorylated (ser129) α-syn (p-syn), co-localize with ubiquitin and p62, and are thioflavin-S-positive and proteinase-k resistant. Over time, the α-syn aggregates progressively compact and eventually lead to neuronal degeneration (193,194,248,249). Thus, the intrastriatal injection of α-syn PFFs can be used to model pathological synucleinopathy and nigrostriatal toxicity in mice. Here, we tested the hypothesis that developmental dieldrin

exposure increases susceptibility to synucleinopathy and associated toxicity in the α-syn PFF model. First, we explored the effects of a developmental dieldrin exposure in male and female mice on levels of α-syn and DA markers and neuroinflammation in the striatum (Chapter 2). Next, we investigated whether this exposure alters toxicity in a synucleinopathy model in both sexes (Chapter 3). Lastly, we presented the observed sex differences in the α-syn PFF model (Chapter 4).

While many factors have been implicated in increased PD risk by epidemiological studies, we focused here on dieldrin, a persistent organic pollutant and organochlorine pesticide, as a representative compound. According to the developmental origins of health and disease (DOHaD) hypothesis, environmental exposures to chemicals, diet, and pesticides during critical periods of development, especially during the prenatal and perinatal period, can alter disease risk later in life (Figure 5.1) (181). The effects of these early exposures can persist into adulthood even if the absence of the persistent presence of a compound.

In this study, we adopted the developmental dieldrin exposure paradigm to model potential effects of developmental exposure to dieldrin on PD risk. There are multiple lines of evidence that suggest an association between dieldrin exposure and increased PD risk; however, the molecular mechanisms by which dieldrin increases risk are not clear. The overall goal of this study is to establish if developmental dieldrin exposure increases susceptibility to synucleinopathy, thereby expanding on findings showing a male-specific increase in susceptibility to MPTP. Our results show clear sex-specific effects of developmental dieldrin exposure on the nigrostriatal system(Chapter 2) and on toxicity in the α-syn PFF model (Chapter 3).

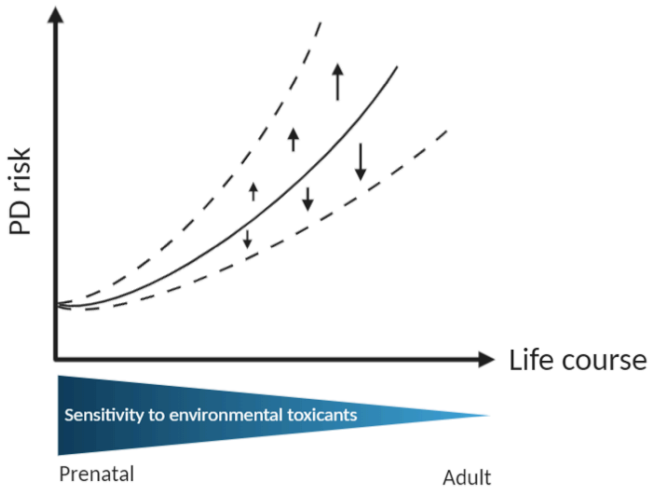

Figure 5.1 Developmental Origins of health and disease

Developmental dieldrin exposure leads to male-specific exacerbation of synucleinopathy

In Chapter 3, we hypothesized that developmental dieldrin exposure would exacerbate PFF-induced α-syn pathology and/or exacerbate the response to the pathology. As summarized in (Figure 3.5), our results showed a male-specific exacerbation of PFF-induced motor deficits on challenging beam by developmental dieldrin exposure. Neuropathological analysis showed that the dieldrin exposure did not affect PFF-induced nigral p-syn pathology (Figure 3.7) or degeneration (Figure 3.12). Dieldrin also did not affect overall loss of striatal DA levels, but did lead to greater deficits in DA turnover in dieldrin exposed male mice (Figure 3.8, Figure 3.9). Such changes in DA turnover suggest that mishandling of the DA in the striatum may be responsible for the motor behavior findings. These results raise important questions for future studies to explore:

- What is the effect of developmental dieldrin exposure on the uptake and release of DA in the striatum? What is the effect of the two-hit (dieldrin/PFF) model on these processes?
- Is the synaptic architecture (e.g. spine density) of DAergic synapses in the striatum altered in this model?
- What are the mechanisms by which dieldrin leads to synaptic changes in the striatum?

Dieldrin induced sex-specific effects in the nigrostriatal pathway may underlie the male-specific increase in susceptibility

In Chapter 2, we explored dieldrin-induced changes in the nigrostriatal system to investigate which mechanisms may underlie the observed dieldrin-induced increase in toxicity. We identified sex-specific changes in expression of neuroinflammatory genes at 12 weeks of age after developmental dieldrin exposure, but did not observe dieldrin-induced changes in overall levels of α-syn. These findings replicate previous results in this exposure paradigm (129). We also did not observe dieldrin-induced changes in overall levels of DAT or VMAT2, or in the DAT:VMAT2 ratio in male or female animals. This is in contrast to the previous report, which showed increased DAT and VMAT2 in both male and female animals, as well as a male-specific increase in DAT:VMAT2 ratio (129).

Consistent with our previous results showing sex-specific effects of dieldrin exposure on the nigral epigenome and transcriptome, we identified sex-specific effects of dieldrin on neuroinflammatory gene expression. Since this was a curated set of genes, we also observed a very high degree of connectivity between these genes in STRING protein-protein network

analysis (77.8% of male DEGs and 88.8% of female DEGs). For both networks, the most enriched gene ontology terms were related to the cellular response to cytokines.

No single inflammatory pathway is apparent in the list of differentially regulated genes from either sex and these results are not consistent with canonical pro- or anti-inflammatory effects. In interpreting these results, it is critical to remember that gene expression was measured in developmentally exposed offspring at 12 weeks of age, when dieldrin is no longer detectable in the brain. Thus, these expression changes may not reflect a typical acute or even chronic inflammatory response. As with our previous epigenetic study, these observed changes likely reflect a persistent change in the baseline state of this system, such that the system responds differently to the second hit.

Despite the lack of a clear pro- or anti-inflammatory gene signature, these gene expression results establish that developmental dieldrin exposure induces distinct sex-specific effects on neuroinflammatory pathways. While these changes are not consistent with canonical pro- or anti-inflammatory effects, they provide multiple avenues for follow-up studies in the two-hit model. In addition, these observations are consistent with previous results demonstrating that dieldrin exposure exacerbates MPTP-induced increases in expression of glial fibrillary acidic protein (GFAP) levels in the striatum, suggesting that dieldrin exposure leads to a greater neuroinflammatory response to a second insult. These results also add to a growing recognition of an important role of neuroinflammation in the α-syn PFF model and in human PD (30,202,227–234). While we were unable to specifically test expression of neuroinflammatory genes after the application of PFFs in this study, our results raise important questions for future studies in this novel two-hit paradigm.

- Does dieldrin change the baseline state of neuroinflammatory pathways, thereby leading to the observed increase in susceptibility? This is particularly important to explore in the α-syn PFF model given the role of neuroinflammation in α-syn PFF induced nigral degeneration (202).
- Do the identified differentially expressed genes play a role in mediating the sex-specific effects of dieldrin on susceptibility to PFFs? Are these genes relevant in other PD-related exposures?
- Are the observed sex-specific differences in neuroinflammatory pathways reflective of differential neuroinflammatory responses in males and females in human PD?
- Given that some of the genes are expressed in endothelial cells, is blood brain barrier permeability affected by developmental exposure to dieldrin?

A model of dieldrin-induced increases in neuronal susceptibility

Based on the results reported here, our previous characterization of epigenetic changes induced by developmental dieldrin exposure, and the previously known mechanisms of dieldrin toxicity, we propose a model for how developmental dieldrin exposure leads to increased susceptibility to synucleinopathy (Figure 5.2) (129,191). In this model, exposure to dieldrin occurs during prenatal and postnatal development. The half-life of dieldrin in mouse brain is less than a week, so no detectable dieldrin remains in the brain of F1 offspring by a few weeks after weaning (129,179,270). When dieldrin is present in the developing brain, it is thought to act on developing DA neurons by inhibiting $GABA_A$ receptor-mediated chloride flux, resulting in increased neuronal activity (184,185,187,189,271,272). Based on previous results, we propose

that this net increase in neuronal activity modifies the dopamine system through persistent changes in epigenetic mechanisms, leading to dysregulation of genes important for dopamine neuron development and maintenance (191). These stable changes then alter the susceptibility of this system to future insults, likely via alterations in striatal dopamine synapses that manifest as increased DA turnover upon application of PFFs. Supporting this model, the present work identified a dieldrin-induced, male-specific exacerbation of PFF-induced deficits in striatal DA handling and motor behavior. Further studies in our lab will focus on exploring the synaptic mechanisms underlying this phenotype and will aim to connect the observed epigenetic changes with these mechanisms. In addition, in a current study, we are tracking the longitudinal patterns of dieldrin-induced epigenetic changes from birth to 12 weeks of age to determine if dieldrin-induced epigenetic changes are maintained from birth or if they represent an altered longitudinal trajectory of epigenetic changes.

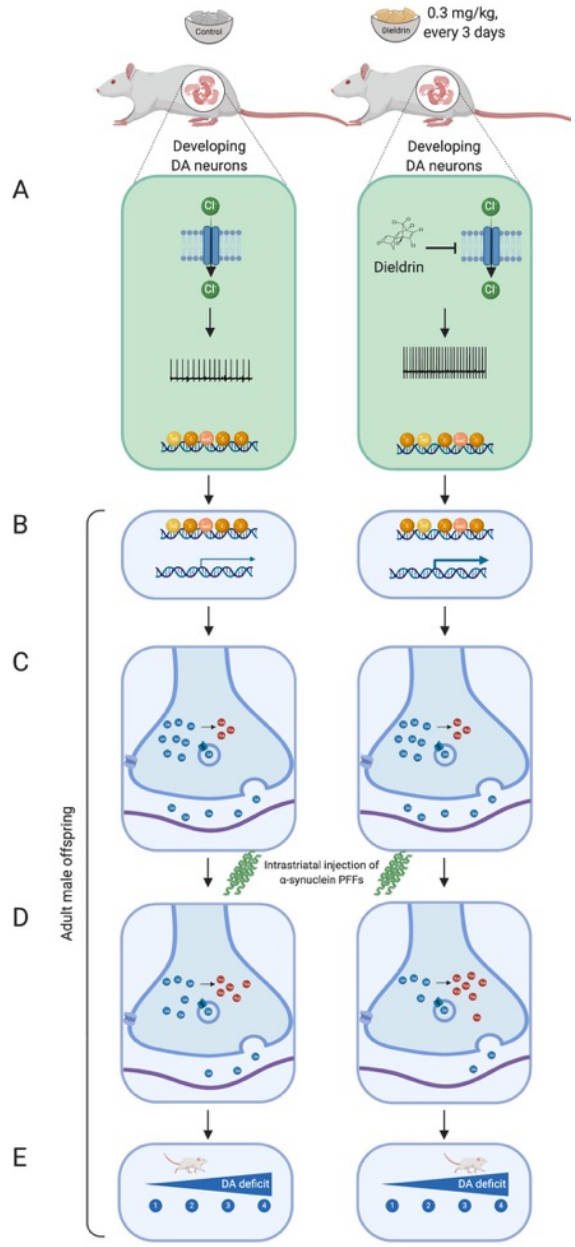

Figure 5.2 Proposed mechanism by which developmental dieldrin exposure leads to exacerbation of PFF-induced toxicity. Dams are fed vehicle or dieldrin containing food starting 1 month prior to mating and continuing through weaning of F1 pups. Dieldrin inhibits chloride influx through $GABA_A$ receptors resulting in increased neuronal activity (A). This change in activity produces epigenetic changes throughout the lifespan even when dieldrin is no longer present (B). These epigenetic changes affect dopamine neuron development and maintenance, producing stable changes in striatal dopamine synapse function (C). These synaptic changes lead to increased susceptibility to PFF-induced synucleinopathy (D, E). Created in BioRender.

Sex-specific effects in the α-syn PFF model

While we expected to see a male-specific exacerbation of PFF-induced toxicity by developmental dieldrin exposure in Chapter 3, the finding that PFFs alone did not induce motor deficits in female animals was quite surprising. As discussed in Chapter 4, this is the first study to show sex differences in sensorimotor function in the PFF model. Despite male and female animals showing similar levels of PFF-induced pathology, female mice showed no motor behavior deficits (Table 5.1). While these data at first appear contradictory, we also found that female animals show less than 20% loss of ipsilateral nigral TH immunoreactivity between saline- and PFF-injected groups, whereas males showed a ~35% PFF-induced loss (Figure 4.9). Together, these data suggest that female mice may have reduced or slower loss of nigral DA neurons that manifests as a behavioral resilience compared to their male counterparts. This is consistent with the reduced incidence of PD and severity of disease course in human females (10–18,236).

Overall, our results underscore the importance of including both sexes in disease models, especially when here is a known sex difference in the human disease (as in PD). Given the inherent sex-specific sensitivity in this model without surgical or pharmacological intervention, the α-syn PFF model could be a powerful system for exploring mechanisms underlying sex differences in PD, and could be used to investigate both disease pathogenesis and development of treatments and interventions.

Outcome Measure	Male	Female
Motor behavior deficit	YES	NO
Nigral p-syn accumulation	YES	YES
Striatal DA loss	YES	YES
Deficits in striatal DA turnover	YES	YES
Loss of THir nigral neurons	YES	YES

Table 5.1 Summary of sex differences in the PFF model

Concluding Remarks

Overall, the experiments in this dissertation established a two-hit model of neuronal susceptibility in DAergic system, revealed sex differences in α-syn PFF PD model and explored potential mechanisms by which dieldrin increased susceptibility to α-syn PFF-induced synucleinopathy. Our work is consistent with current literature and the clinical characteristics of human PD, particularly in terms of progression of neuropathology and sex differences. Given the large environmental contribution to PD risk, understanding the mechanisms underlying environment-induced changes that lead sporadic PD is important for developing early biomarkers to improve early diagnosis and identifying novel potentially neuroprotective therapeutic targets.

BIBLIOGRAPHY

BIBLIOGRAPHY

1. Parkinson J. On the Shaking Palsy. Sherwood, Heely and Jones. 1817;223–36.

2. Titova N, Padmakumar C, Lewis SJG, Chaudhuri KR. Parkinson's: a syndrome rather than a disease? Vol. 124, Journal of Neural Transmission. Springer-Verlag Wien; 2017. p. 907–14.

3. Jellinger KA. Neuropathobiology of non-motor symptoms in Parkinson disease. Vol. 122, Journal of Neural Transmission. Springer-Verlag Wien; 2015. p. 1429–40.

4. Hirsch L, Jette N, Frolkis A, Steeves T, Pringsheim T. The Incidence of Parkinson's Disease: A Systematic Review and Meta-Analysis. Vol. 46, Neuroepidemiology. S. Karger AG; 2016. p. 292–300.

5. Lorraine V Kalia and Anthony E Lang. Parkinson's disease. Lancet [Internet]. 2015 [cited 2019 Sep 7];24(1):92–8. Available from: http://dx.doi.org/10.1016/S0140-6736(14)61393-3

6. Lau LML De, Breteler MMB. Lau and Bretler 2006 - Lancet neurology Epidemiology of PD.pdf. Epidemiol Park Dis. 2006;5(June):525–35.

7. Hirtz D, Thurman DJ, Gwinn-Hardy K, Mohamed M, Chaudhuri AR, Zalutsky R. How common are the "common" neurologic disorders? Vol. 68, Neurology. 2007. p. 326–37.

8. Kowal SL, Dall TM, Chakrabarti R, Storm M V., Jain A. The current and projected economic burden of Parkinson's disease in the United States. Mov Disord. 2013 Mar;28(3):311–8.

9. Dorsey ER, Constantinescu R, Thompson JP, Biglan KM, Holloway RG, Kieburtz K, et al. Projected number of people with Parkinson disease in the most populous nations, 2005 through 2030. Neurology. 2007;68(5):384–6.

10. Elbaz A, Bower JH, Maraganore DM, McDonnell SK, Peterson BJ, Ahlskog JE, et al. Risk tables for parkinsonism and Parkinson's disease. J Clin Epidemiol [Internet]. 2002 Jan [cited 2019 Sep 20];55(1):25–31. Available from: http://www.ncbi.nlm.nih.gov/pubmed/11781119

11. Haaxma CA, Bloem BR, Borm GF, Oyen WJG, Leenders KL, Eshuis S, et al. Gender differences in Parkinson's disease. J Neurol Neurosurg Psychiatry [Internet]. 2007 Aug [cited 2019 Sep 10];78(8):819–24. Available from: http://www.ncbi.nlm.nih.gov/pubmed/17098842

12. Alves G, Müller B, Herlofson K, HogenEsch I, Telstad W, Aarsland D, et al. Incidence of Parkinson's disease in Norway: the Norwegian ParkWest study. J Neurol Neurosurg

Psychiatry [Internet]. 2009 Aug [cited 2019 Sep 20];80(8):851–7. Available from: http://www.ncbi.nlm.nih.gov/pubmed/19246476

13. Baldereschi M, Di Carlo A, Rocca WA, Vanni P, Maggi S, Perissinotto E, et al. Parkinson's disease and parkinsonism in a longitudinal study: two-fold higher incidence in men. ILSA Working Group. Italian Longitudinal Study on Aging. Neurology [Internet]. 2000 Nov 14 [cited 2019 Sep 20];55(9):1358–63. Available from: http://www.ncbi.nlm.nih.gov/pubmed/11087781

14. Dluzen DE, McDermott JL. Gender differences in neurotoxicity of the nigrostriatal dopaminergic system: implications for Parkinson's disease. J Gend Specif Med [Internet]. 2000 [cited 2019 Sep 28];3(6):36–42. Available from: http://www.ncbi.nlm.nih.gov/pubmed/11253381

15. Taylor KSM, Cook JA, Counsell CE. Heterogeneity in male to female risk for Parkinson's disease. J Neurol Neurosurg Psychiatry [Internet]. 2007 Aug [cited 2019 Sep 20];78(8):905–6. Available from: http://www.ncbi.nlm.nih.gov/pubmed/17635983

16. Van Den Eeden SK. Incidence of Parkinson's Disease: Variation by Age, Gender, and Race/Ethnicity. Am J Epidemiol. 2003 Jun 1;157(>11):1015–22.

17. Wooten GF, Currie LJ, Bovbjerg VE, Lee JK, Patrie J. Are men at greater risk for Parkinson's disease than women? J Neurol Neurosurg Psychiatry [Internet]. 2004 Apr [cited 2019 Sep 20];75(4):637–9. Available from: http://www.ncbi.nlm.nih.gov/pubmed/15026515

18. Georgiev D, Hamberg K, Hariz M, Forsgren L, Hariz G-M. Gender differences in Parkinson's disease: A clinical perspective. Acta Neurol Scand [Internet]. 2017 Dec [cited 2019 Sep 28];136(6):570–84. Available from: http://www.ncbi.nlm.nih.gov/pubmed/28670681

19. Gillies GE, Pienaar IS, Vohra S, Qamhawi Z. Sex differences in Parkinson ' s disease. Front Neuroendocrinol [Internet]. 2014 [cited 2019 Sep 9];35(3):370–84. Available from: http://dx.doi.org/10.1016/j.yfrne.2014.02.002

20. Fahn S. Description of Parkinson's disease as a clinical syndrome. Ann N Y Acad Sci [Internet]. 2006 Jan 24 [cited 2019 Sep 14];991(1):1–14. Available from: %3CGo

21. Litvan I, Bhatia KP, Burn DJ, Goetz CG, Lang AE, McKeith I, et al. Movement disorders society scientific issues committee report: SIC task force appraisal of clinical diagnostic criteria for Parkinsonian disorders. Mov Disord [Internet]. 2003 [cited 2019 Aug 23];18(5):467–86. Available from: http://www.ncbi.nlm.nih.gov/pubmed/12722160

22. Olanow CW, Stern MB, Sethi K. The scientific and clinical basis for the treatment of Parkinson disease (2009). Neurology. 2009 May 26;72(21 SUPPL. 4).

23. Chaudhuri KR, Healy DG, Schapira AH. Non-motor symptoms of Parkinson's disease:

diagnosis and management. Lancet Neurol [Internet]. 2006 Mar [cited 2019 Sep 14];5(3):235–45. Available from: https://linkinghub.elsevier.com/retrieve/pii/S1474442206703738

24. Chaudhuri KR, Schapira AH. Non-motor symptoms of Parkinson's disease: dopaminergic pathophysiology and treatment. Vol. 8, The Lancet Neurology. 2009. p. 464–74.

25. Khoo TK, Yarnall AJ, Duncan GW, Coleman S, O'Brien JT, Brooks DJ, et al. The spectrum of nonmotor symptoms in early Parkinson disease. Neurology [Internet]. 2013 Jan 15 [cited 2019 Aug 23];80(3):276–81. Available from: http://www.ncbi.nlm.nih.gov/pubmed/23319473

26. Song W, Guo X, Chen K, Chen X, Cao B, Wei Q, et al. The impact of non-motor symptoms on the Health-Related Quality of Life of Parkinson's disease patients from Southwest China. Park Relat Disord. 2014 Feb;20(2):149–52.

27. Chaudhuri KR, Prieto-Jurcynska C, Naidu Y, Mitra T, Frades-Payo B, Tluk S, et al. The nondeclaration of nonmotor symptoms of Parkinson's disease to health care professionals: An international study using the nonmotor symptoms questionnaire. Mov Disord. 2010 Apr 30;25(6):704–9.

28. AuYong N, Keener AM, Bordelon YM, Portera-Cailliau C, Pouratian N. A New Neuroanatomy of Basal Ganglia Circuitry. In: Genomics, Circuits, and Pathways in Clinical Neuropsychiatry. Elsevier Inc.; 2016. p. 301–15.

29. Albin RL, Young AB, Penney JB. The functional anatomy of basal ganglia disorders. Trends Neurosci. 1989;12(10):366–75.

30. Kordower JH, Olanow CW, Dodiya HB, Chu Y, Beach TG, Adler CH, et al. Disease duration and the integrity of the nigrostriatal system in Parkinson's disease. Brain [Internet]. 2013 Aug [cited 2019 Sep 7];136(Pt 8):2419–31. Available from: http://www.ncbi.nlm.nih.gov/pubmed/23884810

31. Kurowska Z, Kordower JH, Stoessl AJ, Burke RE, Brundin P, Yue Z, et al. Is Axonal Degeneration a Key Early Event in Parkinson's Disease? J Parkinsons Dis [Internet]. 2016 [cited 2019 Sep 7];6(4):703–7. Available from: http://www.ncbi.nlm.nih.gov/pubmed/27497486

32. LEWY, FH. Paralysis agitans. I. Pathologische Anatomie. Handb der Neurol. 1912;3:920–58.

33. Wakabayashi K, Tanji K, Mori F, Takahashi H. The Lewy body in Parkinson's disease: molecules implicated in the formation and degradation of alpha-synuclein aggregates. [Internet]. Oct, 2007 p. 494–506. Available from: http://www.ncbi.nlm.nih.gov/pubmed/18018486

34. Benskey MJ, Perez RG, Manfredsson FP. The contribution of alpha synuclein to neuronal

survival and function - Implications for Parkinson's disease. J Neurochem [Internet]. 2016 May [cited 2019 Sep 2];137(3):331–59. Available from: http://www.ncbi.nlm.nih.gov/pubmed/26852372

35. Beach TG, Adler CH, Sue LI, Vedders L, Lue L, White Iii CL, et al. Multi-organ distribution of phosphorylated alpha-synuclein histopathology in subjects with Lewy body disorders. Acta Neuropathol [Internet]. 2010 Jun [cited 2019 Sep 16];119(6):689–702. Available from: http://www.ncbi.nlm.nih.gov/pubmed/20306269

36. Gelpi E, Navarro-Otano J, Tolosa E, Gaig C, Compta Y, Rey MJ, et al. Multiple organ involvement by alpha-synuclein pathology in Lewy body disorders. Mov Disord [Internet]. 2014 Jul [cited 2019 Sep 16];29(8):1010–8. Available from: http://www.ncbi.nlm.nih.gov/pubmed/24395122

37. Braak H, Del Tredici K. Neuropathological Staging of Brain Pathology in Sporadic Parkinson's disease: Separating the Wheat from the Chaff. Vol. 7, Journal of Parkinson's Disease. IOS Press; 2017. p. S73–87.

38. Braak H, Del Tredici K, Rüb U, de Vos RAI, Jansen Steur ENH, Braak E, et al. Staging of brain pathology related to sporadic Parkinson's disease. Neurobiol Aging [Internet]. 2003 Mar [cited 2019 Sep 7];24(2):197–211. Available from: http://dx.doi.org/

39. Braak H, Ghebremedhin E, Rüb U, Bratzke H, Del Tredici K. Stages in the development of Parkinson's disease-related pathology. Cell Tissue Res [Internet]. 2004 Oct [cited 2019 Sep 7];318(1):121–34. Available from: http://www.ncbi.nlm.nih.gov/pubmed/15338272

40. Del Tredici K, Braak H. Sporadic Parkinson's disease: Development and distribution of α-synuclein pathology. Vol. 42, Neuropathology and Applied Neurobiology. Blackwell Publishing Ltd; 2016. p. 33–50.

41. Engelender S, Isacson O. The Threshold Theory for Parkinson's Disease. Vol. 40, Trends in Neurosciences. Elsevier Ltd; 2017. p. 4–14.

42. Spillantini MG, Schmidt ML, Lee VM, Trojanowski JQ, Jakes R, Goedert M. Alpha-synuclein in Lewy bodies. Nature [Internet]. 1997;388(6645):839–40. Available from: https://www.ncbi.nlm.nih.gov/pubmed/9278044

43. Kim WS, Kågedal K, Halliday GM. Alpha-synuclein biology in Lewy body diseases. Alzheimers Res Ther [Internet]. 2014 [cited 2019 Sep 14];6(5):73. Available from: http://www.ncbi.nlm.nih.gov/pubmed/25580161

44. Weinreb PH, Zhen W, Poon AW, Conway KA, Lansbury PT. NACP, a protein implicated in Alzheimer's disease and learning, is natively unfolded. Biochemistry [Internet]. 1996 Oct 29 [cited 2019 Sep 15];35(43):13709–15. Available from: http://www.ncbi.nlm.nih.gov/pubmed/8901511

45. Uversky VN. What does it mean to be natively unfolded? - Uversky - 2003 - European

Journal of Biochemistry - Wiley Online Library. Eur J Biochem [Internet]. 2002 [cited 2019 Sep 15];12(May 2001):2–12. Available from: http://onlinelibrary.wiley.com/doi/10.1046/j.0014-2956.2001.02649.x/full

46. Dyson HJ, Wright PE. Intrinsically unstructured proteins and their functions. Nat Rev Mol Cell Biol [Internet]. 2005 Mar [cited 2019 Sep 15];6(3):197–208. Available from: http://www.ncbi.nlm.nih.gov/pubmed/15738986

47. Davidson WS, Jonas A, Clayton DF, George JM. Stabilization of alpha-synuclein secondary structure upon binding to synthetic membranes. J Biol Chem [Internet]. 1998 Apr 17 [cited 2019 Sep 6];273(16):9443–9. Available from: http://www.ncbi.nlm.nih.gov/pubmed/9545270

48. Bussell R, Eliezer D. A structural and functional role for 11-mer repeats in alpha-synuclein and other exchangeable lipid binding proteins. J Mol Biol [Internet]. 2003 Jun 13 [cited 2019 Sep 15];329(4):763–78. Available from: http://www.ncbi.nlm.nih.gov/pubmed/12787676

49. Chandra S, Chen X, Rizo J, Jahn R, Südhof TC. A broken alpha -helix in folded alpha -Synuclein. J Biol Chem [Internet]. 2003 Apr 25 [cited 2019 Sep 15];278(17):15313–8. Available from: http://www.ncbi.nlm.nih.gov/pubmed/12586824

50. Jao CC, Der-Sarkissian A, Chen J, Langen R. Structure of membrane-bound alpha-synuclein studied by site-directed spin labeling. Proc Natl Acad Sci U S A [Internet]. 2004 Jun 1 [cited 2019 Sep 15];101(22):8331–6. Available from: http://www.ncbi.nlm.nih.gov/pubmed/15155902

51. Middleton ER, Rhoades E. Effects of curvature and composition on α-synuclein binding to lipid vesicles. Biophys J [Internet]. 2010 Oct 6 [cited 2019 Sep 15];99(7):2279–88. Available from: http://www.ncbi.nlm.nih.gov/pubmed/20923663

52. Jensen MB, Bhatia VK, Jao CC, Rasmussen JE, Pedersen SL, Jensen KJ, et al. Membrane curvature sensing by amphipathic helices: a single liposome study using α-synuclein and annexin B12. J Biol Chem [Internet]. 2011 Dec 9 [cited 2019 Sep 15];286(49):42603–14. Available from: http://www.ncbi.nlm.nih.gov/pubmed/21953452

53. Bartels T, Choi JG, Selkoe DJ. α-Synuclein occurs physiologically as a helically folded tetramer that resists aggregation. Nature. 2011 Sep 1;477(7362):107–11.

54. Uversky VN, Li J, Fink AL. Evidence for a partially folded intermediate in alpha-synuclein fibril formation. J Biol Chem [Internet]. 2001 Apr 6 [cited 2019 Sep 15];276(14):10737–44. Available from: http://www.ncbi.nlm.nih.gov/pubmed/11152691

55. Caughey B, Lansbury PT. Protofibrils, pores, fibrils, and neurodegeneration: separating the responsible protein aggregates from the innocent bystanders. Annu Rev Neurosci [Internet]. 2003 [cited 2019 Sep 14];26:267–98. Available from: http://www.ncbi.nlm.nih.gov/pubmed/12704221

56. Ingelsson M. Alpha-synuclein oligomers-neurotoxic molecules in Parkinson's disease and other lewy body disorders. Vol. 10, Frontiers in Neuroscience. Frontiers Media S.A.; 2016.

57. Serpell LC, Berriman J, Jakes R, Goedert M, Crowther RA. Fiber diffraction of synthetic α-synuclein filaments shows amyloid-like cross-β conformation. Proc Natl Acad Sci U S A. 2000 Apr 25;97(9):4897–902.

58. Uversky VN, Li J, Bower K, Fink AL. Synergistic effects of pesticides and metals on the fibrillation of α-synuclein: Implications for Parkinson's disease. In: NeuroToxicology. 2002. p. 527–36.

59. Conway KA, Harper JD, Lansbury PT. Accelerated in vitro fibril formation by a mutant alpha-synuclein linked to early-onset Parkinson disease. Nat Med [Internet]. 1998 Nov [cited 2019 Sep 16];4(11):1318–20. Available from: http://www.ncbi.nlm.nih.gov/pubmed/9809558

60. Hashimoto M, Hsu LJ, Xia Y, Takeda A, Sisk A, Sundsmo M, et al. Oxidative stress induces amyloid-like aggregate formation of NACP/alpha-synuclein in vitro. Neuroreport [Internet]. 1999 Mar 17 [cited 2019 Oct 1];10(4):717–21. Available from: http://www.ncbi.nlm.nih.gov/pubmed/10208537

61. Goldman JE, Yen SH, Chiu FC, Peress NS. Lewy bodies of Parkinson's disease contain neurofilament antigens. Science [Internet]. 1983 Sep 9 [cited 2019 Sep 7];221(4615):1082–4. Available from: http://www.ncbi.nlm.nih.gov/pubmed/6308771

62. Beyer K, Domingo-Sàbat M, Ariza A. Molecular pathology of lewy body diseases. Vol. 10, International Journal of Molecular Sciences. 2009. p. 724–45.

63. Shahmoradian SH, Lewis AJ, Genoud C, Hench J, Moors TE, Navarro PP, et al. Lewy pathology in Parkinson's disease consists of crowded organelles and lipid membranes. Nat Neurosci. 2019 Jul 1;22(7):1099–109.

64. Lill CM. Genetics of Parkinson's disease. Mol Cell Probes [Internet]. 2016;30(6):386–96. Available from: http://dx.doi.org/10.1016/j.mcp.2016.11.001

65. Blauwendraat C, Nalls MA, Singleton AB. The genetic architecture of Parkinson's disease. Lancet Neurol. 2019 Sep;

66. Polymeropoulos MH, Lavedan C, Leroy E, Ide SE, Dehejia A, Dutra A, et al. Mutation in the alpha-synuclein gene identified in families with Parkinson's disease. Science (80-) [Internet]. 1997;276(5321):2045–7. Available from: https://www.ncbi.nlm.nih.gov/pubmed/9197268

67. Krüger R, Kuhn W, Müller T, Woitalla D, Graeber M, Kösel S, et al. Ala30Pro mutation in the gene encoding alpha-synuclein in Parkinson's disease. Nat Genet [Internet]. 1998 Feb [cited 2019 Sep 14];18(2):106–8. Available from: http://www.ncbi.nlm.nih.gov/pubmed/9462735

68. Zarranz JJ, Alegre J, Gómez-Esteban JC, Lezcano E, Ros R, Ampuero I, et al. The new mutation, E46K, of alpha-synuclein causes Parkinson and Lewy body dementia. Ann Neurol [Internet]. 2004 Feb [cited 2019 Sep 14];55(2):164–73. Available from: http://www.ncbi.nlm.nih.gov/pubmed/14755719

69. Chartier-Harlin M-C, Kachergus J, Roumier C, Mouroux V, Douay X, Lincoln S, et al. Alpha-synuclein locus duplication as a cause of familial Parkinson's disease. Lancet (London, England) [Internet]. [cited 2019 Sep 14];364(9440):1167–9. Available from: http://www.ncbi.nlm.nih.gov/pubmed/15451224

70. Singleton AB, Farrer M, Johnson J, Singleton AB, Hague S, Kachergus J, et al. alpha-Synuclein locus triplication causes Parkinson's disease. Science (80-) [Internet]. 2003 Oct 31 [cited 2019 Sep 14];302(5646):841. Available from: https://www.ncbi.nlm.nih.gov/pubmed/14593171

71. Ibanez P, Bonnet AM, Debarges B, Lohmann E, Tison F, Pollak P, et al. Causal relation between alpha-synuclein gene duplication and familial Parkinson's disease. Lancet [Internet]. 2004;364(9440):1169–71. Available from: %3CGo

72. Flagmeier P, Meisl G, Vendruscolo M, Knowles TPJ, Dobson CM, Buell AK, et al. Mutations associated with familial Parkinson's disease alter the initiation and amplification steps of α-synuclein aggregation. Proc Natl Acad Sci U S A. 2016 Sep 13;113(37):10328–33.

73. Oliveira LMAAA, Falomir-Lockhart LJ, Botelho MG, Lin KHH, Wales P, Koch JC, et al. Elevated α-synuclein caused by SNCA gene triplication impairs neuronal differentiation and maturation in Parkinson's patient-derived induced pluripotent stem cells. Cell Death Dis [Internet]. 2015 [cited 2019 Sep 24];6(11):e1994–e1994. Available from: http://www.pubmedcentral.nih.gov/articlerender.fcgi?artid=PMC4670926

74. Zimprich A, Biskup S, Leitner P, Lichtner P, Farrer M, Lincoln S, et al. Mutations in LRRK2 cause autosomal-dominant parkinsonism with pleomorphic pathology. Neuron. 2004 Nov 18;44(4):601–7.

75. Paisán-Ruíz C, Jain S, Evans EW, Gilks WP, Simón J, Van Der Brug M, et al. Cloning of the gene containing mutations that cause PARK8-linked Parkinson's disease. Neuron. 2004 Nov 18;44(4):595–600.

76. Williams ET, Chen X, Moore DJ. VPS35, the retromer complex and Parkinson's disease. Vol. 7, Journal of Parkinson's Disease. IOS Press; 2017. p. 219–33.

77. Lill CM, Roehr JT, McQueen MB, Kavvoura FK, Bagade S, Schjeide BM, et al. Comprehensive research synopsis and systematic meta-analyses in Parkinson's disease genetics: The PDGene database. PLoS Genet [Internet]. 2012;8(3):e1002548. Available from: http://dx.doi.org/10.1371/journal.pgen.1002548

78. Kitada T, Asakawa S, Hattori N, Matsumine H, Yamamura Y, Minoshima S, et al. Mutations in the parkin gene cause autosomal recessive juvenile parkinsonism. Nature.

1998 Apr 9;392(6676):605–8.

79. Shendelman S, Jonason A, Martinat C, Leete T, Abeliovich A. DJ-1 Is a redox-dependent molecular chaperone that inhibits α-synuclein aggregate formation. PLoS Biol. 2004 Nov;2(11).

80. Brooks J, Ding J, Simon-Sanchez J, Paisan-Ruiz C, Singleton AB, Scholz SW. Parkin and PINK1 mutations in early-onset Parkinson's disease: Comprehensive screening in publicly available cases and control. J Med Genet. 2009 Jun;46(6):375–81.

81. Pankratz N, Pauciulo MW, Elsaesser VE, Marek DK, Halter CA, Wojcieszek J, et al. Mutations in DJ-1 are rare in familial Parkinson disease. Neurosci Lett. 2006 Nov 20;408(3):209–13.

82. Sidransky E, Nalls MA, Aasly JO, Aharon-Peretz J, Annesi G, Barbosa ER, et al. Multicenter analysis of glucocerebrosidase mutations in Parkinson's disease. N Engl J Med. 2009 Oct 22;361(17):1651–61.

83. Nalls MA, Blauwendraat C, Vallerga CL, Heilbron K, Bandres-Ciga S, Chang D, et al. Identification of novel risk loci, causal insights, and heritable risk for Parkinson's disease: a meta-analysis of genome-wide association studies. Lancet Neurol. 2019 Dec 1;18(12):1091–102.

84. Nalls MA, Pankratz N, Lill CM, Do CB, Hernandez DG, Saad M, et al. Large-scale meta-analysis of genome-wide association data identifies six new risk loci for Parkinson's disease. Nat Genet [Internet]. 2014 [cited 2019 Sep 8];46(9):ng.3043-ng.3043. Available from: http://dx.doi.org/10.1038/ng.3043

85. Lill CM. Genetics of Parkinson's disease, Molecular and Cellular Probes. Handb Clin Neurol [Internet]. 2016 [cited 2019 Sep 16];147:211–27. Available from: http://dx.doi.org/10.1016/j.mcp.2016.11.001

86. Hamza TH, Chen H, Hill-Burns EM, Rhodes SL, Montimurro J, Kay DM, et al. Genome-wide gene-environment study identifies glutamate receptor gene grin2a as a parkinson's disease modifier gene via interaction with coffee. PLoS Genet. 2011 Aug;7(8).

87. Hill-Burns EM, Singh N, Ganguly P, Hamza TH, Montimurro J, Kay DM, et al. A genetic basis for the variable effect of smoking/nicotine on Parkinson's disease. Pharmacogenomics J. 2012;1–8.

88. Bellou V, Belbasis L, Tzoulaki I, Evangelou E, Ioannidis JPA. Environmental risk factors and Parkinson's disease: An umbrella review of meta-analyses. Vol. 23, Parkinsonism and Related Disorders. Elsevier Ltd; 2016. p. 1–9.

89. Savica R, Grossardt BR, Bower JH, Ahlskog JE, Rocca WA. Risk factors for Parkinson's disease may differ in men and women: An exploratory study. Vol. 63, Hormones and Behavior. 2013. p. 308–14.

90. Zhang Y, Chen K, Sloan SA, Bennett ML, Scholze AR, O'Keeffe S, et al. An RNA-sequencing transcriptome and splicing database of glia, neurons, and vascular cells of the cerebral cortex. J Neurosci [Internet]. 2014;34(36):11929–47. Available from: https://www.ncbi.nlm.nih.gov/pubmed/25186741

91. Noyce AJ, Bestwick JP, Silveira-Moriyama L, Hawkes CH, Giovannoni G, Lees AJ, et al. Meta-analysis of early nonmotor features and risk factors for Parkinson disease. Ann Neurol [Internet]. 2012 Dec [cited 2019 Sep 16];72(6):893–901. Available from: http://www.ncbi.nlm.nih.gov/pubmed/23071076

92. Yang F, Trolle Lagerros Y, Bellocco R, Adami H-O, Fang F, Pedersen NL, et al. Physical activity and risk of Parkinson's disease in the Swedish National March Cohort. Brain [Internet]. 2015 Feb [cited 2019 Sep 16];138(Pt 2):269–75. Available from: http://www.ncbi.nlm.nih.gov/pubmed/25410713

93. Etminan M, Gill SS, Samii A. Intake of vitamin E, vitamin C, and carotenoids and the risk of Parkinson's disease: A meta-analysis. Vol. 4, Lancet Neurology. 2005. p. 362–5.

94. Jiang W, Ju C, Jiang H, Zhang D. Dairy foods intake and risk of Parkinson's disease: a dose-response meta-analysis of prospective cohort studies. Eur J Epidemiol. 2014;29(9):613–9.

95. Mortimer JA, Borenstein AR, Nelson LM. Associations of welding and manganese exposure with Parkinson disease; Review and meta-Analysis. Neurology. 2012 Sep 11;79(11):1174–80.

96. Palin O, Herd C, Morrison KE, Jagielski AC, Wheatley K, Thomas GN, et al. Systematic review and meta-analysis of hydrocarbon exposure and the risk of Parkinson's disease. Park Relat Disord. 2015 Mar 1;21(3):243–8.

97. Pezzoli G, Cereda E. Exposure to pesticides or solvents and risk of Parkinson disease. Vol. 80, Neurology. 2013. p. 2035–41.

98. van der Mark M, Brouwer M, Kromhout H, Nijssen P, Huss A, Vermeulen R. Is pesticide use related to Parkinson disease? Some clues to heterogeneity in study results. Vol. 120, Environmental Health Perspectives. 2012. p. 340–7.

99. Ascherio A, Chen H, Weisskopf MG, O'Reilly E, McCullough ML, Calle EE, et al. Pesticide exposure and risk for Parkinson's disease. Ann Neurol [Internet]. 2006 Aug [cited 2019 Sep 5];60(2):197–203. Available from: http://www.ncbi.nlm.nih.gov/pubmed/16802290

100. Brown TP, Rumsby PC, Capleton AC, Rushton L, Levy LS. Pesticides and Parkinson's disease - Is there a link? Vol. 114, Environmental Health Perspectives. 2006. p. 156–64.

101. Semchuk KM, Love EJ, Lee RG. Parkinson's disease and exposure to rural environmental factors: a population based case-control study. Can J Neurol Sci [Internet]. 1991 [cited 2019 Sep 5];18(3):279–86. Available from: http://www.ncbi.nlm.nih.gov/pubmed/1913361

102. Semchuk KM, Love EJ, Lee RG. Parkinson's disease and exposure to agricultural work and pesticide chemicals. Neurology [Internet]. 1992 Jul [cited 2019 Aug 25];42(7):1328–35. Available from: http://www.ncbi.nlm.nih.gov/pubmed/1620342

103. Steenland K, Hein MJ, Cassinelli RT, Prince MM, Nilsen NB, Whelan EA, et al. Polychlorinated biphenyls and neurodegenerative disease mortality in an occupational cohort. Epidemiology. 2006 Jan;17(1):8–13.

104. Tanner CM, Langston JW. Do environmental toxins cause Parkinson's disease? A critical review. Neurology [Internet]. 1990 Oct [cited 2019 Sep 5];40(10 Suppl 3):suppl 17-30; discussion 30-1. Available from: http://www.ncbi.nlm.nih.gov/pubmed/2215971

105. Tanner CM, Aston DA. Epidemiology of Parkinson's disease and akinetic syndromes. Curr Opin Neurol [Internet]. 2000 Aug [cited 2019 Sep 5];13(4):427–30. Available from: http://www.ncbi.nlm.nih.gov/pubmed/10970060

106. Tanner CM, Kamel F, Ross GW, Hoppin JA, Goldman SM, Korell M, et al. Rotenone, paraquat, and Parkinson's disease. Environ Health Perspect [Internet]. 2011 Jun [cited 2019 Sep 5];119(6):866–72. Available from: http://www.ncbi.nlm.nih.gov/pubmed/21269927

107. Wirdefeldt K, Adami H-O, Cole P, Trichopoulos D, Mandel J. Epidemiology and etiology of Parkinson's disease: a review of the evidence. Eur J Epidemiol [Internet]. 2011 Jun [cited 2019 Sep 5];26(Supplement 1):S1–58. Available from: http://www.ncbi.nlm.nih.gov/pubmed/21626386

108. Caudle WM, Guillot TS, Lazo CR, Miller GW. Industrial toxicants and Parkinson's disease. Vol. 33, NeuroToxicology. 2012. p. 178–88.

109. Elbaz A, Clavel J, Rathouz PJ, Moisan F, Galanaud J-P, Delemotte B, et al. Professional exposure to pesticides and Parkinson disease. Ann Neurol [Internet]. 2009 Oct [cited 2019 Sep 5];66(4):494–504. Available from: http://www.ncbi.nlm.nih.gov/pubmed/19847896

110. Freire C, Koifman S. Pesticide exposure and Parkinson's disease: Epidemiological evidence of association. Vol. 33, NeuroToxicology. 2012. p. 947–71.

111. Hatcher JM, Pennell KD, Miller GW. Parkinson's disease and pesticides: a toxicological perspective. Vol. 29, Trends in Pharmacological Sciences. 2008. p. 322–9.

112. Le Couteur DG, McLean AJ, Taylor MC, Woodham BL, Board PG. Pesticides and Parkinson's disease. Biomed Pharmacother [Internet]. 1999 Apr [cited 2019 Aug 25];53(3):122–30. Available from: http://www.ncbi.nlm.nih.gov/pubmed/10349500

113. Priyadarshi A, Khuder SA, Schaub EA, Shrivastava S. A meta-analysis of Parkinson's disease and exposure to pesticides. Neurotoxicology [Internet]. 2000 Aug [cited 2019 Sep 5];21(4):435–40. Available from: http://www.ncbi.nlm.nih.gov/pubmed/11022853

114. Priyadarshi A, Khuder SA, Schaub EA, Priyadarshi SS. Environmental risk factors and Parkinson's disease: a metaanalysis. Environ Res [Internet]. 2001 Jun [cited 2019 Sep 5];86(2):122–7. Available from: http://www.ncbi.nlm.nih.gov/pubmed/11437458

115. Ritz B, Yu F. Parkinson's disease mortality and pesticide exposure in California 1984-1994. Int J Epidemiol [Internet]. 2000 [cited 2019 Sep 5];29(2):323–9. Available from: https://www.ncbi.nlm.nih.gov/pubmed/10817132

116. Goldman SM. Trichloroethylene and Parkinson's disease: Dissolving the puzzle. Expert Review of Neurotherapeutics. 2010 Jun;10(6):835–7.

117. Seegal RF, Marek KL, Seibyl JP, Jennings DL, Molho ES, Higgins DS, et al. Occupational exposure to PCBs reduces striatal dopamine transporter densities only in women: A β-CIT imaging study. Neurobiol Dis. 2010 May;38(2):219–25.

118. De Miranda BR, Greenamyre JT. Trichloroethylene, a ubiquitous environmental contaminant in the risk for Parkinson's disease. Environ Sci Process Impacts [Internet]. 2020 Jan 30 [cited 2020 Mar 27]; Available from: http://www.ncbi.nlm.nih.gov/pubmed/31996877

119. Brown TP, Rumsby PC, Capleton AC, Rushton L. Pesticides and Parkinson's disease-is there a link? Pestic Park Dis there a link? [Internet]. 2006; Available from: http://dx.doi.org/10.2307/3436503

120. Moretto A, Colosio C. Biochemical and toxicological evidence of neurological effects of pesticides: The example of Parkinson's disease. Vol. 32, NeuroToxicology. 2011. p. 383–91.

121. Hancock DB, Martin ER, Mayhew GM, Stajich JM, Jewett R, Stacy MA, et al. Pesticide exposure and risk of Parkinson's disease: a family-based case-control study. BMC Neurol [Internet]. 2008 Mar 28 [cited 2020 Mar 27];8:6. Available from: http://www.ncbi.nlm.nih.gov/pubmed/18373838

122. Hayes WJ. Pesticides studied in man. Williams & Wilkins; 1982. 672 p.

123. Kanthasamy AG, Kitazawa M, Kanthasamy A, Anantharam V. Dieldrin-induced neurotoxicity: relevance to Parkinson's disease pathogenesis. Neurotoxicology [Internet]. 2005 Aug [cited 2019 Aug 25];26(4):701–19. Available from: http://www.ncbi.nlm.nih.gov/pubmed/16112328

124. Corrigan FM, Murray L, Wyatt CL, Shore RF. Diorthosubstituted polychlorinated biphenyls in caudate nucleus in Parkinson's disease. Exp Neurol. 1998;150(2):339–42.

125. Corrigan FM, Wienburg CL, Shore RF, Daniel SE, Mann D. Organochlorine insecticides in substantia nigra in Parkinson's disease. J Toxicol Environ Health A [Internet]. 2000 Feb 25 [cited 2019 Aug 25];59(4):229–34. Available from: http://www.ncbi.nlm.nih.gov/pubmed/10706031

126. Fleming L, Mann JB, Bean J, Briggle T, Sanchez-Ramos JR. Parkinson's disease and brain levels of organochlorine pesticides. Ann Neurol [Internet]. 1994 Jul [cited 2019 Aug 25];36(1):100–3. Available from: http://www.ncbi.nlm.nih.gov/pubmed/7517654

127. Weisskopf MG, Knekt P, O'Reilly EJ, Lyytinen J, Reunanen A, Laden F, et al. Persistent organochlorine pesticides in serum and risk of Parkinson disease. Neurology. 2010;74(13):1055–61.

128. Alter SP, Lenzi GM, Bernstein AI, Miller GW. Vesicular integrity in Parkinson's disease. Curr Neurol Neurosci Rep [Internet]. 2013 [cited 2019 Sep 5];13(7):362. Available from: https://www.ncbi.nlm.nih.gov/pubmed/23690026

129. Richardson JR, Caudle WM, Wang M, Dean ED, Pennell KD, Miller GW. Developmental exposure to the pesticide dieldrin alters the dopamine system and increases neurotoxicity in an animal model of Parkinson's disease. FASEB J [Internet]. 2006;20(10):1695–7. Available from: http://www.fasebj.org/doi/10.1096/fj.06-5864fje

130. Maroteaux L, Campanelli JT, Scheller RH. Synuclein: a neuron-specific protein localized to the nucleus and presynaptic nerve terminal. J Neurosci [Internet]. 1988 Aug [cited 2019 Sep 6];8(8):2804–15. Available from: http://www.ncbi.nlm.nih.gov/pubmed/3411354

131. Burré J, Sharma M, Tsetsenis T, Buchman V, Etherton MR, Südhof TC. α-Synuclein promotes SNARE-complex assembly in vivo and in vitro. Science (80-). 2010 Sep 24;329(5999):1663–7.

132. Burré J, Sharma M, Südhof TC. Systematic mutagenesis of α-synuclein reveals distinct sequence requirements for physiological and pathological activities. J Neurosci. 2012 Oct 24;32(43):15227–42.

133. Vargas-Medrano J, Krishnamachari S, Villanueva E, Godfrey WH, Lou H, Chinnasamy R, et al. Novel FTY720-based compounds stimulate neurotrophin expression and phosphatase activity in dopaminergic cells. ACS Med Chem Lett. 2014 Jul 10;5(7):782–6.

134. Choi BK, Choi MG, Kim JY, Yang Y, Lai Y, Kweon DH, et al. Large α-synuclein oligomers inhibit neuronal SNARE-mediated vesicle docking. Proc Natl Acad Sci U S A. 2013 Mar 5;110(10):4087–92.

135. Scott D, Roy S. α-Synuclein inhibits intersynaptic vesicle mobility and maintains recycling-pool homeostasis. J Neurosci. 2012 Jul 25;32(30):10129–35.

136. Abeliovich A, Schmitz Y, Fariñas I, Choi-Lundberg D, Ho WH, Castillo PE, et al. Mice lacking alpha-synuclein display functional deficits in the nigrostriatal dopamine system. Neuron [Internet]. 2000 [cited 2019 Sep 6];25(1):239–52. Available from: https://www.ncbi.nlm.nih.gov/pubmed/10707987

137. Perez RG, Waymire JC, Lin E, Liu JJ, Guo F, Zigmond MJ. A Role for α-Synuclein in the Regulation of Dopamine Biosynthesis. J Neurosci [Internet]. 2002;22(8):3090–9. Available

from: http://www.ncbi.nlm.nih.gov/pubmed/11943812

138. Perez RG, Hastings TG. Could a loss of alpha-synuclein function put dopaminergic neurons at risk? J Neurochem [Internet]. 2004 Jun [cited 2019 Sep 6];89(6):1318–24. Available from: http://www.ncbi.nlm.nih.gov/pubmed/15189334

139. Yu S, Zuo X, Li Y, Zhang C, Zhou M, Zhang YA, et al. Inhibition of tyrosine hydroxylase expression in α-synuclein-transfected dopaminergic neuronal cells. Neurosci Lett [Internet]. 2004;367(1):34–9. Available from: https://linkinghub.elsevier.com/retrieve/pii/S0304394004006755

140. Peng X, Peng XM, Tehranian R, Dietrich P, Stefanis L, Perez RG. Alpha-synuclein activation of protein phosphatase 2A reduces tyrosine hydroxylase phosphorylation in dopaminergic cells. J Cell Sci [Internet]. 2005 Aug 1 [cited 2019 Sep 6];118(Pt 15):3523–30. Available from: http://www.ncbi.nlm.nih.gov/pubmed/16030137

141. Wang J, Lou H, Pedersen CJ, Smith AD, Perez RG. 14-3-3ζ contributes to tyrosine hydroxylase activity in MN9D cells: Localization of dopamine regulatory proteins to mitochondria. J Biol Chem. 2009 May 22;284(21):14011–9.

142. Lou H, Montoya SE, Alerte TNM, Wang J, Wu J, Peng X, et al. Serine 129 phosphorylation reduces the ability of α-synuclein to regulate tyrosine hydroxylase and protein phosphatase 2A in vitro and in vivo. J Biol Chem. 2010 Jun 4;285(23):17648–61.

143. Gombash SE, Manfredsson FP, Kemp CJ, Kuhn NC, Fleming SM, Egan AE, et al. Morphological and behavioral impact of AAV2/5-mediated overexpression of human wildtype alpha-synuclein in the rat nigrostriatal system. PLoS One [Internet]. 2013 Nov 27 [cited 2020 Apr 24];8(11):e81426. Available from: http://www.ncbi.nlm.nih.gov/pubmed/24312298

144. Lee FJ, Liu F, Pristupa ZB, Niznik HB. Direct binding and functional coupling of alpha-synuclein to the dopamine transporters accelerate dopamine-induced apoptosis. FASEB J [Internet]. 2001;15(6):916–26. Available from: http://www.ncbi.nlm.nih.gov/pubmed/11292651

145. Dauer W, Kholodilov N, Vila M, Trillat AC, Goodchild R, Larsen KE, et al. Resistance of α-synuclein null mice to the parkinsonian neurotoxin MPTP. Proc Natl Acad Sci U S A. 2002 Oct 29;99(22):14524–9.

146. Wersinger C, Sidhu A. Attenuation of dopamine transporter activity by alpha-synuclein. Neurosci Lett [Internet]. 2003;340(3):189–92. Available from: http://www.ncbi.nlm.nih.gov/pubmed/12672538

147. WERSINGER C, PROU D, VERNIER P, SIDHU A. Modulation of dopamine transporter function by α-synuclein is altered by impairment of cell adhesion and by induction of oxidative stress. FASEB J [Internet]. 2003 Nov [cited 2019 Sep 6];17(14):2151–3. Available from: http://www.fasebj.org/doi/10.1096/fj.03-0152fje

148. Fountaine TM, Wade-Martins R. RNA interference-mediated knockdown of α-synuclein protects human dopaminergic neuroblastoma cells from MPP+ toxicity and reduces dopamine transport. J Neurosci Res [Internet]. 2007 Feb 1 [cited 2019 Sep 6];85(2):351–63. Available from: http://doi.wiley.com/10.1002/jnr.21125

149. Fountaine TM, Venda LL, Warrick N, Christian HC, Brundin P, Channon KM, et al. The effect of alpha-synuclein knockdown on MPP+ toxicity in models of human neurons. Eur J Neurosci [Internet]. 2008;28(12):2459–73. Available from: http://www.pubmedcentral.nih.gov/articlerender.fcgi?artid=PMC3132457

150. Wong YC, Luk K, Purtell K, Burke Nanni S, Stoessl AJ, Trudeau L-E, et al. Neuronal vulnerability in Parkinson disease: Should the focus be on axons and synaptic terminals? Mov Disord [Internet]. 2019 Sep 4 [cited 2019 Oct 1]; Available from: http://www.ncbi.nlm.nih.gov/pubmed/31483900

151. Caudle WM, Richardson JR, Wang MZ, Taylor TN, Guillot TS, McCormack AL, et al. Reduced vesicular storage of dopamine causes progressive nigrostriatal neurodegeneration. J Neurosci. 2007;27:8138–48.

152. Guillot TS, Shepherd KR, Richardson JR, Wang MZ, Li YJ, Emson PC, et al. Reduced vesicular storage of dopamine exacerbates methamphetamine-induced neurodegeneration and astrogliosis. J Neurochem. 2008;106:2205–17.

153. Taylor TN, Caudle WM, Shepherd KR, Noorian A, Jackson CR, Iuvone PM, et al. Nonmotor symptoms of Parkinson's disease revealed in an animal model with reduced monoamine storage capacity. J Neurosci [Internet]. 2009;29(25):8103–13. Available from: https://www.ncbi.nlm.nih.gov/pubmed/19553450

154. Taylor TN, Caudle WM, Miller GW. VMAT2-Deficient Mice Display Nigral and Extranigral Pathology and Motor and Nonmotor Symptoms of Parkinson's Disease. Park Dis [Internet]. 2011;2011(124165):124165. Available from: https://www.ncbi.nlm.nih.gov/pubmed/21403896

155. Lohr KM, Bernstein AI, Stout KA, Dunn AR, Lazo CR, Alter SP, et al. Increased vesicular monoamine transporter enhances dopamine release and opposes Parkinson disease-related neurodegeneration in vivo. Proc Natl Acad Sci U S A [Internet]. 2014;111(27):9977–82. Available from: https://www.ncbi.nlm.nih.gov/pubmed/24979780

156. Mor DE, Tsika E, Mazzulli JR, Gould NS, Kim H, Daniels MJ, et al. Dopamine induces soluble α-synuclein oligomers and nigrostriatal degeneration. Nat Neurosci [Internet]. 2017;20(11):1560–8. Available from: http://www.nature.com/doifinder/10.1038/nn.4641

157. Venda LL, Cragg SJ, Buchman VL, Wade-Martins R. α-Synuclein and dopamine at the crossroads of Parkinson's disease. Trends Neurosci [Internet]. 2010;33(12):559–68. Available from: https://linkinghub.elsevier.com/retrieve/pii/S0166223610001359

158. Roy S. Synuclein and dopamine: the Bonnie and Clyde of Parkinson's disease. Nat Neurosci [Internet]. 2017;20(11):1514–5. Available from: http://www.nature.com/articles/s41593-017-0035-7

159. Bridi JC, Hirth F. Mechanisms of α-Synuclein Induced Synaptopathy in Parkinson's Disease. Front Neurosci [Internet]. 2018;12(FEB). Available from: http://journal.frontiersin.org/article/10.3389/fnins.2018.00080/full

160. Conway KA, Rochet JC, Bieganski RM, Lansbury J. Kinetic stabilization of the α-synuclein protofibril by a dopamine-α-synuclein adduct. Science (80-). 2001 Nov 9;294(5545):1346–9.

161. Volles MJ, Lee SJ, Rochet JC, Shtilerman MD, Ding TT, Kessler JC, et al. Vesicle permeabilization by protofibrillar α-synuclein: Implications for the pathogenesis and treatment of Parkinson's disease. Biochemistry. 2001 Jul 3;40(26):7812–9.

162. Gaugler MN, Genc O, Bobela W, Mohanna S, Ardah MT, El-Agnaf OM, et al. Nigrostriatal overabundance of α-synuclein leads to decreased vesicle density and deficits in dopamine release that correlate with reduced motor activity. Acta Neuropathol. 2012 May;123(5):653–69.

163. Bové J, Prou D, Perier C, Przedborski S. Toxin-induced models of Parkinson's disease. NeuroRx. 2005;2(3):484–94.

164. Simola N, Morelli M, Carta AR. The 6-hydroxydopamine model of Parkinson's disease. Neurotox Res [Internet]. 2007 Apr [cited 2019 Oct 1];11(3–4):151–67. Available from: http://www.ncbi.nlm.nih.gov/pubmed/17449457

165. Tieu K. A guide to neurotoxic animal models of Parkinson's disease. Cold Spring Harb Perspect Med. 2011 Sep;1(1).

166. Przedborski S, Jackson-Lewis V, Djaldetti R, Liberatore G, Vila M, Vukosavic S, et al. The parkinsonian toxin MPTP: action and mechanism. Restor Neurol Neurosci [Internet]. 2000 [cited 2019 Sep 28];16(2):135–42. Available from: http://www.ncbi.nlm.nih.gov/pubmed/12671216

167. Jackson-Lewis V, Przedborski S. Protocol for the MPTP mouse model of Parkinson's disease. Nat Protoc. 2007 Feb;2(1):141–51.

168. Betarbet R, Sherer TB, MacKenzie G, Garcia-Osuna M, Panov A V, Greenamyre JT. Chronic systemic pesticide exposure reproduces features of Parkinson's disease. Nat Neurosci [Internet]. 2000 Dec [cited 2019 Sep 28];3(12):1301–6. Available from: http://www.ncbi.nlm.nih.gov/pubmed/11100151

169. Miller GW. Paraquat: The Red Herring of Parkinson's Disease Research. Toxicol Sci [Internet]. 2007 Nov [cited 2019 Sep 28];100(1):1–2. Available from: https://academic.oup.com/toxsci/article/1627080/Paraquat:

170. Corrigan F, Wienburg C, Shore R, Daniel S, Mann D. Organochlorine insecticides in substantia nigra in Parkisnon's disease. J Toxicol Environ Heal Part A Curr Issues. 2000;59(4):229–34.

171. Kitazawa M, Anantharam V, Kanthasamy AG. Dieldrin induces apoptosis by promoting caspase-3-dependent proteolytic cleavage of protein kinase Cdelta in dopaminergic cells: relevance to oxidative stress and dopaminergic degeneration. Neuroscience [Internet]. 2003;119(4):945–64. Available from: https://www.ncbi.nlm.nih.gov/pubmed/12831855

172. Kitazawa M, Anantharam V, Kanthasamy AG. Dieldrin-induced oxidative stress and neurochemical changes contribute to apoptopic cell death in dopaminergic cells. Free Radic Biol Med [Internet]. 2001;31(11):1473–85. Available from: http://linkinghub.elsevier.com/retrieve/pii/S0891584901007262

173. Chun HS, Gibson GE, Degiorgio LA, Zhang H, Kidd VJ, Son JH. Dopaminergic cell death induced by MPP(+), oxidant and specific neurotoxicants shares the common molecular mechanism. J Neurochem. 2001;76(4):1010–21.

174. Sun F, Anantharam V, Latchoumycandane C, Kanthasamy A, Kanthasamy AG. Dieldrin induces ubiquitin-proteasome dysfunction in α-synuclein overexpressing dopaminergic neuronal cells and enhances susceptibility to apoptotic cell death. J Pharmacol Exp Ther. 2005 Oct;315(1):69–79.

175. Sanchez-Ramos J, Facca A, Basit A, Song S. Toxicity of Dieldrin for Dopaminergic Neurons in Mesencephalic Cultures. Exp Neurol [Internet]. 1998;150(2):263–71. Available from: http://linkinghub.elsevier.com/retrieve/pii/S0014488697967704

176. Sharma RP, Winn DS, Low JB. Toxic, neurochemical and behavioral effects of dieldrin exposure in mallard ducks. Arch Environ Contam Toxicol [Internet]. 1976 [cited 2019 Sep 17];5(1):43–53. Available from: http://www.ncbi.nlm.nih.gov/pubmed/1015862

177. Wagner SR, Greene FE. Dieldrin-induced alterations in biogenic amine content of rat brain. Toxicol Appl Pharmacol. 1978;43(1):45–55.

178. Heinz G, Hill E. Dopamine and norepinephrine depletion in ring doves fed DDE, dieldrin, and Aroclor 1254. Elsevier Pharmacol JF Contrera - Toxicol Appl [Internet]. 1980 [cited 2019 Sep 17]; Available from: https://www.sciencedirect.com/science/article/pii/0041008X8090383X

179. Hatcher JM, Richardson JR, Guillot TS, McCormack AL, Di Monte DA, Jones DP, et al. Dieldrin exposure induces oxidative damage in the mouse nigrostriatal dopamine system. Exp Neurol [Internet]. 2007;204(2):619–30. Available from: https://linkinghub.elsevier.com/retrieve/pii/S0014488606006480

180. Baird J, Jacob C, Barker M, Fall C, Hanson M, Harvey N, et al. Developmental Origins of Health and Disease: A Lifecourse Approach to the Prevention of Non-Communicable Diseases. Healthcare [Internet]. 2017 Mar 8 [cited 2020 Mar 28];5(1):14. Available from:

http://www.ncbi.nlm.nih.gov/pubmed/28282852

181. Heindel JJ, Vandenberg LN. Developmental origins of health and disease: A paradigm for understanding disease cause and prevention. Vol. 27, Current Opinion in Pediatrics. Lippincott Williams and Wilkins; 2015. p. 248–53.

182. Cory-Slechta DA, Thiruchelvam M, Richfield EK, Barlow BK, Brooks AI. Developmental pesticide exposures and the Parkinson's disease phenotype. In: Birth Defects Research Part A - Clinical and Molecular Teratology [Internet]. 2005 [cited 2020 Mar 28]. p. 136–9. Available from: http://www.ncbi.nlm.nih.gov/pubmed/15751039

183. Lohr KM, Chen M, Hoffman CA, McDaniel MJ, Stout KA, Dunn AR, et al. Vesicular Monoamine Transporter 2 (VMAT2) Level Regulates MPTP Vulnerability and Clearance of Excess Dopamine in Mouse Striatal Terminals. Toxicol Sci [Internet]. 2016 [cited 2019 Sep 27];153(1):79–88. Available from: http://www.ncbi.nlm.nih.gov/pubmed/27287315

184. Narahashi T. Neuronal ion channels as the target sites of insecticides. Pharmacol Toxicol [Internet]. 1996 Jul [cited 2019 Sep 17];79(1):1–14. Available from: http://www.ncbi.nlm.nih.gov/pubmed/8841090

185. Okada H, Matsushita N, Kobayashi K, Kobayashi K. Identification of GABAA receptor subunit variants in midbrain dopaminergic neurons. J Neurochem. 2004;89(1):7–14.

186. Lauder J, Liu J, … LD-P on, 1998 undefined. GABA as a trophic factor for developing monoamine neurons. europepmc.org [Internet]. [cited 2019 Sep 17]; Available from: https://europepmc.org/abstract/med/9777640

187. Liu J, Morrow AL, Devaud L, Grayson DR, Lauder JM. GABA A Receptors Mediate Trophic Effects of GABA on Embryonic Brainstem Monoamine Neurons In Vitro. 1997.

188. Narahashi T, Carter D, Frey J, Ginsburg K, letters KN-T, 1995 undefined. Sodium channels and GABAA receptor-channel complex as targets of environmental toxicants. Elsevier [Internet]. [cited 2019 Sep 17]; Available from: https://www.sciencedirect.com/science/article/pii/037842749503482X

189. Paladini CA, Tepper JM. GABA(A) and GABA(B) antagonists differentially affect the firing pattern of substantia nigra dopaminergic neurons in vivo. Synapse. 1999 Jun 1;32(3):165–76.

190. Gezer AO, Kochmanski J, VanOeveren SE, Cole-Strauss A, Kemp CJ, Patterson JR, et al. Developmental exposure to the organochlorine pesticide dieldrin causes male-specific exacerbation of α-synuclein-preformed fibril-induced toxicity and motor deficits. bioRxiv [Internet]. 2020 Feb 6 [cited 2020 Mar 6];2020.02.03.932681. Available from: https://doi.org/10.1101/2020.02.03.932681

191. Kochmanski J, VanOeveren SE, Patterson JR, Bernstein AI, Patterson JR, Bernstein AI. Developmental Dieldrin Exposure Alters DNA Methylation at Genes Related to

Dopaminergic Neuron Development and Parkinson's Disease in Mouse Midbrain. Toxicol Sci [Internet]. 2019 Jun 1 [cited 2019 Sep 22];169(2):593–607. Available from: http://dx.doi.org/10.1093/toxsci/kfz069

192. Jagmag SA, Tripathi N, Shukla SD, Maiti S, Khurana S. Evaluation of models of Parkinson's disease. Vol. 9, Frontiers in Neuroscience. Frontiers Media S.A.; 2016.

193. Paumier KL, Luk KC, Manfredsson FP, Kanaan NM, Lipton JW, Collier TJ, et al. Intrastriatal injection of pre-formed mouse α-synuclein fibrils into rats triggers α-synuclein pathology and bilateral nigrostriatal degeneration. Neurobiol Dis. 2015 Oct 1;82:185–99.

194. Luk KC, Kehm V, Carroll J, Zhang B, O'Brien P, Trojanowski JQ, et al. Pathological α-synuclein transmission initiates Parkinson-like neurodegeneration in nontransgenic mice. Science (80-). 2012 Nov 16;338(6109):949–53.

195. Duffy MF, Collier TJ, Patterson JR, Kemp CJ, Fischer DL, Stoll AC, et al. Quality Over Quantity: Advantages of Using Alpha-Synuclein Preformed Fibril Triggered Synucleinopathy to Model Idiopathic Parkinson's Disease. Front Neurosci [Internet]. 2018 [cited 2019 Sep 2];12:621. Available from: http://www.ncbi.nlm.nih.gov/pubmed/30233303

196. Volpicelli-Daley LA, Luk KC, Patel TP, Tanik SA, Riddle DM, Stieber A, et al. Exogenous α-Synuclein Fibrils Induce Lewy Body Pathology Leading to Synaptic Dysfunction and Neuron Death. Neuron. 2011 Oct 6;72(1):57–71.

197. Volpicelli-Daley LA, Luk KC, Lee VMY. Addition of exogenous α-synuclein preformed fibrils to primary neuronal cultures to seed recruitment of endogenous α-synuclein to Lewy body and Lewy neurite-like aggregates. Vol. 9, Nature Protocols. Nature Publishing Group; 2014. p. 2135–46.

198. Luk KC, Song C, O'Brien P, Stieber A, Branch JR, Brunden KR, et al. Exogenous α-synuclein fibrils seed the formation of Lewy body-like intracellular inclusions in cultured cells. Proc Natl Acad Sci U S A. 2009 Nov 24;106(47):20051–6.

199. Luk KC, Kehm V, Carroll J, Zhang B, O'Brien P, Trojanowski JQ, et al. Pathological alpha-synuclein transmission initiates Parkinson-like neurodegeneration in nontransgenic mice. Science (80-) [Internet]. 2012;338(6109):949–53. Available from: https://www.ncbi.nlm.nih.gov/pubmed/23161999

200. Patterson JR, Duffy MF, Kemp CJ, Howe JW, Collier TJ, Stoll AC, et al. Time course and magnitude of alpha-synuclein inclusion formation and nigrostriatal degeneration in the rat model of synucleinopathy triggered by intrastriatal α-synuclein preformed fibrils. Neurobiol Dis [Internet]. 2019 Oct [cited 2019 Sep 9];130:104525. Available from: http://www.ncbi.nlm.nih.gov/pubmed/31276792

201. Patterson JR, Polinski NK, Duffy MF, Kemp CJ, Luk KC, Volpicelli-Daley LA, et al. Generation of Alpha-Synuclein Preformed Fibrils from Monomers and Use In vivo |

Protocol. JOVE [Internet]. 2019; Available from: https://www.jove.com/video/59758/generation-alpha-synuclein-preformed-fibrils-from-monomers-use

202. Duffy MF, Collier TJ, Patterson JR, Kemp CJ, Luk KC, Tansey MG, et al. Lewy body-like alpha-synuclein inclusions trigger reactive microgliosis prior to nigral degeneration. J Neuroinflammation [Internet]. 2018 May 1 [cited 2019 Sep 25];15(1):129. Available from: https://www.ncbi.nlm.nih.gov/pubmed/29716614

203. Sortwell CE, Collier TJ, Duffy MF, Luk KC, Kemp CJ, Kanaan NM, et al. Optimization of synucleinopathy and nigrostriatal degeneration induced by Injection of α-Synuclein preformed fibrils into rat striatum. Mov Disord [Internet]. 2017;32(S2). Available from: http://scholar.google.com/scholar?q=Optimization

204. Jorgenson JL. Aldrin and dieldrin: a review of research on their production, environmental deposition and fate, bioaccumulation, toxicology, and epidemiology in the United States. Environ Health Perspect [Internet]. 2001;109 Suppl(March):113–39. Available from: http://www.pubmedcentral.nih.gov/articlerender.fcgi?artid=1240548&tool=pmcentrez&rendertype=abstract

205. de Jong G. Long-term health effects of aldrin and dieldrin. A study of exposure, health effects and mortality of workers engaged in the manufacture and formulation of the insecticides aldrin and dieldrin. Toxicol Lett [Internet]. 1991;Suppl:1–206. Available from: http://www.ncbi.nlm.nih.gov/pubmed/2014520

206. Meijer SN, Halsall CJ, Harner T, Peters AJ, Ockenden WA, Johnston AE, et al. Organochlorine pesticide residues in archived UK soil. Environ Sci Technol [Internet]. 2001 May 15 [cited 2019 Sep 17];35(10):1989–95. Available from: http://www.ncbi.nlm.nih.gov/pubmed/11393978

207. Weisskopf MG, Knekt P, O'Reilly EJ, Lyytinen J, Reunanen A, Laden F, et al. No Title. Neurology [Internet]. 2010 Mar 30 [cited 2019 Aug 25];74(13). Available from: http://www.ncbi.nlm.nih.gov/pubmed/20350979

208. Kitazawa M, Anantharam V, and AK-FRB, 2001 undefined. Dieldrin-induced oxidative stress and neurochemical changes contribute to apoptopic cell death in dopaminergic cells. Elsevier [Internet]. [cited 2019 Sep 17]; Available from: https://www.sciencedirect.com/science/article/pii/S0891584901007262

209. Miller GW, Erickson JD, Perez JT, Penland SN, Mash DC, Rye DB, et al. Immunochemical analysis of vesicular monoamine transporter (VMAT2) protein in Parkinson's disease. Exp Neurol [Internet]. 1999;156(1):138–48. Available from: http://www.ncbi.nlm.nih.gov/pubmed/10192785

210. Uhl GR. Hypothesis: the role of dopaminergic transporters in selective vulnerability of cells in Parkinson's disease. Ann Neurol [Internet]. 1998 May [cited 2019 Sep

24];43(5):555–60. Available from: http://www.ncbi.nlm.nih.gov/pubmed/9585349

211. Allis CD, Jenuwein T. The molecular hallmarks of epigenetic control. Nat Rev Genet [Internet]. 2016;17(8):487–500. Available from: https://www.ncbi.nlm.nih.gov/pubmed/27346641

212. Faulk C, Dolinoy DC. Timing is everything. Epigenetics [Internet]. 2011;6(7):791–7. Available from: http://www.tandfonline.com/doi/abs/10.4161/epi.6.7.16209

213. Cheng Y, Bernstein A, Chen D, Jin P. 5-Hydroxymethylcytosine: A new player in brain disorders? Exp Neurol [Internet]. 2015;268:3–9. Available from: http://dx.doi.org/10.1016/j.expneurol.2014.05.008

214. Jakovcevski M, Akbarian S. Epigenetic mechanisms in neurological disease. Nat Med [Internet]. 2012;18(8):1194–204. Available from: http://www.pubmedcentral.nih.gov/articlerender.fcgi?artid=3596876&tool=pmcentrez&rendertype=abstract

215. Labbe C, Lorenzo-Betancor O, Ross OA. Epigenetic regulation in Parkinson's disease. Acta Neuropathol [Internet]. 2016;132(4):515–30. Available from: http://dx.doi.org/10.1007/s00401-016-1590-9

216. Lardenoije R, Pishva E, Lunnon K, van den Hove DL. Neuroepigenetics of Aging and Age-Related Neurodegenerative Disorders. Prog Mol Biol Transl Sci [Internet]. 2018;158:49–82. Available from: http://dx.doi.org/10.1016/bs.pmbts.2018.04.008

217. Marques S, Outeiro TF. Epigenetics: Development and Disease. Epigenetics Dev Dis [Internet]. 2013;61:507–25. Available from: http://link.springer.com/10.1007/978-94-007-4525-4

218. Miranda-Morales E, Meier K, Sandoval-Carrillo A, Salas-Pacheco J, Vazquez-Cardenas P, Arias-Carrion O. Implications of DNA Methylation in Parkinson's Disease. Front Mol Neurosci [Internet]. 2017;10:225. Available from: http://dx.doi.org/10.3389/fnmol.2017.00225

219. Wullner U, Kaut O, deBoni L, Piston D, Schmitt I. DNA methylation in Parkinson's disease. J Neurochem [Internet]. 2016;139 Suppl:108–20. Available from: http://dx.doi.org/10.1111/jnc.13646

220. Yang Z, Wang KKW. Glial fibrillary acidic protein: From intermediate filament assembly and gliosis to neurobiomarker. Vol. 38, Trends in Neurosciences. Elsevier Ltd; 2015. p. 364–74.

221. Gonzales C, Zaleska MM, Riddell DR, Atchison KP, Robshaw A, Zhou H, et al. Alternative method of oral administration by peanut butter pellet formulation results in target engagement of BACE1 and attenuation of gavage-induced stress responses in mice. Pharmacol Biochem Behav [Internet]. 2014;126:28–35. Available from:

https://www.ncbi.nlm.nih.gov/pubmed/25242810

222. Masuda-Suzukake M, Nonaka T, Hosokawa M, Oikawa T, Arai T, Akiyama H, et al. Prion-like spreading of pathological alpha-synuclein in brain. Brain [Internet]. 2013;136(Pt 4):1128–38. Available from: https://www.ncbi.nlm.nih.gov/pubmed/23466394

223. Redmann M, Wani WY, Volpicelli-Daley L, Darley-Usmar V, Zhang J. Trehalose does not improve neuronal survival on exposure to alpha-synuclein pre-formed fibrils. Redox Biol [Internet]. 2017;11:429–37. Available from: https://linkinghub.elsevier.com/retrieve/pii/S22132317163

224. Sasaki A, Arawaka S, Sato H, Kato T. Sensitive western blotting for detection of endogenous Ser129-phosphorylated α-synuclein in intracellular and extracellular spaces. Sci Rep [Internet]. 2015;5(1):14211. Available from: http://www.nature.com/articles/srep14211

225. Cliburn RA, Dunn AR, Stout KA, Hoffman CA, Lohr KM, Bernstein AI, et al. Immunochemical localization of vesicular monoamine transporter 2 (VMAT2) in mouse brain. J Chem Neuroanat [Internet]. 2016;83–84:82–90. Available from: https://www.ncbi.nlm.nih.gov/pubmed/27836486

226. Livak KJ, Schmittgen TD. Analysis of relative gene expression data using real-time quantitative PCR and the 2-ΔΔCT method. Methods. 2001;25(4):402–8.

227. Mogi M, Harada M, Narabayashi H, Inagaki H, Minami M, Nagatsu T. Interleukin (IL)-1β, IL-2, IL-4, IL-6 and transforming growth factor-α levels are elevated in ventricular cerebrospinal fluid in juvenile parkinsonism and Parkinson's disease. Neurosci Lett. 1996 Jun;211(1):13–6.

228. Imamura K, Hishikawa N, Sawada M, Nagatsu T, Yoshida M, Hashizume Y. Distribution of major histocompatibility complex class II-positive microglia and cytokine profile of Parkinson's disease brains. Acta Neuropathol. 2003 Dec;106(6):518–26.

229. Croisier E, Moran LB, Dexter DT, Pearce RKB, Graeber MB. Microglial inflammation in the parkinsonian substantia nigra: Relationship to alpha-synuclein deposition. J Neuroinflammation. 2005 Jun;2.

230. Dijkstra AA, Ingrassia A, De Menezes RX, Van Kesteren RE, Rozemuller AJM, Heutink P, et al. Evidence for immune response, axonal dysfunction and reduced endocytosis in the substantia nigra in early stage Parkinson's disease. PLoS One. 2015 Jun;10(6).

231. Braak H, Tredici K Del, Rüb U, de Vos RAI, Steur ENHJ, Braak E. Staging of brain pathology related to sporadic Parkinson's disease. Neurobiol Aging. 2003;24:197–211.

232. Kannarkat GT, Cook D a, Lee J-K, Chang J, Chung J, Sandy E, et al. Common genetic variant association with altered HLA expression, synergy with pyrethroid exposure, and risk for Parkinson's disease: an observational and case–control study. npj Park Dis.

2015;1(January):15002.

233. Harms AS, Cao S, Rowse AL, Thome AD, Li X, Mangieri LR, et al. MHCII Is Required for -Synuclein-Induced Activation of Microglia, CD4 T Cell Proliferation, and Dopaminergic Neurodegeneration. J Neurosci. 2013 Jun;33(23):9592–600.

234. Liu X, Zhan Z, Li D, Xu L, Ma F, Zhang P, et al. Intracellular MHC class II molecules promote TLR-triggered innate immune responses by maintaining activation of the kinase Btk. Nat Immunol [Internet]. 2011 May [cited 2019 Sep 25];12(5):416–24. Available from: http://www.ncbi.nlm.nih.gov/pubmed/21441935

235. De Miranda BR, Fazzari M, Rocha EM, Castro S, Greenamyre JT. Sex Differences in Rotenone Sensitivity Reflect the Male-to-Female Ratio in Human Parkinson's Disease Incidence. Toxicol Sci. 2019;

236. Gillies GE, Pienaar IS, Vohra S, Qamhawi Z. Sex differences in Parkinson's disease. Front Neuroendocrinol. 2014;35(3):370–84.

237. Rice D, Barone S. Critical periods of vulnerability for the developing nervous system: evidence from humans and animal models. Environ Health Perspect [Internet]. 2000;108 Suppl(s3):511–33. Available from: http://dx.doi.org/10.1289/ehp.00108s3511

238. Heyer DB, Meredith RM. Environmental toxicology: Sensitive periods of development and neurodevelopmental disorders. Neurotoxicology [Internet]. 2017;58:23–41. Available from: http://dx.doi.org/10.1016/j.neuro.2016.10.017

239. Miodovnik A. Environmental neurotoxicants and developing brain. Mt Sinai J Med [Internet]. [cited 2019 Sep 25];78(1):58–77. Available from: http://www.ncbi.nlm.nih.gov/pubmed/21259263

240. Dauer W, Przedborski S. Parkinson's Disease. Neuron [Internet]. 2003;39(6):889–909. Available from: https://linkinghub.elsevier.com/retrieve/pii/S0896627303005683

241. Farrer MJ. Genetics of Parkinson disease: paradigm shifts and future prospects. Nat Rev Genet [Internet]. 2006 Apr [cited 2019 Sep 5];7(4):306–18. Available from: http://www.nature.com/doifinder/10.1038/nrg1831

242. Toxicological profile for Aldrin/Dieldrin. 2002.

243. de la Fuente-Fernandez R, Schulzer M, Mak E, Sossi V. Trials of neuroprotective therapies for Parkinson's disease: problems and limitations. Park Relat Disord [Internet]. 2010;16(6):365–9. Available from: https://www.ncbi.nlm.nih.gov/pubmed/20471298

244. Forno LS, DeLanney LE, Irwin I, Langston JW. Similarities and differences between MPTP-induced parkinsonsim and Parkinson's disease. Neuropathologic considerations. Adv Neurol [Internet]. 1992;60:600–8. Available from: http://europepmc.org/abstract/med/8380528

245. Freundt EC, Maynard N, Clancy EK, Roy S, Bousset L, Sourigues Y, et al. Neuron-to-neuron transmission of alpha-synuclein fibrils through axonal transport. Ann Neurol [Internet]. 2012;72(4):517–24. Available from: https://www.ncbi.nlm.nih.gov/pubmed/23109146

246. Luk KC, Kehm VM, Zhang B, O'Brien P, Trojanowski JQ, Lee VM. Intracerebral inoculation of pathological alpha-synuclein initiates a rapidly progressive neurodegenerative alpha-synucleinopathy in mice. J Exp Med [Internet]. 2012;209(5):975–86. Available from: https://www.ncbi.nlm.nih.gov/pubmed/22508839

247. Recasens A, Dehay B, Bove J, Carballo-Carbajal I, Dovero S, Perez-Villalba A, et al. Lewy body extracts from Parkinson disease brains trigger alpha-synuclein pathology and neurodegeneration in mice and monkeys. Ann Neurol [Internet]. 2014;75(3):351–62. Available from: https://www.ncbi.nlm.nih.gov/pubmed/24243558

248. Osterberg VR, Spinelli KJ, Weston LJ, Luk KC, Woltjer RL, Unni VK. Progressive aggregation of alpha-synuclein and selective degeneration of lewy inclusion-bearing neurons in a mouse model of parkinsonism. Cell Rep [Internet]. 2015;10(8):1252–60. Available from: https://www.ncbi.nlm.nih.gov/pubmed/25732816

249. Luk KC, Covell DJ, Kehm VM, Zhang B, Song IY, Byrne MD, et al. Molecular and Biological Compatibility with Host Alpha-Synuclein Influences Fibril Pathogenicity. Cell Rep [Internet]. 2016;16(12):3373–87. Available from: https://www.ncbi.nlm.nih.gov/pubmed/27653697

250. Polinski NK, Volpicelli-Daley LA, Sortwell CE, Luk KC, Cremades N, Gottler LM, et al. Best practices for generating and using alpha-synuclein pre-formed fibrils to model Parkinson's disease in rodents. J Parkinsons Dis [Internet]. 2018;8(2):303–22. Available from: http://www.medra.org/servlet/aliasResolver?alias=iospress&doi=10.3233/JPD-171248

251. Tarutani A, Suzuki G, Shimozawa A, Nonaka T, Akiyama H, Hisanaga SI, et al. The effect of fragmented pathogenic α-synuclein seeds on prion-like propagation. J Biol Chem. 2016 Sep 2;291(36):18675–88.

252. Abdelmotilib H, Maltbie T, Delic V, Liu Z, Hu X, Fraser KB, et al. α-Synuclein fibril-induced inclusion spread in rats and mice correlates with dopaminergic Neurodegeneration. Neurobiol Dis. 2017 Sep 1;105:84–98.

253. Fleming SM, Salcedo J, Fernagut PO, Rockenstein E, Masliah E, Levine MS, et al. Early and progressive sensorimotor anomalies in mice overexpressing wild-type human α-synuclein. In: Journal of Neuroscience. 2004. p. 9434–40.

254. Hwang D-YY, Fleming SM, Ardayfio P, Moran-Gates T, Kim H, Tarazi FI, et al. 3,4-Dihydroxyphenylalanine reverses the motor deficits in Pitx3-deficient Aphakia mice: Behavioral characterization of a novel genetic model of Parkinson's disease. J Neurosci. 2005 Feb;25(8):2132–7.

255. Glajch KE, Fleming SM, Surmeier DJ, Osten P. Sensorimotor assessment of the unilateral 6-hydroxydopamine mouse model of Parkinson's disease. Behav Brain Res. 2012 May;230(2):309–16.

256. Dirr ER, Ekhator OR, Blackwood R, Holden JG, Masliah E, Schultheis PJ, et al. Exacerbation of sensorimotor dysfunction in mice deficient in Atp13a2 and overexpressing human wildtype alpha-synuclein. Behav Brain Res. 2018 May;343:41–9.

257. Neal ML, Fleming SM, Budge KM, Boyle AM, Kim C, Alam G, et al. Pharmacological inhibition of CSF1R by GW2580 reduces microglial proliferation and is protective against neuroinflammation and dopaminergic neurodegeneration. FASEB J. 2020 Jan;34(1):1679–94.

258. West MJ, Slomianka L, Gundersen HJ. Unbiased stereological estimation of the total number of neurons in thesubdivisions of the rat hippocampus using the optical fractionator. Anat Rec [Internet]. 1991 Dec [cited 2019 Sep 25];231(4):482–97. Available from: http://www.ncbi.nlm.nih.gov/pubmed/1793176

259. Ip CW, Cheong D, Volkmann J. Stereological estimation of dopaminergic neuron number in the mouse substantia nigra using the optical fractionator and standard microscopy equipment. J Vis Exp. 2017 Sep 1;2017(127).

260. Chan P, Di Monte DA, Langston JW, Janson AM. (+)MK-801 does not prevent MPTP-induced loss of nigral neurons in mice. J Pharmacol Exp Ther [Internet]. 1997 Jan [cited 2019 Sep 25];280(1):439–46. Available from: http://www.ncbi.nlm.nih.gov/pubmed/8996226

261. Fleming SM, Mulligan CK, Richter F, Mortazavi F, Lemesre V, Frias C, et al. A pilot trial of the microtubule-interacting peptide (NAP) in mice overexpressing alpha-synuclein shows improvement in motor function and reduction of alpha-synuclein inclusions. Mol Cell Neurosci. 2011 Mar;46(3):597–606.

262. Tillerson JL, Caudle WM, Revero ME, Miller GW. Detection of Behavioral Impairments Correlated to Neurochemical Deficits in Mice Treated with Moderate Doses of. Exp Neurol. 2002;90:80–90.

263. Goldberg MS, Fleming SM, Palacino JJ, Cepeda C, Lam HA, Bhatnagar A, et al. Parkin-deficient Mice Exhibit Nigrostriatal Deficits but not Loss of Dopaminergic Neurons. J Biol Chem. 2003;

264. Chen L, Ding Y, Cagniard B, Van Laar AD, Mortimer A, Chi W, et al. Unregulated cytosolic dopamine causes neurodegeneration associated with oxidative stress in mice. J Neurosci [Internet]. 2008;28(2):425–33. Available from: http://www.ncbi.nlm.nih.gov/pubmed/18184785

265. Guillot TS, Richardson JR, Wang MZ, Li YJ, Taylor TN, Ciliax BJ, et al. PACAP38 increases vesicular monoamine transporter 2 (VMAT2) expression and attenuates

methamphetamine toxicity. Neuropeptides. 2008;42:423–34.

266. Wang YM, Gainetdinov RR, Fumagalli F, Xu F, Jones SR, Bock CB, et al. Knockout of the vesicular monoamine transporter 2 gene results in neonatal death and supersensitivity to cocaine and amphetamine. Neuron. 1998/01/14. 1997;19(6):1285–96.

267. Gainetdinov RR, Fumagalli F, Wang Y, Jones SR, Levey AI, Miller GW, et al. Increased MPTP Neurotoxicity in Vesicular Monoamine Transporter 2 Heterozygote Knockout Mice. J Neurochem. 1998 May;70(5):1973–8.

268. Colebrooke RE, Humby T, Lynch PJ, McGowan DP, Xia J, Emson PC. Age-related decline in striatal dopamine content and motor performance occurs in the absence of nigral cell loss in a genetic mouse model of Parkinson's disease. Eur J Neurosci. 2006 Nov;24(9):2622–30.

269. Ulusoy A, Björklund T, Buck K, Kirik D. Dysregulated dopamine storage increases the vulnerability to α-synuclein in nigral neurons. Neurobiol Dis [Internet]. 2012;47(3):367–77. Available from: https://linkinghub.elsevier.com/retrieve/pii/S0969996112001982

270. Aldrin and dieldrin: health and safety guide. 1989.

271. Lauder JM, Liu J, Devaud L, Morrow AL. GABA as a trophic factor for developing monoamine neurons. Perspect Dev Neurobiol. 1998;5(2–3):247–59.

272. Narahashi T, Carter DB, Frey J, Ginsburg K, Hamilton BJ, Nagata K, et al. Sodium channels and GABAA receptor-channel complex as targets of environmental toxicants. Toxicol Lett. 1995;82–83:239–45.

273. Swerdlow RH, Parker WD, Currie LJ, Bennett JP, Harrison MB, Trugman JM, et al. Gender ratio differences between Parkinson's disease patients and their affected relatives. Parkinsonism Relat Disord [Internet]. 2001 Apr [cited 2019 Sep 20];7(2):129–33. Available from: http://www.ncbi.nlm.nih.gov/pubmed/11248594

274. Shulman LM, Bhat V. Gender disparities in Parkinson's disease. Expert Rev Neurother [Internet]. 2006 Mar [cited 2019 Sep 20];6(3):407–16. Available from: http://www.ncbi.nlm.nih.gov/pubmed/16533144

275. Hamm RJ, Pike BR, O'dell DM, Lyeth BG, Jenkins LW. The Rotarod Test: An Evaluation of Its Effectiveness in Assessing Motor Deficits Following Traumatic Brain Injury. J Neurotrauma. 1994;11(2):187–96.

276. Benedetti MD, Maraganore DM, Bower JH, McDonnell SK, Peterson BJ, Ahlskog JE, et al. Hysterectomy, menopause, and estrogen use preceding Parkinson's disease: an exploratory case-control study. Mov Disord [Internet]. 2001 Sep [cited 2019 Sep 30];16(5):830–7. Available from: http://www.ncbi.nlm.nih.gov/pubmed/11746612

277. Saunders-Pullman R, Gordon-Elliott J, Parides M, Fahn S, Saunders HR, Bressman S. The effect of estrogen replacement on early Parkinson's disease. Neurology [Internet]. 1999

Apr 22 [cited 2019 Sep 30];52(7):1417–21. Available from: http://www.ncbi.nlm.nih.gov/pubmed/10227628

278. Tsang KL, Ho SL, Lo SK. Estrogen improves motor disability in parkinsonian postmenopausal women with motor fluctuations. Neurology [Internet]. 2000 Jun 27 [cited 2019 Sep 30];54(12):2292–8. Available from: http://www.ncbi.nlm.nih.gov/pubmed/10881255

279. Liu B, Dluzen DE. Oestrogen and nigrostriatal dopaminergic neurodegeneration: animal models and clinical reports of Parkinson's disease. Clin Exp Pharmacol Physiol [Internet]. 2007 Jul [cited 2019 Sep 30];34(7):555–65. Available from: http://www.ncbi.nlm.nih.gov/pubmed/17581209

280. Currie LJ, Harrison MB, Trugman JM, Bennett JP, Wooten GF. Postmenopausal estrogen use affects risk for Parkinson disease. Arch Neurol [Internet]. 2004 Jun [cited 2019 Sep 30];61(6):886–8. Available from: http://www.ncbi.nlm.nih.gov/pubmed/15210525

281. Kaminsky Z, Wang S-C, Petronis A. Complex disease, gender and epigenetics. Ann Med [Internet]. 2006 [cited 2019 Sep 30];38(8):530–44. Available from: http://www.ncbi.nlm.nih.gov/pubmed/17438668

282. Czech DP, Lee J, Sim H, Parish CL, Vilain E, Harley VR. The human testis-determining factor SRY localizes in midbrain dopamine neurons and regulates multiple components of catecholamine synthesis and metabolism. J Neurochem [Internet]. 2012 Jul [cited 2019 Sep 30];122(2):260–71. Available from: http://www.ncbi.nlm.nih.gov/pubmed/22568433

283. Cantuti-Castelvetri I, Keller-McGandy C, Bouzou B, Asteris G, Clark TW, Frosch MP, et al. Effects of gender on nigral gene expression and parkinson disease. Neurobiol Dis [Internet]. 2007 Jun [cited 2019 Sep 30];26(3):606–14. Available from: http://www.ncbi.nlm.nih.gov/pubmed/17412603

284. Simunovic F, Yi M, Wang Y, Stephens R, Sonntag KC. Evidence for gender-specific transcriptional profiles of nigral dopamine neurons in Parkinson Disease. PLoS One. 2010 Jan 25;5(1).